CHEMICAL ENGINEERING SCIENCE
GENIE CHIMIQUE

VOL. 10 1959 No. 3

Grössen, Einheiten und Einheitensysteme

U. GRIGULL

Farbenfabriken Bayer A. G., Leverkusen, W. Germany

(*Received* 11 *December* 1958)

Zusammenfassung—Die Beschlüsse der 10 Generalkonferenz für Mass und Gewicht (1954) sowie die Empfehlungen der "International Organisation for Standardization" (ISO) und anderer internationaler Fachorganisationen zeigen das Bestreben, zu grösserer Einheitlichkeit in dem Gebrauch von physikalischen Grössen und ihren Einheiten zu gelangen. In der Bundesrepublik Deutschland hat der *Verein Deutscher Ingenieure* kürzlich Empfehlungen ausgesprochen, die dem gleichen Ziel dienen sollen und über die im folgenden berichtet wird.

Abstract—The resolutions of the 10th General Conference on Weights and Measures (1954) and the recommendations of the International Organisation for Standardization (ISO) and of other international organisations indicate the desire to achieve greater uniformity in the use of physical quantities and their units. In the German Federal Republic the *Verein Deutscher Ingenieure* has recently made recommendations intended to serve the same purpose, which are reported on in the following.

Résumé—Les résolutions de la 10e Conférence Générale des Poids et Mesures (1954), les recommendations de l'Organisation Internationale pour la Normalisation (ISO – OIN) et d'autres organisations internationales manifestent le désir d'achever une plus grande uniformité dans l'emploi de grandeurs physiques et de leurs unités. Pour la République Fédérale Allemande, l'auteur indique les recommandations rédigées par le *Verein Deutscher Ingenieure*.

1. EINLEITUNG

MIT grosser Aufmersamkeit wird in allen Kulturstaaten die neuere Entwicklung auf dem Gebiet der Einheiten und Einheitensysteme verfolgt, die durch die Beschlüsse der 10. Generalkonferenz für Mass und Gewicht vom Jahre 1954 ausgelöst wurde. Diese Konferenz setzte 6 Grundeinheiten fest und empfahl die allgemeine Verwendung des durch diese Grundeinheiten bestimmten Einheitensystems in den Ländern der Meterkonvention.

Diese 6 Grundeinheiten sind:

das *Meter* (m) als Einheit der *Länge*,
das *Kilogramm* (kg) als Einheit der *Masse*,
die *Sekunde* (s) als Einheit der *Zeit*,
das *Ampere* (A) als Einheit der elektrischen *Stromstärke*,
der *Grad Kelvin* (°K) als Einheit der thermodynamischen *Temperatur*,
die *Candela* (cd) als Einheit der *Lichtstärke*.

Das zu diesen Grundeinheiten kohärente Einheitensystem wird im folgenden mit "Internationales Einheitensystem" bezeichnet. Häufig spricht man auch abkürzend vom MKS-System oder vom MKSA-System.

Andere internationale Fachorganisationen schlossen sich dem Vorgehen der Generalkonferenz an, so die "International Organization for Standardization" (ISO), die "International Union for Pure and Applied Physics" (IUPAP), die "International Union for Pure and Applied Chemistry" (IUPAC) und die "International Electrical Commission" (IEC). In vielen Dokumenten dieser Organisationen, die auch Einheiten

anderer Systeme oder systemfreie Einheiten enthalten, ist das Internationale Einheitensystem deutlich hervorgehoben und empfohlen.

Angesichts dieser Entwicklung mussten sich auch die deutschen Ingenieure die Frage vorlegen, ob ein weiteres Festhalten am metrischen technischen Einheitensystem vernünftig sei. Bei der zunehmenden Verflechtung der Ingenieurwissenschaften mit Physik, Chemie und physikalischer Chemie, wie sie gerade für die Verfahrenstechnik (Chemical Engineering) typisch ist, erwies sich das technische Einheitensystem als hinderlich für eine gegenseitige Verständigung.

Das metrische technische Einheitensystem beruht (im Bereich der Mechanik) auf den Grundeinheiten Meter, Kilogrammkraft und Sekunde. Es unterscheidet sich also vom Internationalen Einheitensystem oder vom (hier nicht weiter behandelten) CGS-System nicht nur durch andere Grundeinheiten, sondern auch dadurch, dass eine diesser Grundeinheiten zu einer anderen Grössenart gehörte. Besonders verwirrend wirkte es, dass das Kilogrammkraft durchweg mit Kilogramm bezeichnet wurde, obwohl bereits die 1. Generalkonferenz (1889) das Kilogramm eindeutig zur Einheit der Masse erklärte und seither diese Festlegung wiederholt bestätigt wurde.

Die oben genannte Frage, ob das metrische technische Einheitensystem im deutschen technischen Schrifttum beibehalten werden sollte, wurde durch den Wissenschaftlichen Beirat des *Vereins Deutscher Ingenieure* (*VDI*) diskutiert und nach langen Beratungen schliesslich verneint. Die Beratungen fanden dadurch ihren Abschluss, dass Empfehlungen, die eine hierzu eingesetzte Kommission augesarbeitet hatte, zusammen mit einem Kommentar von FLEGLER [1] veröffentlicht wurden.

Im folgenden sind diese Empfehlungen im Wortlaut wiedergegeben. Einzelne Punkte, soweit sie insbesondere für die Leser dieser Zeitschrift von Interesse sein können, werden ausführlicher besprochen.

2. EMPFEHLUNGEN DES *VDI*

1. Die in *Z. Ver. dtsch. Ing.* 1950 **92** 161 veröffentlichten Stellungnahmen des Wissenschaftlichen Beirates sind aufzugeben.

2. Unter Kilogramm (kg) ist in Zukunft nur noch das Massenkilogramm zu verstehen. Der Krafteinheit im Technischen Mass-System ist eine andere Bezeichnung als Kilogramm, z.B. die Bezeichnung Kilopond (kp), zu geben.

3. Das Internationale Einheitensystem mit den sechs Grundeinheiten Meter, Kilogramm, Sekunde, Ampere, Grad Kelvin, Candela, ist zu bevorzugen. Für dieses Einheitensystem gilt:

3.1 Die Einheit der Kraft ist das Newton (N),

$$1\ \mathrm{N} = 1\ \mathrm{kg\ m\ s^{-2}}.$$

Das Kilopond ist damit definiert durch die Gleichung

$$1\ \mathrm{kp} = 9{,}80665\ \mathrm{N}.$$

3.2 Die Einheit der Energie (Arbeit, Wärmemenge usw.) ist das Joule (J),

$$1\ \mathrm{J} = 1\ \mathrm{N\ m}.$$

Als weitere Energie-Einheiten können verwendet werden: die Kilowattstunde (kWh),

$$1\ \mathrm{kWh} = 3{,}6 \cdot 10^{6}\ \mathrm{J},$$

das Elektronenvolt

$$1\ \mathrm{eV} = 1{,}602 \cdot 10^{-19}\ \mathrm{J},$$

die Kilokalorie (Internationale Tafel-Kilokalorie vom Jahre 1956), definiert als

$$1\ \mathrm{kcal} = 4186{,}8\ \mathrm{J}.$$

3.3 Die Einheit der Leistung ist das Watt (W),

$$1\ \mathrm{W} = 1\ \mathrm{J/s}.$$

3.4 Die Einheit des Druckes ist das Newton je Quadratmeter,

$$1\ \mathrm{N/m^2} = 1\ \mathrm{kg\ m^{-1}\ s^{-2}}.$$

Als weitere Druckeinheiten können verwendet werden: das Bar,

$$1\ \mathrm{bar} = 10^{5}\ \mathrm{N/m^2},$$

die Technische Atmospähre (at),

$$1\ \mathrm{at} = 1\ \mathrm{kp/cm^2} = 98066{,}5\ \mathrm{N/m^2},$$

die Physikalische Atmosphäre (atm), definiert als

VOL. 10 1959

$1\ \text{atm} = 101\,325\ \text{N/m}^2$,

das Torr, definiert als

$$1\ \text{Torr} = \frac{1}{760}\ \text{atm}$$

$$\left(= \frac{101325}{760}\ \text{N/m}^2 \approx 133{,}32\ \text{N/m}^2\right).$$

4. Es sind Grössengleichungen zu bevorzugen. Bei der Auswahl der in diese Gleichungen einzuführenden Grössen ist zu beachten:

4.1 Als Mass der Menge ist ihre Masse, nicht ihr Gewicht (Masse mal Fallbeschleunigung) zu benutzen.

Dies bedeutet insbesondere:

4.11 Die spezifischen Grössen der Wärmelehre sind auf die Masse, nicht auf das Gewicht zu beziehen.

4.12 Die Wichte (auch spezifisches Gewicht genannt) ist zu vermeiden und die Dichte zu benutzen.

4.2 Elektrische und magnetische Grössen sind so zu definieren, dass die Grössengleichungen in rationaler Schreibweise erscheinen.

4.3 Energie, Arbeit und Wärmemenge sind Grössen gleicher Art. Das Wärmeäquivalent tritt demnach in Grössengleichungen nicht mehr auf.

In Punkt 1 der Empfehlungen wird eine frühere Stellungnahme aufgehoben, die der weiteren Entwicklung im Wege stand; hierauf sei nicht weiter eingegangen. Die übrigen Punkte lassen sich deutlich nach zwei Gesichtspunkten einteilen, nämlich nach Einheiten (Punkt 2 und 3) und nach Grössen (Punkt 4). Diese werden im folgenden getrennt behandelt.

3. Die Empfohlenen Einheiten

Zu Punkt 2

Die lange Diskussion über die Benennung der metrischen technischen Krafteinheit hat ihr vorläufiges Ende dadurch gefunden, dass das Technische Kommitee ISO/TC 12 zwei Namen als gleichberechtigt anerkannte [2]: Kilopond (kp) und kilogramme-force (kgf). Eine Einigung auf eine einzige Bezeichnung gelang nicht, jedoch sollen die beiden Symbole kp und kgf die Vielzahl der bisherigen ersetzen, wie kg_p, kg_f, kg', kg*, Kg, kG. Die IUPAP schloss sich dem Beschluss von ISO/TC 12 an.

In Deutschland wird das Kilopond, das man dort um 1939 vorgeschlagen hatte, im Schulunterricht gebraucht, auch verwendet es der Deutsche Normenausschuss seit 1955 in seinen Normblättern. In Österreich ist das Kilopond gesetzliche Einheit und wird auch in das künftige deutsche Einheitengesetz aufgenommen werden, das man zur Zeit vorbereitet.*

Zu Punkt 3

Hier ist der Kernpunkt der Empfehlungen enthalten, nämlich die Bevorzugung des Internationalen Einheitensystems. Die Urheber dieser Empfehlung waren sich völlig darüber klar, dass man mit einem einzigen kohärenten Einheitensystem niemals auskommt, da man damit häufig sehr unbequeme Zahlenwerte erhalten würde. Hier bietet sich der Ausweg an, *dezimale* Teile und Vielfache der kohärenten Einheiten zu verwenden, für die von 10^{-12} bis 10^{12} die wohlbekannten Vorsatzsilben mit ihren Abkürzungen existieren (Milli für 10^{-3}, Kilo für 10^3 usw.) Manche Einheiten dieser Art haben eigene Namen, z.B. die Tonne (t) für 10^3 kg. Allerdings sind der konsequentien Anwendung dieses Grundsatzes dadurch Grenzen gesetzt, dass die Zeiteinheiten Minute und Stunde nicht dezimal aus der Grundeinheit Sekunde abgeleitet sind.

Die Empfehlung bedeutet doch aber zugleich den Vorschlag, nichtkohärente und nicht dezimal abgeleitete Einheiten in Zukunft (mit der genannten Einschränkung) nach und nach fallen zu lassen, sofern nicht sehr triftige Gründe für ihre Weiterverwendung bestehen. Für den Bereich der Thermodynamik handelt es sich dabei vorzugsweise um die Druckeinheiten at und atm und um die Energieeinheit kcal. Die technische und die physikalische Atmosphäre wären durch das Bar zu ersetzen, das bereits als Millibar in der

* Für den Bereich der Deutschen Demokratischen Republik ist die "Verordnung über die physikalisch-technischen Einheiten" kürzlich in Kraft getreten (Gesetzblatt Teil I. Nr, 56 vom 6. September 1958, S. 647–649). Hierzu gehört die "Tafel der gesetzlichen Einheiten." Mitteilungsblatt Nr. 149 des Deutchen Amtes für Mass und Gewicht vom 8. Oktober 1958.

Meteorologie verwendet wird. An die Stelle der Kilokalorie soll das Kilojoule treten. Natürlich braucht eine solche Umstellung eine vernünftige Übergangszeit, weshalb die Empfehlung auch einige heute übliche Einheiten aufzählt.

Es ist eine sehr bestechende Eigenschaft des Internationalen Einheitensystems, dass man mit ihm die verschiedenen Energiearten in der gleichen Einheit ausdrücken kann. Das wird aus folgender Einheitengleichung deutlich:

$$\mathrm{N.m = kg.m^2/s^2 = J = W.s} \qquad (1)$$

Die einzelnen Terme dieser Gleichung kann man, obwohl sie per definitionem alle dasselbe bedeuten, als Einheiten folgender Energiearten auffassen:

Arbeit (Kraft mal Weg),
kinetische Energie (Masse mal Quadrat der Geschwindigkeit)
Wärmemenge,
elektrische Energie.

Es gibt keinen vernünftigen Grund dafür, mechanische Energien nur in kpm, Wärmemengen in kcal und elektrische Energien in kWh anzugeben und dadurch eine Vielzahl von Umrechnungsfaktoren notwendig zu machen.

Die Anwendung des Internationalen Einheitensystems bietet auch eine Möglichkeit, zwischen metrischen und englisch-amerikanischen Einheiten zu vermitteln. Weder die Kilokalorie (kcal) noch die British thermal unit (B.t.u.) sind in irgend einem Einheitensystem kohärent. Der Ersatz einer gewohnten Einheit durch eine neue ist erfahrungsgemäss umso leichter durchzuführen, je weniger die Umrechnungsfaktoren von Eins abweichen. Da mehrere internationale Gremien bereits verabredet haben, sich im internen Verkehr nur des Internationalen Einheitensystems zu bedienen, ist die folgende Zusammenstellung der Umrechnungsfaktoren für die Druck und Energieeinheiten von Interesse.

$$\begin{aligned} 1\ \mathrm{at} &= 0{,}980665\ \mathrm{bar\ (genau)} \\ 1\ \mathrm{atm} &= 1{,}01325\ \mathrm{bar\ (genau)} \\ 1\ \mathrm{lbf/in^2} &= 0{,}0689476\ \mathrm{bar} \\ 1\ \mathrm{kcal_{IT}} &= 4{,}1868\ \mathrm{kJ\ (genau)} \\ 1\ \mathrm{(B.t.u.)_{IT}} &= 1{,}05506\ \mathrm{kJ} \end{aligned}$$

Dabei ist lbf die Abkürzung für die Krafteinheit pound-force. Unter $\mathrm{kcal_{IT}}$ und $\mathrm{(B.t.u.)_{IT}}$ sind die Internationale Tafelkilokalorie und die international table British thermal unit zu verstehen, die durch die 5. Internationale Dampftafelkonferenz (London 1956) angenommen sind und nach ihrer Definition nicht mehr auf den Stoffeigenschaften von Wasser basieren.

Die Zusammenstellung zeigt, dass beim Übergang von at oder atm auf bar die Zahlenwerte fast ungeändert bleiben. Dasselbe gilt für den Übergang von $\mathrm{(B.t.u.)_{IT}}$ auf kJ. Wesentliche Umgewöhnungen wären beim Ersatz von $\mathrm{lbf/in^2}$ (auch p.s.i. genannt) durch bar und von $\mathrm{(kcal)_{IT}}$ durch kJ nötig. Im letzteren Falle ensteht nebenbei der Vorteil, dass die spezifische Wärmekapazität von Luft etwa den Zahlenwert Eins erhält (bei 0°C und 1 bar ist $c_p = 1{,}00_5$ kJ/kg grd). In mehreren Ländern (Schweden, Schweiz) gibt es heute schon Wasserdampftafeln, die in den Einheiten bar und Joule abgefasst sind.

VOL. 10 1959

4. Grössen und Grössengleichungen

Die Schwierigkeiten, die aus der Verwendung verschiedener Einheiten und Einheitensysteme entstehen, werden wesentlich gemildert, wenn man die Formelzeichen nicht als Zahlen sondern als physikalische Grössen auffasst. Eine Gleichung zwischen solchen Grössen, eine sogenannte Grössengleichung, beschreibt ein Naturgesetz in seiner allgemeinsten Form ohne das Beiwerk von Umrechnungszahlen. Die Grössengleichung gilt unabhängig von der Wahl bestimmter Einheiten, sie ist auch gegen den späteren Wechsel von Einheiten invariant und legt den Benutzer nicht auf die Verwendung kohärenter Einheiten fest [3], [4], [5], [6].

Zu Punkt 4

Da man mit Hilfe bestimmter einfacher Regeln eine Grössengleichung für beliebige Einheiten umformen kann, ist es zweckmässig, die Grössengleichungen stets als Ausgangsgleichungen anzugeben. Ihre Verwendung wird daher durch den *VDI* besonders empfohlen. Der Vorteil der Grössengleichungen wirkt sich erst dann voll aus, wenn sie für den Ingenieur in der gleichen Form geschrieben werden wie für den Physiker,

Chemiker, Physikochemiker usw. Das setzt aber bestimmte gemeinsame Regeln für die Definition der abgeleiteten Grössen voraus, auf die daher in den letzten Teilen der *VDI*-Empfehlungen eingegangen wird.

***Zu Punkt* 4.1.** Natürlich braucht die Definition abgeleiter Grössen nicht von der Wahl irgendwelcher Einheiten oder Grundeinbeiten abzuhängen. Trotzdem kann gelegentlich die Auswahl der Grundeinheiten auch auf die Grössendefinition einwirken. Ein solcher Fall liegt offenbar beim metrischen technischen Einheitensystem vor. Weil die Ingenieure die Krafteinheit Kilopond (kilogramme-force) zur Grundeinheit und damit die Kraft zur Grundgrösse gewählt hatten, bevorzugten sie auch das Gewicht (im Sinne einer Kraft) als Mass für die Menge und zugleich als Bezugsgrösse für spezifischen Grössen der Thermodynamik. Dabei handelte es sich nicht um das örtliche Gewicht G, sondern um das Normgewicht G_n, das mit der Masse m durch die Gleichung

$$G_n = m \cdot g_n \tag{2}$$

zusammenhängt, in der g_n die Norm-Fallbeschleunigung bedeutet ($g_n = 9{,}80665$ m/s²).

Nehmen wir wieder die spezifische Wärmekapazität von Luft als Beispiel, so erhalten wir folgende beiden Gleichungen:
für die Ingenieure

$$c_p' = \frac{C}{G_n} = 0{,}240 \ \frac{\text{kcal}_{\text{IT}}}{\text{kp grd}} \tag{3}$$

und für die Physiker

$$c_p = \frac{C}{m} = 0{,}240 \ \frac{\text{kcal}_{\text{IT}}}{\text{kg grd}} \tag{4}$$

wobei C die Wärmekapazität bedeutet. Obwohl c_p' und c_p Grössen verschiedener Art sind, haben die Zahlenwerte den gleichen Betrag. Zwischen den beiden Grössen besteht die Grössengleichung

$$c_p = c_p' \cdot g_n \tag{5}$$

und zwischen kg und kp die Einheitengleichung

$$\text{kp} = \text{kg} \cdot g_n \tag{6}$$

Üblicherweise haben die Ingenieure bisher die Grösse c_p' mit c_p bezeichnet und die Krafteinheit kp mit kg. Sie schrieben also die Gleichung

$$c_p = 0{,}240 \ \frac{\text{kcal}_{\text{IT}}}{\text{kg grd}}, \tag{7}$$

die äusserlich mit Gl. (4) identisch war, in Wirklichkeit aber Gl. (3) bedeuten sollte. Diese laxe Schreibweise, die manches Missverständnis hervorrief [6], [7], [8], erleichtert jetzt die durch den *VDI* emfohlene Umstellung (Punkt 4.11). Es ergibt sich das Kuriosum, dass in der technischen Literatur bisherige Gleichungen nach Art von Gleichung (7) stehen bleiben können, obwohl die Grösse auf der linken Seite ihre Definition geändert hat und die Einheit auf der rechten Seite zu einer anderen Grössenart gehört.

Die im metrischen technischen Einheitensystem kohärente Masseneinheit (kp s²/m = 9,80665 kg) hatte in Deutschland nie einen eigenen Namen. Da die spezifischen Grössen, wie oben erwähnt, bisher auf das Normgewicht (in kp) bezogen wurden, kam diese Masseneinheit als Bezugseinheit nicht in Frage. Durch diesen glücklichen Umstand können bei der empfohlenen Umstellung die Zahlenwerte der spezifschen Grössen ungeändert bleiben.

Auch das spezifische Volumen v wurde bisher durch den Ingenieur anders als durch den Physiker definiert. Für den Ingenieur war

$$v' = 1/\gamma$$

mit γ als Wichte (spezifisches Gewicht), wobei eigentlich die Wichte bei der Norm-Fallbeschleunigung g_n gemeint war, während für den Physiker v die reziproke Dichte ρ bedeutete:

$$v = 1/\rho$$

Der Ingenieur bezeichnete bisher v' mit v und unterschied nicht zwischen g und g_n, wodurch manche Grössengleichung eine fast unverständliche Form erhielt [6], [7], [8]. Um diese Mehrdeutigkeiten zu beseitigen, empfiehlt der *VDI* im Punkt 4.12, die Wichte überhaupt nicht mehr zu benutzen. Das spezifische Volumen soll nach Punkt 4.11 $v = 1/\rho$ definiert werden. In Schwerkraftproblemen würde man die örtliche Wichte besser durch $\rho\, g$ ersetzen.

Die praktische Folge dieser Emphfehlungen würde sein, dass die örtliche Fallbeschleunigung g nur noch in Gleichungen auftritt, die Schwer-

kraftprobleme beschreiben. Die Norm-Fallbeschleunigung tritt überhaupt nicht mehr auf, die Wichte (spezifisches Gewicht) ist entbehrlich.

Der Punkt 4.2 Empfehlungen, der sich mit elektrischen Grössen beschäftigt, sei hier übergangen.

Zu Punkt 4.3. Es ist seit langen bekannt, dass Energie, Arbeit und Wärmemenge Grössen gleicher Grössenart sind. Das bedeutet aber, dass jede Energieeinheit zugleich als Einheit der Wärmemenge aufgefasst werden kann, z.B. J, erg, kWh, kp m, kcal, B.t.u., eV. In der technischen Literatur herrschte vielfach die Ansicht vor, dass mechanische Arbeit nur in kp m, Wärmemenge nur in kcal gemessen werden dürfte, weshalb die Umrechnungszahl zwischen diesen beiden Einheiten

$$\text{kcal}_{\text{IT}} = 426{,}935 \text{ kp m},$$

mit einem eigenen Symbol (A) in die entsprechenden Gleichungen aufgenommen und mit der besonderen Bezeichnung " mechanisches Wärmeäquivalent " belegt wurde. Da aber irgend eine Einheitenvorschrift nicht mit dem Charakter der Grössengleichung verträglich ist, darf in Grössengleichungen auch keine Umrechnungszahl zwischen Einheiten erscheinen, was in Punkt 4.3 der *VDI*-Empfehlungen ausdrücklich festgestellt wird. Auch verdient die Zahl 426,935 sowenig einen eigenen Namen oder ein eigenes Symbol, wie irgend eine andere Umrechnungszahl zwischen Einheiten.

5. Schlussbemerkung

Die Empfehlungen des *VDI*, die vorstehend kommentiert wurden, werden seit einigen Monaten in einem Teil der deutschen technischen Literatur angewendet. Obwohl die Beobachtungszeit noch sehr kurz ist, lässt sich schon heute erkennen, dass das Interesse der Fachwelt sehr gross ist und dass ernsthafte Schwierigkeiten nicht aufgetreten sind. Die positiven Kommentare der Leser überwiegen bei weitem die negativen.

Die Autoren dieser Empfehlungen hatten sich das Ziel gesetzt, eine bessere Verständigung zwischen Ingenieuren und Naturwissenschaftlern zu erreichen. Die Chancen, die hierzu in der Benutzung von Grössengleichungen und von einheitlichen Einheiten liegen, sollen voll ausgenutzt werden. Dass dabei auch alte Gewohnheiten aufgegeben werden müssen, ist unvermeidlich.

Literatur

[1] Flegler E. Z. *Ver. dtsch. Ing.* 1958 **100**, 1100.

[2] Stille U. *DIN-Mitt.* 1958 **37** 58 (bes. S.59).

[3] Flegler E. Z. *Ver. dtsch. Ing.* 1952 **94** 928, 1009.

[4] Stille U. *Messen und Rechnen in der Physik.* Braunschweig, 1955.

[5] Wallot J. *Grössengleichungen, Einheiten und Dimensionen.* (2. Aufl.), Leipzig 1957.

[6] Grigull U. *Brennst.-Wärmekr.* 1957 **9** 219.

[7] Klinkenberg A. *Chem. Engng. Sci.* 1955 **4** 130, 167.

[8] Grassman P. Z. *Ver. dtsch. Ing.* 1956 **98** 1829.

Chemical Engineering Science, 1959, Vol. 10, pp. 139 to 149. Pergamon Press Ltd., London. Printed in Great Britain

The influence of the initial filtration velocity and of vibrations on the resistance of a polystyrene filtercake

P. J. Bakker, P. M. Heertjes and J. L. Hibou
Laboratory of Chemical Engineering of the Technical University, Delft.

(*Received* 8 *March* 1958; *in revised form* 27 *August* 1958)

Abstract—The influence of the initial filtration velocity and of vibrations on the resistance of a filtercake of polystyrene spheres of known diameter and formed over three different well-defined filters has been studied.

The influence of the initial filtration velocity could be expressed mathematically, showing an increase of a cake resistance zero at an infinite velocity, to a maximum value at a velocity zero. The parameters in this equation depend besides on the system on the particle size.

The influence of vibrations on the cake resistance has been studied qualitatively. In general it has been observed that the mean resistance increases by vibration and with increasing amplitude and frequency. The influence is larger if the cake has a high resistance and is not very stable. For the case of a well-defined vibration, a mathematical expression for the relative cake resistance as a function of the frequency could be derived.

By successive filtration, filtration under vibration and re-filtration, interesting phenomena have been observed.

A qualitative explanation of the phenomena, based on the structure of a cake as a function of the initial filtration velocity and based again on the structure of foregoing layers, has been given.

Résumé—L'influence de la vitesse initiale de filtration et de vibrations sur la résistance d'un gâteau de sphères de polystyrène de diamètre connue formé sur trois filtres différents bien définis, a été étudiée.

L'influence de la vitesse initiale de filtration a pu être exprimée mathématiquement, montrant une augmentation de la résistance du gâteau, nulle pour une vitesse infinie, à une valeur maximum pour une vitesse nulle. Ces paramètres de cette équation dépendent du système et de la grandeur des particles.

L'influence des vibrations sur la résistance du gâteau a été étudiée qualitativement. En général il a été observé que les vibrations augmentent la résistance moyenne et ceci d'autant plus que l'amplitude et la fréquence sont plus grandes. L'influence est plus grande si le gâteau a une grande résistance et s'il n'est pas très stable. Pour le cas d'une vibration bien définie, une expression mathématique donnant la résistance relative du gâteau en fonction de la fréquence a pu être trouvée.

Dans le cas d'une filtration suivie de filtration avec vibration puis de nouveau par une filtration simple, des observations intéressantes ont pu être faites.

Une explication qualitative du phénomène, fondée sur la structure du gâteau en tant que fonction de la vitesse initiale de filtration et sur la structure des couches précédents a été donnée.

Zusammenfassung—Der Einfluss der anfänglichen Filtrationsgeschwindigkeit und von Schwingungen auf den Widerstand eines Filterkuchens aus Polystyrolkugeln bekannten Durchmessers wurde untersucht, wobei der Filterkuchen über drei wohldefinierten Filtern gebildet wurde.

Der Einfluss der anfänglichen Filtrationsgeschwindigkeit konnte mathematisch ausgedrückt werden; der Kuchenwiderstand Null bei unendlicher Geschwindigkeit erreichte einen Maximalwert bei einer Geschwindigkeit Null. Die Parameter dieser Gleichung hängen ausserdem von der Teilchengrösse ab.

Der Einfluss von Schwingungen auf den Kuchenwiderstand wurde qualitativ untersucht. Im allgemeinen wurde beobachtet, dass der mittlere Widerstand infolge von Schwingungen und mit steigender Amplitude und Frequenz anstieg. Der Einfluss ist grösser, wenn der Kuchen

einen hohen Widerstand hat und nicht sehr fest ist. Für den Fall einer wohldefinierten Schwingung konnte ein mathematischer Ausdruck für den relativen Kuchenwiderstand als Funktion der Frequenz abgeleitet werden.

Wenn einer geowöhnlichen Filtration eine solche mit Schwingung und dann wieder eine gewöhnliche Filtration folgten, konnten interessante Beobachtungen gemacht werden.

Die Erscheinungen konnten qualitativ gedeutet werden, wobei man von der Struktur des Kuchens als Funktion der anfänglichen Filtrationsgeschwindigkeit und von der Struktur der vorhergehenden Schichten ausging.

Introduction

In filtration, vibrations often have a strong effect on the filtration velocity. In former publications [1], [2] and [3] precautions have been described which had to be taken against an influence of vibrations on the results.

Because of the technical importance of this phenomenon it has been undertaken to study the influence of vibrations on the resistance of a filtercake. To facilitate a possible explanation, a well-defined system has been chosen, viz. slurries of spherical particles of polystyrene* in water, filtered over well-defined filters.

The use of these systems enabled us to study more quantitatively than was previously possible [2] the influence of the initial filtration velocity and (or) of the filter resistance on the packing of the filtercake.

Experimental

The apparatus used was almost equal to another set-up described earlier [1]. Nevertheless a sketch (see Fig. 1) and a short description of its use will be given.

The slurry to be filtered is prepared and stored in a vessel A (30 l) provided with a stirrer and a heating coil controlled by a contact thermometer. Via a membrane valve the slurry flows into the actual filtration apparatus B. This apparatus (see detail) consists of a perforated brass plate, on top of which the filtercloth is placed, a brass funnel and a cylindrical plexiglass container provided with an overflow.

The filtrate formed is assembled in the container C, the filtrate volume can be measured by means of the calibrated burette D. Vacuum is applied to C and D by means of the water-jet pump H. The big vessel F connected with the vacuum system serves as a buffer, the needle-valve G enables the introduction of a small but constant amount of air into the system. In this way a constant vacuum (read on manometer E) can be maintained under the filter, ensuring a constant filtration pressure (vacuum + hydrostatic waterhead). The suspension overflowing from B into I is periodically returned to A, via J and K, by means of compressed air. After each run the filtrate is assembled in L, pumped to N by M, prefiltered over a small filter P to remove algae, fine dust particles, etc., and stored in *Q*. This prefiltered liquid is used to prepare the slurries in A to which it is transported with the aid of compressed air. As liquid water has been used, small amounts of a wetting agent (Teepol or Triton X 100) have been added to the water to promote monodispersivity. The water temperature was 25°C ($\eta_{water} = 8{\cdot}937\ 10^{-3}$, $\rho_{polystyrene} = 1{\cdot}045$).

With the apparatus as described filtration pressures equal to $17{\cdot}10^4$ (head of ~ 170 cm of water) have been used.

For a much smaller filtration pressure ($8{\cdot}10^3 = \sim 8$ cm of water) the apparatus was changed into a gravity filter. The vacuum system was disconnected and the filtrate flowed via an overflow into the container C. No details will be given.

Three filter "cloths" have been used: a nylon filter (nylon: 4,000 openings/cm²), and two nickel filters (Ni I: 729 circular openings ($\phi = 250\ \mu$)/cm²; Ni II: 2704 circular openings ($\phi = 75\ \mu$)/cm². The polystyrene mixture was graded in fractions by sieving. The following sieve fractions have been used: 125–150 μ, 150–175 μ, 175–210 μ, 350–420 μ, 500–600 μ, 600–710 μ, 710–1,000 μ, 1,200–1,400 μ, 1,400–1,700 μ, 1,700–2,000 μ and 2,000–2,400 μ.

*The "Chemische Werke Hüls" at Recklinghausen, Germany, had the courtesy to put a large amount of polystyrene pearls of wide size spectrum (30–3000 μ) at our disposal. Our thanks to this firm for their support may be expressed here.

VOL. 10 1959

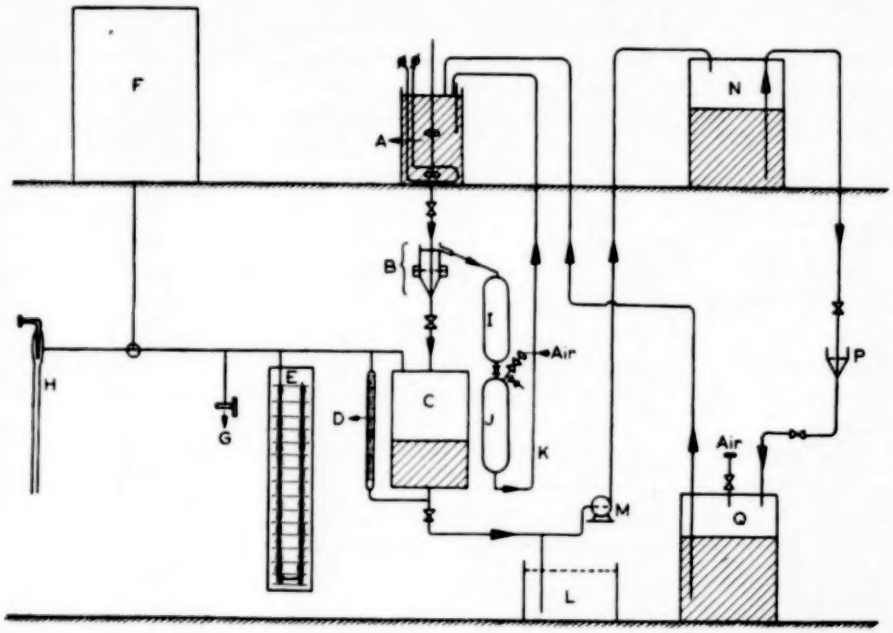

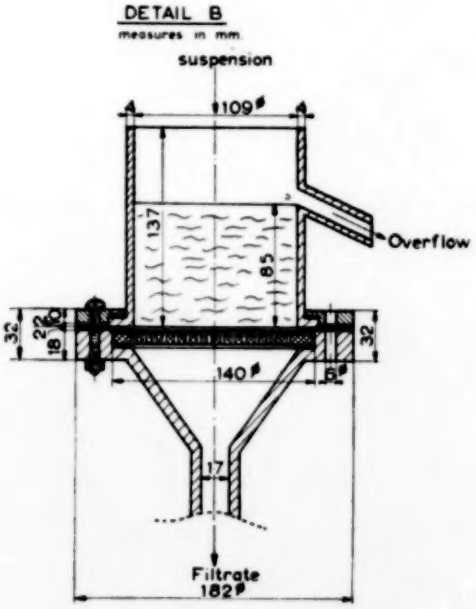

FIG. 1. Sketch of the filtration set-up.

The filter was mounted in a frame. Vibrations were applied to this frame. Two different devices were used. The first consisted of a wheel rotating around a horizontal axis. To this wheel pieces of rubber-tubing were attached in which small iron rods were fastened. The rubber ends touched the bearing bars of the filter support with a frequency proportional to the number of revolutions of the wheel. The amount of impacts per minute on the bars will be called the frequency of vibration (F).

The second device consisted of a constant speed motor, coupled to a variator which enabled to regulate the speed between 500 and 3,000 rev/min (F). The variator was coupled to an excentric allowing for an amplitude varying from 0–5 mm. The vibration created this way was of a sinusoid form.

The magnitudes measured during a run were $dV^*/\alpha\theta$ and V as a function of the time of filtration θ. Measurements were carried out in the laminar regime of flow. The specific resistance of the cake r, the resistance of the cake R_k, the resistance of the filter R_f, the total resistance of cake and filter R and the initial filtration velocity U_0, were defined and calculated by means of:

$$\frac{1}{A}\cdot\frac{dV}{d\theta}=\frac{1}{\eta}\cdot\frac{\Delta P}{R} \tag{1}$$

$$U_0=\left(\frac{1}{A}\frac{dV}{d\theta}\right)_{V=0}=\frac{1}{\eta}\frac{\Delta P}{R_f} \tag{2}$$

$$R=R_f+R_k \tag{3}$$

$$r=\frac{A}{c}\frac{dR_k}{dV}=\frac{A}{c}\frac{dR}{dV} \tag{4}$$

Measurements were carried out at a constant filtration pressure. Unless extraordinary effects occurred straight R-V lines were obtained, from the slope of which r was found. This r is a *mean* resistance.

Results

(with Boehm, Kroon and Veenhof)

(a) The influence of the filtration velocity on the cake resistance

It has been described earlier [2] that the cake resistance as far as filtration variables is concerned depends on the concentration of the slurry and on the initial filtration velocity U_0, or if the filtration pressure is constant, on the resistance R_f of the filter. An increase of r with decreasing U_0 has been observed. No mathematical relation could be found, because of a too large scattering of the results. This was in all probability caused by the not too well defined system used.

The better defined system used here has enabled us to find for this system a mathematical relation between r and U_0 (or R_f), which takes the form of an exponential function:

$$r=r_a\exp-\left(\frac{b_2}{R_f}\right)^d \tag{5}$$

or

$$r=r_a\exp-\left(\frac{U_0}{b_1}\right)^d \tag{6}$$

Combination of equations (2), (5) and (6) gives $b_1 b_1=\nabla P/\eta$. In these equations r_a signifies the specific resistance of a cake formed at an initial filtration velocity zero (or for a finite filtration pressure, at an infinite resistance), in which case the filtercake will be of the densest packing possible. Moreover, the packing of a filtercake formed over a filter which resistance approaches zero will approach that of the slurry. For the dilute suspensions used the resistance of such a cake will be very small. It has been assumed that the cake resistance for $R_f=0$, will be zero. The experiments carried out do not contradict the last supposition.

In Table 1 the values of r_A, b_1, b_2 and d as calculated for six series of polystyrene in water have been collected. The conditions of the experiments were: concentration $=6{\cdot}66\times10^{-3}$, $\Delta P=16{\cdot}3\times10^4$, the R_f of the nylon cloth used has been changed from 20×10^6 to 285×10^6.

In Fig. 2 the results for the series 4 and 6 are represented graphically, the dots are the measured data, the crosses are calculated with the aid of equation (5).

In Fig. 3, r has been plotted as a function of $\bar{d}_p$ (arithmetic mean) at constant values of R_f. The one system investigated so far does not yet permit us to draw any conclusions as to the significance of the magnitudes introduced. It

*See nomenclature.

VOL. 10 1959

Table 1.

Series no.	d_p *range* in* μ	r_a	b_1	b_2	d
1	125–150	110×10^6	0·126	145×10^6	0·67
2	175–210	149×10^6	0·193	95×10^6	0·87
3	350–420	91×10^6	0·610	30×10^6	2·07
4	500–600	114×10^6	0·572	32×10^6	1·73
5	600–710	135×10^6	0·359	51×10^6	1·10
6	710–1000	162×10^6	0·352	52×10^6	1·00

*The d_p range given is that of the corresponding sieve openings.

may suffice to note that apparently these magnitudes depend on the particle size. For the polystyrene cakes investigated the lowest values of r_a and b_2 and the highest values of d and b are found for particles of 350–420 μ. The change with particle size is gradual with the exception of r_a for the small-sized fractions. It has to be observed, however, that the inaccuracy in the calculated value of r_a may be large. On the other hand, the values as found lie within the actual possibilities. This conclusion can be drawn from percolation data on consolidated polystyrene cakes, obtained by introducing polystyrene spheres into the filter apparatus containing water, consolidated by careful and prolonged tapping against the wall of the filter. This has been continued until the cake has the highest possible packing density under these conditions.

Some of the resistances found with these cakes were:

$d_p = 1200$–$1400\ \mu$, $r = 1280 \times 10^6$;
$d_p = 1400$–$1700\ \mu$, $r = 865 \times 10^6$;
$d_p = 1700$–$2000\ \mu$, $r = 620 \times 10^6$;
$d_p = 2000$–$2400\ \mu$, $r = 413 \times 10^6$.

Analogous experiments with glass spheres (see later) gave the results that for:

$d_p = 1400$–$2000\ \mu$, $r = 362 \times 10^6$;
$d_p = 2000$–$4000\ \mu$, $r = 206 \times 10^6$.

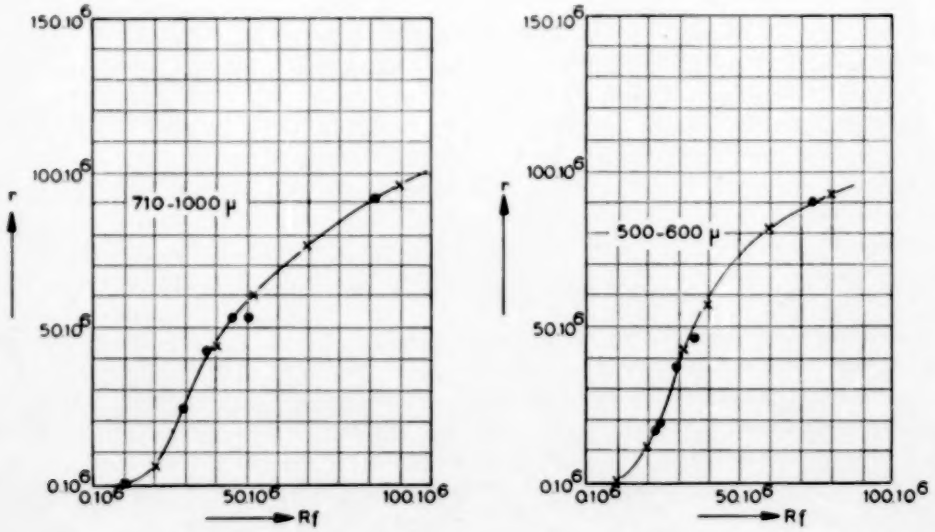

FIG. 2. The specific resistance of a cake r as a function of the resistance of the filter R_f for two sieve fractions of polystyrene.

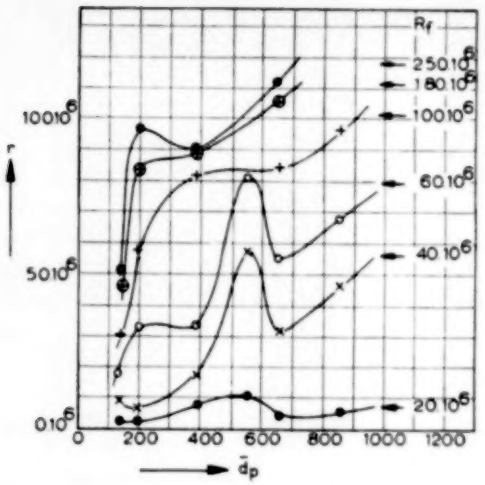

Fig. 3. The specific resistance of cakes of polystyrene as a function of the particle diameter d_p.

The results showed excellent reproducibility, demonstrated by the fact that the total resistance was linear with the amount of particles.

From the above it can be concluded that the r_a values as found are possible. The influence of the particle diameter as found for the cake resistance of the consolidated cakes has not been found for the r_a values which represent the resistance of cakes formed by filtration at the highest packing density possible under filtration conditions. Of course this does not necessarily need to be the case, because the mechanism of the cake, built-up for both types of cake, is in fact quite different.

From Fig. 3 it can be concluded that the general tendency is that at constant R_f, r increases with $\bar{d}_p$, although maxima and minima occur.

The differences observed in the resistances of cakes of polystyrene- and glass-spheres seem to indicate the existence of an influence of the surface-tension solid–liquid on the cake-resistance. Experiments with water containing different quantities of Teepol, presented in Fig. 4* as the cake resistances, measured at constant R_f, for the fraction 175–210 μ and $\Delta P = 16{\cdot}3 \times 10^4$, as a function of the surface tension liquid–air (σ_{LG}) show such an influence if as may reasonably

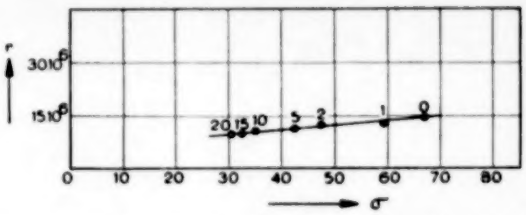

Fig. 4. The specific resistance of a cake in liquids of different surface tension.

be assumed the change in σ_{LG} is accompanied by a change in σ_{SL}.

It seems worthwhile to investigate what actual change in σ_{SL} causes the observed change in r. This has not yet been done.

(*b*) *The effect of vibrations*

(*i*) ***The filter.*** It has been found that vibrations do not cause a change in the filter resistance, except in those cases where air is trapped under the filter, the openings are small ($\sim 75\ \mu$) and the frequency is high ($F = 3000$). In these cases, however, the observed increase in resistance is small and of the order of some per cent.

(*ii*) ***The cake.*** Vibrations in general increase the resistance of cakes. The effect increases with increasing amplitude and cake-resistance. This holds for vibrating while filtering or while percolating. Reproducible results are not easy to obtain especially with particles of large diameter and sometimes with cakes of high resistance.

(*c*) *Combined filtration and vibration*

In those cases, where vibrations were applied from the very beginning of the filtration, linear $R - V$ relations were obtained, which enabled to determine the resistance r_F of the vibrated cake. The effect of the vibrations could then be expressed in a relative increase of the cake resistance $\Delta r = (r_F - r)/r$, if r is the resistance of a cake formed without vibration.

It has been found that the relation between Δr and F at a constant amplitude again can be expressed as an exponential function. Including that for $F = 0$, $\Delta r = 0$, the following equation fits the results:

$$\Delta r = a \exp - \left(\frac{b}{F}\right)^d \qquad (7)$$

*The number near the points represent the amount of Teepol added in ml/30 l. of water.

VOL. 10 1959

Table 2.

d_p *range* (μ)	*Conc.*	*Amplitude* (mm)	a	b	d	r	$r_{F\to\infty}$
150–175	$2{\cdot}5 \times 10^{-3}$	$1\frac{1}{4}$	1·49	1200	1·83	$6{\cdot}84 \times 10^6$	$17{\cdot}0 \times 10^6$
		$2\frac{1}{2}$	1·46	1100	1·57		$16{\cdot}8 \times 10^6$
		5	1·50	1000	1·65		$17{\cdot}1 \times 10^6$
350–420	$5{\cdot}0 \times 10^{-3}$	–*	0·74	1800	1·36	$0{\cdot}98 \times 10^6$	$1{\cdot}70 \times 10^6$
		$2\frac{1}{2}$	0·99	850	0·61		$1{\cdot}95 \times 10^6$
500–600	$5{\cdot}0 \times 10^{-3}$	–*	0·46	1000	2·92	$0{\cdot}61 \times 10^6$	$0{\cdot}89 \times 10^6$
		$2\frac{1}{2}$	0·64	900	2·68		$1{\cdot}00 \times 10^6$
		5	0·70	650	1·81		$1{\cdot}04 \times 10^6$

*In this case the amplitude could not be measured, but nevertheless the cake was vibrated.

The value of a signifies the maximum relative increase possible at a certain amplitude.

In Table 2 the calculated values of a, b and d, obtained with experiments where vibrations were applied from the very beginning, with a nylon filter ($R_f = 2{\cdot}69 \times 10^6$), with a pressure difference of $7{\cdot}8 \times 10^3$ and over an F range of 500–3000 have been collected. The maximum (extrapolated) value of r_F for $F = \infty$ [$r_{F\to\infty} = (1 + a)\, r$] as well as the resistance of the cake formed without vibration (r) has been included. The vibrations were applied either on top or at the bottom of the filter.

The relation between r_F of a vibrated cake and R_f can also be expressed by equation (5). However, as compared with a non-vibrated cake the magnitude of the constants changes. For a sieve fraction 175–210 μ, $F^1 = 540$, $\Delta P = 17{\cdot}4 \times 10^4$, $c = 6{\cdot}66 \times 10^{-3}$, R_f region of the Dynal filter used $45 \times 10^6 \to 230 \times 10^6$,* the following values have been calculated from the results:

	r_a	b_2	d
without vibration:	130×10^6	126×10^6	1·0
with vibration:	170×10^6	66×10^6	2·3

*The fraction taken was from a different stock as used before. Moreover instead of one of the three filters used normally, a Dynal filter cloth was taken because this could be cleaned with diluted hydrochloric acid.

From these data it can be calculated that the value of r_F/r at $R_f = 40 \times 10^6$ is equal to 1, that it rises rapidly to 3·1 at $R_f = 60 \times 10^6$ and then decreases slowly to 2·3 at $R_f = 200 \times 10^6$. In view of the accuracy of the measurements, the difference between the ratio 3·1 and 2·3 is not significant.

The conclusion can be drawn that the increase of the resistance by vibration is larger if the cake is formed at a relatively low initial velocity and therefore has a corresponding relatively high resistance, showing an increasing influence by decreasing the flow velocity, reaching constancy below a certain velocity.

(*d*) *Alternating periods of filtration and vibration*

Interesting phenomena are encountered if a filtration is started without vibration (period 1), if then vibrations are applied either while continuing the filtration or while percolating (period 2) and if finally a filtration without vibrations is carried out (period 3). The phenomena observed depend strongly on the type of cake formed in period 1. Two limiting cases will be considered. If the cake is formed at a high initial velocity and therefore has a low resistance, vibration in period 2, while filtrating, immediately shows a change in the R–V relation. The straight R–V line obtained has a larger slope than in the period 1. Continuing the filtration without vibrations in period 3 results again in a straight R–V line, with

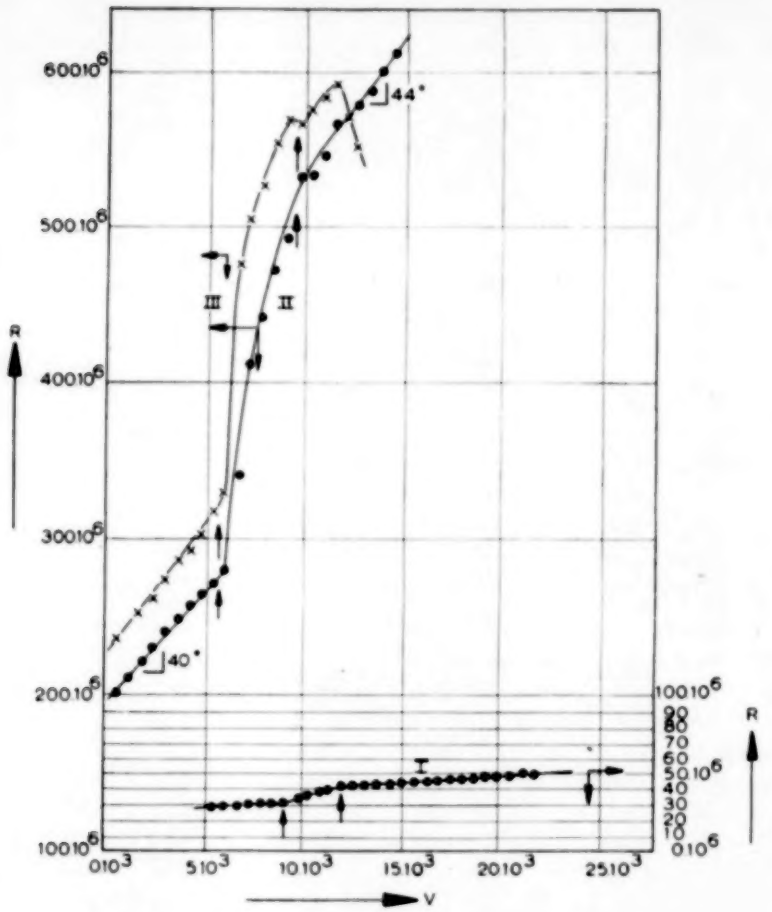

Fig. 5. The influence of vibrations on the form of the R–V line.

the same or a smaller slope as measured in period 1. The cakes thus formed are of a relatively low resistance.

For a cake formed at a low initial filtration velocity, therefore with a rather high resistance, the behaviour is quite different. As soon as the vibration has been started a sharp and, compared with the first case, relatively larger increase in R occurs. A second difference is that the R–V line for the period 2 is not straight, but curved downwards. On stopping the vibrations but continuing the filtration (period 3) the behaviour again shows a difference with the former case.

First a sharp drop in the total resistance occurs; this can be followed by an increase of R. In some cases several repetitions take place with a gradual decrease in the differences between the consecutive maxima and minima. Finally again a linear R–V relation is found if the filtration is prolonged long enough. The slope of this line is larger than that of the original cake, the limiting case being that by extrapolation the line passes the starting point of period 1 ($V = 0$, $R = R_f$).

For inbetween cases the phenomena are in-between. The smaller the original cake resistance, the smaller the drop of R at the end of period 2, the more the undulating part of the R–V line disappears, the smaller the increase in slope of the straight R–V line in period 3, as compared with that in period 1. It is not necessarily so that the drop in R occurs immediately after the vibrations have been stopped.

To substantiate the above three examples have been presented in a graphical form in Fig. 5. The filtrations have been carried out for the fraction 175–210 μ, in a concentration of $6{\cdot}66 \times 10^{-3}$, filtered over nylon cloth with $\Delta P = 16{\cdot}3 \times 10^4$. The two arrows mark the period 2 of vibration ($F^1 = 540$). To increase the cloth resistance several layers of nylon have been used or the cloth was not cleaned thoroughly.

Line I represents the results of a cake with a relatively low resistance (note the value of R_f, to be found by linear extrapolation of the R–V line of period 1).

Line II is for a cake with a higher resistance. This is an inbetween case as described. Immediately after vibration is stopped, a normal cake filtration follows, the cake showing a somewhat higher resistance than that of the cake formed in period 1.

Line III is for a still higher original cake-resistance showing a still sharper increase in R on vibration in period 2, followed by the period of unrest mentioned.

The straight R–V line of period 3 has not yet appeared here, because the filtration has not been prolonged long enough.

The phenomena just described can be altered by uncontrollable outside influences or even by small experimental changes. It is for this reason that no rigorous quantitative treatment can yet be given. Some of these influences need mentioning.

It can happen that while carrying out a filtration the resistance suddenly increases above the normal, especially if slurries with large particles are used. In most cases these changes could be attributed to some outside vibration, such as a resonating water tap.

In the second place, especially for thin cakes and with small driving forces the constancy of the slurry inlet is very important. The regulation is not easy for small quantities. A too large inlet stream causes a whirling-up of the cake layers already formed, causing a decrease in resistance. Moreover, with these thin cakes the disturbance can cause deblocking as well as blocking upon vibration. It has often been observed that vibration of a thin cake was accompanied by a decrease in the total resistance, sometimes without an increase afterwards. This happened more frequently with nickel filters, than with the nylon filter. A change of r from $7{\cdot}2 \times 10^6$ to $1{\cdot}7 \times 10^6$ can occur in such cases.

This influence has been avoided as much as possible, but could not always be prevented.

In the third place it may be remarked that air under the filter causes a small increase in the resistence of the filter. For nylon cloth R_f changes from $2{\cdot}69 \times 10_6$ to $2{\cdot}87 \times 10_6$.

In view of these facts, only a few data will be given. These data (see Table 3) will be presented as mean values of a number of experiments of the cake resistances before and after the period of vibration ($F = 3000$), therefore of period 1 and of period 3.

In series 1 and 2, carried out with thin cakes, always a permanent decrease of R on vibration has been observed. In the other series on vibration after a small decrease of R an increase followed, to higher value than that of the final value at the end of period 1.

Table 3.

No.	*Number of experiments*	*Filter*	*Conc.*	d_p *range* (μ)	r *before vibration*	r *after vibration*
1	22	Ni I	10×10^{-3}	350–420	$0{\cdot}19 \times 10^6$	$0{\cdot}14 \times 10^6$
*2	8	Ni I	10×10^{-3}	350–420	$0{\cdot}15 \times 10^6$	$0{\cdot}14 \times 10^6$
3	40	Ni II	$3{\cdot}33 \times 10^{-3}$	150–175	$2{\cdot}63 \times 10^6$	$2{\cdot}78 \times 10^6$
4	13	Ni II	$6{\cdot}66 \times 10^{-3}$	150–175	$2{\cdot}67 \times 10^6$	$2{\cdot}85 \times 10^6$
5	8	nylon	$6{\cdot}66 \times 10^{-3}$	150–175	$1{\cdot}67 \times 10^6$	$2{\cdot}28 \times 10^6$

*During vibration in this series no filtration took place, the cake was percolated.

The results given substantiate some of the statements made above.

Discussion

The key to an understanding of many of the results obtained may be the results published earlier [2] and repeated here in a more quantitative manner, on the influence of the initial filtration velocity on the building up of the cake. For the filters used the very first layers of the cake formed over the filter govern the building up of the rest of the cake, of course under the condition that the cake is not very thick and phenomena such as packing compressibility do not occur. The packing of the very first layers of a cake is now governed for a certain filter by the initial filtration velocity. At a high velocity, a cake is built up of a low† density and of a low resistance; at a low initial filtration velocity a cake of higher density and of greater resistance is formed.

For the less dense-packed cakes, as a result of the great flow velocity, large stabilizing forces or pressures must exist. The stabilizing forces are counteracted by the cake pressure, which is maximum near the filter and zero at the top of the cake. The cake pressure tends to increase the density of the packing and therefore the resistance of the cake.

If the balance of forces is disturbed, e.g. by vibration, an increase of density is to be expected, the more so, if the stabilizing forces are small, the frequency is high and the amplitude large.

Let us now, as a limiting example, consider the behaviour of a cake of low density and relatively great stability under flow and vibration. Vibrations of low frequency will not have much effect on such a cake, however increasing the frequency will finally result in a cake consolidation starting near the filter. If during the vibration filtration is continued, the layers on top (which are in their original packing) will determine the structure of the newly formed layers giving these the original top packing density, whilst the consolidated layers near the filter will grow. The effect resembles the retarded packing compressibility as described by Rietema [5].

Therefore a constant, but higher, mean resistance will be found for the vibrated cake. If the vibration is ended, the top layers will still have the corresponding original packing and therefore the same or a smaller cake resistance as that of the original cake will be found on continued filtration for the newly formed cake.

As a second limiting case, the behaviour of a cake formed at low initial filtration velocity of high density and low stability will be considered. At a lower frequency than in the former case, vibrations will affect the cake density, furthermore the layers affected will be thicker. If it is assumed that the whole layer already formed will be affected, the results will be twofold. First of all in the beginning a rapid increase in resistance, which is much larger than in the first case, will occur. Because the driving force will decrease with time, the relative effect will decrease. Therefore the R–V line obtained will be concave to the V axis. In the second place the top layers of the cake, when vibration is continued long enough, will be of a higher packing density than that of the original cake. A cake formed on these layers by normal filtration will therefore have a higher density than the top layers of the original cake. The resulting mean resistance of the cake cannot be higher than when the total cake has been formed under vibration from the very beginning. Therefore the extrapolated R–V line for the last filtration in this limiting case must pass through the point $V = 0$, $R = R_f$. The cases just discussed have been realized, as can be seen from the results presented.

The qualitative explanation of the other phenomena mentioned follows from the above. When a cake is formed directly under vibration, a straight R–V line might be expected, and has been found.

The irregular behaviour of vibrated cakes of high density and resistance, when vibration is stopped, cannot, however, be deduced from the above. It is possible that an explanation lies in the observation that vibration will cause a state of unrest in the cake. It is conceivable that if

†The indication high and low are used here as before in a relative sense. All the cakes considered are far removed from the densest packing possible.

VOL. 10 1959

the vibrations have not yet resulted in a packing stable with respect to conditions of flow, stabilizing forces and vibration, the particles will adjust themselves again to the new conditions of flow. This phenomenon will be more marked with less stable cakes. It may be remarked that an analogous behaviour have been described earlier [4] for cakes consolidated by flow only.

Conclusion

For the type of relation between the cake resistance and the initial filtration velocity an exponential function has been found. The parameters in the equations derived depend on the size of the particles and on the concentration. The same type of correlation has been found for the relation between Δr, the fractional increase of the cake resistance by vibration, and the frequency of the vibration. Here, for one particle size besides depending on the initial filtration velocity and on the concentration, the parameters depend on the amplitude of the vibration.

Vibrations cause an increase of the cake resistance. The increase in general is larger with increasing frequency, amplitude and original resistance. A possible explanation of the behaviour of cakes under vibration, and after vibration, has been given, based on the disturbance of the balance between stabilizing forces and cake pressure and on the phenomenon that the packing of a layer of particles is determined by the packing of the foregoing layers, whereas for the type of filters used the packing of the first layers is determined by the velocity with which these particles reach the filter. On these principles the results obtained could be explained qualitatively.

Notation

a	= maximum relative increase of resistance	
A	= surface of filter	cm^2
b	= parameter	rev/min^{-1}
b_1	= parameter	$cm\ sec^{-1}$
b_2	= parameter	cm^{-1}
c	= concentration	$g\ cm^{-3}$
d	= parameter	no dimension
d_p	= diameter of particle	μ ($= 10^{-4}$ cm)
F	= frequency	rev/min^{-1}
F^1	= impacts pro minute	$impacts/min^{-1}$
ΔP	= pressure difference over filter	$g\ cm^{-1}\ sec^{-2}$
r	= mean specific resistance of a cake of one g per cm^2 filter surface	$cm\ g^{-1}$
r_a	= cake resistance for $R_f = \infty$	$cm\ g^{-1}$
r_F	= cake resistance of a vibrated cake	$cm\ g^{-1}$
Δr	= relative increase of cake resistance	no dimension
R	= resistance of filtercloth plus cake of one cm^2 filter surface	cm^{-1}
R_f	= resistance of filtercloth of one cm^2 filter surface	cm^{-1}
R_k	= resistance of the cake on cm^2 filter surface	cm^{-1}
U_0	= initial filtration velocity	$cm\ sec^{-1}$
V	= volume of filtrate	cm^3
σ	= surface tension	$dyne\ cm^{-1}$
ρ	= density	$g\ cm^{-3}$
η	= viscosity	$g\ cm^{-1}\ sec^{-1}$
θ	= time	sec

References

[1] Heertjes P. M. and van der Haas H. *Rec. Trav. Chim. Pays-Bas.* 1949 **68** 361.

[2] Heertjes P. M. *Chem. Engng. Sci.* 1957 **6** 190.

[3] Heertjes P. M. *Chem. Engng. Sci.* 1957 **6** 269.

[4] Heertjes P. M. and Nijman J. *Chem. Engng. Sci.* 1957 **7** 15.

[5] Rietema K. Thesis Delft, 1952.

Chemical Engineering Science, 1959, Vol. 10, pp. 150 to 156. Pergamon Press Ltd. London. Printed in Great Britain

The flow of granular solids through orifices

R. T. FOWLER and J. R. GLASTONBURY
Chemical Engineering Department, University of Sydney, N.S.W.

(*Received* 20 *March* 1958)

Abstract—The factors affecting the flow of granular solids through orifices of different diameter and shapes under gravity conditions has been investigated at various heads. Different granular materials such as sand, sugar, rape seed, wheat and rice were used and the best equation was found to be :—

$$\frac{W}{\rho_B A\sqrt{(2g\,D_h)}} = 0{\cdot}236\left(\frac{D_h}{\lambda\, d}\right)^{0{\cdot}185}$$

where W is the weight discharged per second, ρ_B the bulk density of the solids, A is the flow area of the orifice of hydraulic diameter $D_h d$ is the average arithmetic screen diameter and λ is the average shape factor of the particles.

The effect of head and container diameter was found to be insignificant in the 347 runs used in the statistical analysis.

The equation allows the prediction of flow rates through various orifices with an over-all accuracy of $\pm$ 10 per cent.

Résumé—Les auteurs ont étudié les facteurs qui affectent l'écoulement de grains solides, par gravité à différentes hauteurs à travers des orifices de formes et de diamètres différents. Divers matériaux granulaires ont été utilisés, tels que sable, sucre, graines de colza, blé et riz et l'équation qui convient le mieux est :

$$\frac{W}{\rho_B A\sqrt{(2g\,D_h)}} = 0{,}236\left(\frac{D_h}{\lambda\, d_{av}}\right)^{0{,}185}$$

dans laquelle W = débit massique par seconde, ρ_B = densité globale des solides, A = l'aire d'écoulement de l'orifice de diamètre hydraulique D_h, d_{av} = le diamètre moyen arithmétique du tamis et λ = le facteur de forme moyen des particules.

L'effet de la hauteur et du diamètre du récipient a été jugé insignifiant au cours des 347 essais d'analyse statistique.

L'équation permet de prévoir les vitesses d'écoulement à travers divers orifices, avec une précision moyenne de $\pm$ 10 per cent.

Zusammenfassung—Die Einflussgrössen auf das Fliessen körniger Feststoffe durch Öffnungen verschiedener Durchmesser und Form unter dem Einfluss der Schwerkraft wurden für veränderte Druckhöhen untersucht. Verwendet wurden verschiedene körnige Stoffe wie Sand, Zucker, Rübsamen, Weizen und Reis. Als beste Gleichung ergab sich folgende :

$$\frac{W}{\rho_B A\sqrt{(2g\,D_h)}} = 0{,}236\left(\frac{D_h}{\lambda\, d_{av}}\right)^{0{,}185}$$

Hierin ist W der Gewichtsstrom, ρ_B die Schüttdichte der Feststoffe, A die durchströmte Fläche der Öffnung mit dem hydraulischen Durchmesser D_h, d_{av} der arithmetische Mittelwert des Siebdurchmessers und λ der mittlere Formfaktor der Teilchen.

Der Einfluss der Druckhöhe und des Behälterdurchmessers ergab sich als unbedeutend in den 347 Versuchen, die der statistischen Auswertung zugrunde lagen.

Die Gleichung erlaubt die Vorausberechnung von Fliessgeschwindigkeiten durch unterschidliche Öffnungen mit einer gesamten Genauigkeit von $\pm$ 10 per cent.

Introduction

There has been very little systematic work published in the literature in the last 50 years upon the flow characteristics of granular solids flowing through orifices from hoppers or bins. Due to the lack of any reliable formula for predicting the flow rate of granular solids the design of bins or hoppers has been to some extent of an empirical nature. It is the purpose of this paper to investigate the flow of granular material through various orifices from vertical-sided hoppers to find the effect of such variables as bulk density, head, orifice diameter and shape, particle diameter and shape and container diameter upon the discharge rate.

In the past most of the early work upon flow of solids has been a by-product of research into pressure distributions in hoppers or bins for design purposes [1, 2, 3]. The first investigation into the flow of solids appeared in 1911 by Ketchum [4]. He used wheat and showed that the flow was independent of the head and varied as the cube of the orifice diameter. Ketchum, using glass-sided bins, showed that the flow of solids was an intermittent flow caused by the rapid formation and collapse of domes or bridges which built up in the mass of the material.

Deming and Mehring [5], in 1929, examined the flow of granular solids from conical bins or containers and proposed an equation of the form:

$$W = \frac{100\, D^{5/2}\, \rho_B}{\mu \left[34{\cdot}6 + (67{\cdot}4 + 444 \sin \tfrac{1}{2}\phi)\right] \left[(d/D) + 0{\cdot}130 - 0{\cdot}161\, \mu\right]} \text{ g/min} \qquad (1)$$

with D and d in mm.

This equation (1) should be valid for flat bottomed containers if the value of $\phi = 180^\circ - 2\theta$ where $\theta = \tan^{-1} \mu$ is used as the conical angle.

Takahashi [6], in 1933, carried out a large number of runs using different materials and published an equation which he claimed to explain the flow of granular solids.

$$V = \frac{k\sqrt{gD}}{f(\mu) + a\,(d/D)} \qquad (2)$$

It will be noted that this equation does not involve a head term. Takahashi does not appear to have claimed any specific accuracy for his equation and also does not show how he derived it.

Newton, Dunham and Simpson [7], in 1945, published some results on the flow of catalyst pellets from a hopper for feed to a fluidized cracking plant. They found for catalyst pellets 0·1–0·2 in. in diameter that the maximum flow rate given by an equation of the form given below:

$$W = 8{\cdot}50\, D^{2{\cdot}96}\, H^{0{\cdot}04} \text{ lb/min} \qquad (3)$$

where H is in ft and D in in.

They found that the equation (3) was only valid if the orifice diameter exceeded six times the pellet diameter, as for smaller orifice sizes the flow tended to become irregular and was liable to stop. They also investigated the flow patterns and showed that for heads less than $1\frac{1}{2}$ times the container diameter that a stationary cone of material remained at the walls subtending an angle approximately twice the angle of repose of the material.

Brown and Hawksley [8], in 1953, made a thorough examination of the mechanism of flow of solids through orifices and showed that there were at least five distinct regions of movement near the orifice and that the upper surface of the solids did not move until a considerable dilation of the packing had occurred. They did not however give any equation to explain the flow.

Rudd [2] and Jenike [3], in 1954, published papers trying to explain the flow of solids on the basis of the pressures set up in a mass of material and while they gave interesting theories their equations prove to be complex and the factors needed difficult to obtain readily.

Franklin and Johnson [9], in 1955, published a paper in which they give a proposed flow equation of the form:

$$W = \frac{\rho_s\, D^{2{\cdot}93}}{(6{\cdot}288\, \mu + 23{\cdot}16)\,(d + 1{\cdot}889) - 44{\cdot}90} \text{ lb/min} \qquad (4)$$

The equation (4) was derived for circular

orifices only under the conditions of particle size 0·03 to 0·20 in., density 7·3 to 676 lb/lb^3 and orifice diameters 0·236 to 2·28 in. and an over-all accuracy of $\pm$ 7 per cent was claimed.

They also suggested that the equation for flow rate could be influenced by the following factors.

(a) Orifice diameter to particle diameter less than 5.

(b) Column diameter to orifice diameter less than 6·3.

(c) Bed height less than one column diameter.

It will be noted that in equations (1), (2) and (4) the factor of coefficient of friction appears, in the case of Takahashi's equation the method of calculation of $f(\mu)$ is obscure and in the case of equations (1) and (4) the determination of the coefficient of kinetic angle of repose is not easy and subject to considerable error. Franklin and Johnson admit that the coefficient of friction seems to be a characterization factor for other physical properties such as particle shape, roughness and effective size and also void fraction of the bed of packed material. Since it has been shown by Fowler and Chodziesner [10] that the coefficient of friction is a function of particle shape, diameter and roughness it was deleted from this investigation in favour of the more fundamental factors. It was considered that the possible factors that can influence the flow of dry granular solids are as follows:

(i) The orifice diameter or the equivalent hydraulic diameter for orifice shapes other than circular
(ii) The container diameter
(iii) The true spherical particle diameter
(iv) The head of material above the orifice
(v) The true density of the material
(vi) The bulk density of the bed which is a combination of (v), and the void fraction of the bed
(vii) The orifice shape

It will be noted that the fundamental factors affecting angle of repose are included in the above list either by themselves or in combination with others.

The application of dimensionless analysis to the above factors yields an equation of the form:

$$\frac{W}{\rho_s D^2 g D} = f\left(\frac{D}{d_s}\right) \cdot \left(\frac{H}{d_s}\right) \cdot \left(\frac{\rho_s}{\rho_B}\right) \cdot S \cdot \left(\frac{D_c}{d_s}\right) \quad (5)$$

which can be written in a more convenient form as

$$\frac{W}{\rho_s A \sqrt{2g D}} = f\left(\frac{D}{d_s}\right) \cdot \left(\frac{H}{d_s}\right) \cdot \left(\frac{\rho_s}{\rho_B}\right) \cdot S \cdot \left(\frac{D_c}{d_s}\right) \quad (6)$$

Equation (6) resembles the basic equations derived by Deming and Mehring in 1929, except that they used time for discharge of a given weight of solid which is a reciprocal of equation (5).

It was decided to investigate the equation (6) by the use of statistical analysis and a series of experiments were carried out involving all the possible factors.

VOL. 10 1959

Experimental Apparatus and Procedure

Three Pyrex glass cylinders 48 in. in length and of inside diameters of 6$\frac{1}{2}$, 4 and 2$\frac{1}{4}$ in. were selected and clamped vertically in a steel framwork. The tubes were marked to indicate heads of 25, 50, 75 and 100 cm from the base plates. The base plate consisted of 18 s.w.g. brass plate and was so constructed that an orifice plate could be slid into slots in the base plate together with a sliding shutter. The orifice plates were made in 18 s.w.g. brass plate in which the appropriate orifices had been cut. The circular orifices were cut to size in a lathe but the other shapes such as triangle, square, ellipse etc. were cut and filed by hand. Due to hand cutting slight deviations from the nominal size were unavoidable but the areas and perimeters were accurately measured by triangulation using a cathetometer. Details of the orifices are given in Table 1.

The materials used in the tests were sand, rape seed, rice, wheat and sugar. The sand was screened into four size fractions, namely $-20 + 30$, $-30 + 40$, $-40 + 50$ and -50 Tyler mesh by the use of a double deck vibrating screen. The true specific densities of the materials were determined by pyknometers. The shape factor for each material was determined by permeability measurements on a Lea and Nurse [11] apparatus and the shape factor calculated from the Kozeny-Carman equation. The angle of repose (static)

Table 1. *Details of orifices used in flow experiments*

No.	*Shape of orifice*	*Nominal area* (cm^2)	*Actual area* (cm^2)	*Perimeter* (cm)	*Hydraulic diameter* (cm)
1	Circle	20	20·157	15·917	5·066
2	Square		20·347	18·043	4·511
3	Rectangle (1 : 1·5)		19·821	18·889	4·197
4	Triangle (45°)		19·878	20·327	3·912
5	Circle	5	5·027	7·948	2·530
6	Square		5·150	9·078	2·269
7	Rectangle (1: 2)		5·095	9·565	2·131
8	Triangle (45°)		5·002	10·196	1·962
9	Hexagon		4·810	8·164	2·357
10	Pentagon		4·968	8·497	2·339
11	Ellipse (2 : 1)		5·143	8·764	2·347
12	(3 : 1)		4·910	9·637	2·038
13	(4 : 1)		5·740	11·592	1·981
14	Rectangle (1 : 1·4)		5·220	9·289	2·248
15	(1 : 3)		4·876	10·193	1·914
16	(1 : 4·1)		4·923	11·176	1·762
17	(1 : 4·7)		4·843	11·582	1·673
18	(1 : 5·1)		4·910	11·994	1·638
19	Circle	2·8	2·829	5·963	1·898
20	Square		3·820	6·718	1·679
21	Rectangle (1 : 1·5)		2·769	7·074	1·566
22	Triangle (45°)		2·694	7·484	1·440
23	Circle	1·2	1·293	4·031	1·283
24	Square		1·288	4·540	1·135
25	Rectangle (1 : 1·5)		1·205	4·666	1·033
26	Triangle (45°)		1·289	5·176	0·996

Table 2. *Details of physical properties of the materials used in the flow experiments*

Material	*True density* ρ_s (g/ml)	*Average screen particle size* d (cm)	*Average shape factor* λ	*True average spherical particle diameter* $= \lambda d = d_s$	*Angle of repose* (°)
Sand					
− 20 + 30	2·647	0·0661	1·38	0·092	32·0
− 30 + 40	2·647	0·0508	1·31	0·0668	32·5
− 40 + 50	2·647	0·0372	1·33	0·0496	32·5
− 50	2·647	0·0272	1·43	0·0406	33·5
Wheat	1·380	0·3298	1·25	0·4128	25·0
Rice	1·434	0·2805	1·12	0·3156	29·0
Rape seed	1·103	0·1924	1·00	0·1924	19·5
Sugar	1·590	0·0712	1·54	0·1095	37·0

for each material was also determined. The details of the particle properties is given in Table 2.

A series of experiments were planned to cover all possible combinations of orifice size and shape, particle size and head and these resulted in a total of 470 experiments.

Experimental Results and Conclusions

Statistical correlation of 347 results to determine the values of the exponents and constant in equation (7)

$$\frac{W}{\rho_s A\sqrt{2g\,D_h}} = a\left(\frac{\rho_s}{\rho_B}\right)^b\left(\frac{D_h}{d_s}\right)^c\left(\frac{D_c}{d_s}\right)^d\left(\frac{H}{d_s}\right)^e \quad (7)$$

revealed that the significance of the terms $\left(\frac{\rho_s}{\rho_B}\right)$, $\left(\frac{H}{d_s}\right)$ and $\left(\frac{D_c}{D_s}\right)$ was very low and consequently could be ignored.

The value of the orifice shape factor (S) could be explained by using the hydraulic diameter of the orifice defined as $D_h = 4 \times$ free area/perimeter. The final equation evolved based on 247 runs was as follows:

$$\frac{W}{\rho_B A\sqrt{2g\,D_h}} = 0{\cdot}236\left(\frac{D_h}{d_s}\right)^{0{\cdot}185} \quad (8)$$

The individual values of the constant in the equation (8) for each orifice shape was further calculated and is given in Table 3.

Table 3. Values of the constant in equation (8) for various orifice shapes

Orifice shape	*No. of runs*	*Constant a*
Circle	90	0·222
Ellipse	13	0·247
Rectangle	38	0·221
Square	90	0·229
Pentagon	13	0·226
Hexagon	13	0·222
Triangle	90	0·270
Total	347	Weighted = 0·236 Average

It is not possible in this paper to give the full set of 470 runs performed but the results for a random sample of runs is given in Table 4 together with the observed and calculated discharge rates.

The over-all accuracy of equation (8) is $\pm$ 10 per cent which is quite good considering the wide range of orifice shapes, diameters and particle sizes used.

The results of Table 4 are depicted graphically in Fig. 1 where the observed velocity $W/\rho_B A$ cm/sec is plotted against the calculated velocity of $0{\cdot}236\sqrt{2g\,D_h}\left(\frac{D_h}{d_s}\right)^{0{\cdot}185}$ cm/sec.

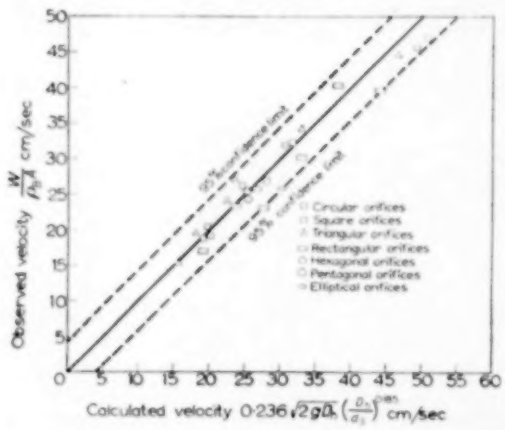

Fig. 1. Graph showing the effect of plotting the observed velocity of flow against the calculated velocity for the results of Table 4.

Further examination of the complete set of 470 results reveals that while equation (8) can be regarded as sufficiently accurate for most design purposes, it is felt that more complex expressions involving a parameter expressing orifice shape would probably reduce the error to even smaller limits. However, the accuracy of determination of such parameters as particle shape factor, bulk density, angle of repose, etc. is of the order of $\pm$ 10 per cent and the incorporation of these factors in any equation will limit the over-all accuracy.

It will be noted that in Table 4 that several results are marked with an asterisk. These results were carried out at a low ratio of orifice hydraulic diameter to mean spherical particle diameter

VOL. 10 1959

Table 4. Random set of results used as a basis for equation (7)

Run No.	*Orifice shape and number*	D_h (cm)	*Material*	d_s (cm)	H (cm)	ρ_B (lb/ft^3)	W_{obs} (lb/sec)	W_{calc} (lb/sec)
2	Circle 1	5·066	Sand	0·0918	50	91·6	2·94	3·22
14	,, 5	2·530	,,	,,	50	,,	0·52	0·50
28	,, 19	1·898	,,	,,	100	88·9	0·24	0·22
39	,, 23	1·283	,,	,,	75	90·6	0·079	0·080
97	,, 1	5·066	,,	0·0496	25	88·5	2·82	3·49
103	Square 2	4·511	,,	,,	75	,,	3·00	3·32
105	Triangle 4	3·912	,,	,,	25	,,	2·82	2·88
116	Square 6	2·269	,,	,,	100	,,	0·52	0·51
132	Triangle 22	1·440	,,	,,	100	,,	0·23	0·20
137	Square 24	1·135	,,	,,	25	,,	0·083	0·080
144	Triangle 26	0·996	,,	,,	100	,,	0·079	0·073
197	Rectangle 3	4·197	Rape	0·1924	100	44·3	1·25	1·18
205	Rectangle 7	2·131	,,	,,	50	,,	0·185	0·189
207	Triangle 8	1·962	,,	,,	50	,,	0·188	0·176
209	Hexagon 9	2·357	,,	,,	50	,,	0·184	0·192
211	Pentagon 10	2·339	,,	,,	50	,,	0·197	0·197
216	Square 20	1·679	,,	,,	100	,,	0·085	0·089
217	Rectangle 21	1·566	,,	,,	50	,,	0·074	0·084
233	Rectangle 3	4·197	Wheat	0·4128	50	53·6	1·13	1·14
*237	Circle 5	2·530	,,	,,	50	,,	0·163	0·220
*246	Hexagon 9	2·357	,,	,,	100	,,	0·146	0·202
*248	Pentagon 10	2·339	,,	,,	100	,,	0·154	0·205
251	Square 2	4·511	Sugar	0·1095	50	56·7	1·61	1·80
261	Rectangle 7	2·131	,,	,,	50	,,	0·264	0·269
267	Pentagon 10	2·339	,,	,,	50	,,	0·270	0·280
284	Triangle 26	0·996	,,	,,	100	,,	0·040	0·040
292	Triangle 4	3·912	Rice	0·3156	100	55·1	1·33	1·27
*293	Circle 5	2·530	,,	,,	50	,,	0·207	0·254
424	Rectangle 16	1·762	Sand	0·0406	100	94·3	0·377	0·394
433	Ellipse 13	1·981	,,	,,	100	,,	0·492	0·500

*These runs were performed at a low $\left(\frac{D_h}{d_s}\right)$ ratio approaching 6 : 1 and the flow consequently tended to be unstable.

approaching 6 : 1. As found by previous workers at this value and lower, the flow of granules tends to become irregular and sporadic and consequently such results have a high error in prediction by equation (8). The influence of head upon the flow rate has been found to be insignificant in the analysis of equation (7) which confirms previous work except for NEWTON, DUNHAM and SIMPSON [8]. However, a very slight effect on the flow rate is noticable at increasing heads but it is debatable as to whether this is due to an increase in bulk density due to packing of the particles or to a head effect in itself.

It was noticed in the results at constant head, orifice diameter and shape, that the effect of reducing the particle diameter for a particular material such as sand was an increase in the flow rate to a maximum at a particle size of 65 mesh Tyler approximately and then a decrease with particle size. This effect was quite marked for finer sizes than 65 mesh as the material lost its "flowability" and tended to flow in lumps or aggregates with sudden jerks. Bridging and scaffolding of the orifice became very noticable and with — 100 mesh sand the material in the 6 in. diameter tube arched even with a 4 in. diameter circular orifice and would only flow when poked. It is apparent therefore for steady flow conditions that the

particle size has a limiting value for each material used.

The value of the term (ρ_s/ρ_B) in equation (7) proved to be insignificant probably due to the small variation of this ratio in the experiments. In most cases of packed beds of materials at random the bed porosity lies between 30 per cent and 50 per cent and the ratio of (ρ_s/ρ_B) is 1·30 to 1·50. In the experiments carried out the value lay between these two extremes and deliberate packing of the columns did not give much variation in this ratio. It was considered however that the incorporation of the bulk density term was desirable instead of using the true density as it is noticable that any variation of bulk density does affect the flow rate. Consequently the value of ρ_B was substituted for ρ_s in equation (8).

The effect of container diameter D_c proved to be insignificant upon the flow rate in the experiments performed. Generally in practice the limiting value of $D_c = d_s$ is never realized and is clearly fantastic. In the experiments the minimum value of (D_c/d_s) was 14·1 with the $2\frac{1}{4}$ in. tube and wheat but no change in the flow rate was detected even when the maximum value of 37·1 was used.

Acknowledgements—The authors are indebted to the Workshop Staff of the Chemical Engineering Department for the fabrication of the apparatus and the various orifices used and one of the authors (J.R.G.) is indebted to the Vacuum Oil Company for an award of a scholarship for the carrying out of this work.

Notation

A = free flow area of orifice
D = diameter of circular orifice
D_h = hydraulic or perimetral diameter $= 4 \times A$/perimeter of orifice
D_c = container diameter
d = average screen size of particles
d_s = spherical diameter of particles
$f(\mu)$ = a function involving the coefficient of kinetic angle of friction θ where $\mu = \tan\theta$
g = gravitational constant
H = head of packing above orifice
λ = shape factor of particles $d_s = \lambda d$
ρ_s = true density of solid
ρ_B = bulk density of packing
S = orifice shape function
V = velocity of discharge from orifice
ϕ = subtended angle of conical portion of container
W = weight discharged/unit time
a, b, c, d, e, k = constants

References

[1] Janssen H. A. *Z. Ver. Dtsch. Ing.* 1895 **39** 1045.
[2] Rudd J. K. *Sugar* 1954 **49** 38.
[3] Jenike A. W. *Chem. Engng.* 1954 **61** 175.
[4] Ketchum M. S. *Walls, Bins and Grain Elevators.* McGraw-Hill, New York 1911.
[5] Deming W. E. and Mehring A. L. *Industr. Engng. Chem.* 1929 **21** 661.
[6] Takahashi H. *Bull. Inst. Phys. Chem. Res., Tokyo* 1933 **12** 984.
[7] Newton R. H., Dunham G. S. and Simpson T. P. *Trans. Amer. Inst. Chem. Engng* 1945 **41** 218.
[8] Brown R. L. and Hawksley P. G. W. *Fuel* 1947 **26** 159.
[9] Franklin F. C. and Johanson L. N. *Chem. Engng. Sci.* 1955 **4** 119.
[10] Fowler R. T. and Chodziesner W. B. Unpublished Report. Chem. Eng. Dept. University of Sydney 1956.
[11] Lea F. C. and Nurse R. W. *Symposium on Particle Size Analysis.* Inst. Chem. Engrs. Lond. 1947.

Chemical Engineering Science, 1959, Vol. 10, pp. 157 to 162. Pergamon Press Ltd. London. Printed in Great Britain.

The influence of variables upon the angle of friction of granular materials

R. T. Fowler and W. B. Chodziesner

Chemical Engineering Department, University of Sydney, N.S.W.

(*Received* 20 *March* 1958)

Abstract—Experiments have been carried out to determine the variables affecting the angle of friction of dry granular materials. It has been found that the angle of friction (θ) of solids sliding on surfaces depends on the shape factor (f_s), specific gravity (s_1), and diameter (D) of the sliding material and on the roughness (ϵ) of the surface. A dimensionless equation has been developed statistically and is of the form

$$\mu = \tan\theta = \frac{a}{f_s^2} + b\left(\frac{\epsilon}{D}\right)^{0.5} + c \cdot s_1 + d$$

where a, b, c and d are constants and have values $a = 0{\cdot}2110$, $b = 0{\cdot}3436$, $c = -0{\cdot}0171$ and $d = 0{\cdot}1834$. The equation is useful in predicting the sliding angle of dry materials within the ranges $f_s = 0{\cdot}67$ to $1{\cdot}00$, $s_1 = 1{\cdot}103$ to $11{\cdot}340$, $D = 0{\cdot}0272$ cm to $0{\cdot}4026$ cm and $\epsilon = 0{\cdot}0272$ cm to $0{\cdot}3134$ cm. The equation developed explains the trends observed by other investigators and may be of use in estimating the angle of slope of chutes, slides, etc., and also the angle of repose of beds of granules.

Résumé—Les auteurs ont fait des expériences afin de déterminer les variables qui affectent l'angle de friction de matériaux granulaires secs. Ils ont trouvé que l'angle de friction (θ) de solides glissant sur des surfaces, dépend du facteur de forme (f_s), du poids spécifique (s_1) et du diamètre (D) du matériau glissant, et de la rugosité (ϵ) de la surface. Une équation sans dimension a été développée statistiquement ; elle est de la forme :

$$\mu = \tan\theta = \frac{a}{f_s^2} + b\left(\frac{\epsilon}{D}\right)^{0,5} + c \cdot s_1 + d$$

où a, b, c et d sont constants et ont pour valeurs :

$$a = 0{,}2110\,; \quad b = 0{,}3436\,; \quad c = -0{,}0171 \quad \text{et} \quad d = 0{,}1834$$

L'équation est utile pour prévoir l'angle de glissement de matériaux sec dans les intervalles $f_s = 0{,}67$ à $1{,}00$, $s_1 = 1{,}103$ à $11{,}340$, $D = 0{,}0272$ cm à $0{,}4026$ cm et $\epsilon = 0{,}0272$ cm à $0{,}3134$ cm. L'equation développér explique les tendances observées par d'autres chercheurs, et peut être utilisée pour estimer la pente de chutes, de glissoirs, etc. et aussi l'angle d'arrêt de lits de matériaux granulés.

Zusammenfassung—Zur Ermittlung der Einflussgrössen auf den Reibungswinkel von trockenen, körnigen Stoffen wurden Versuche angestellt. Danach hing der Reibungswinkel (θ) der auf Flächen gleitenden Feststoffen ab vom Formfaktor (f_s), der relativen Dichte (s_1), dem Durchmesser (D) des gleitenden Materials und der Oberflächenrauhigkeit (ϵ). Eine dimensionslose Gleichung wurde auf statistischem Wege abgeleitet, die folgende Form hatte :

$$\mu = \tan\theta = \frac{a}{f_s^2} + b\left(\frac{\epsilon}{D}\right)^{0,5} + c \cdot s_1 + d$$

Hierin bedeuten a, b, c und d Konstanten mit den Werten $a = 0{,}2110$, $b = 0{,}3436$, $c = -0{,}0171$ und $d = 0{,}1834$. Die Gleichung erlaubt es, Reibungswinkel trockener Stoffe in folgenden Bereichen zu berechnen : $f_s = 0{,}67$ bis $1{,}00$, $s_1 = 1{,}103$ bis $11{,}340$, $D = 0{,}0272$ cm bis $0{,}4026$ cm und $\epsilon = 0{,}0272$ cm bis $0{,}3134$ cm. Die entwickelte Gleichung gibt die Ergebnisse anderer Beobachter richtig wieder und kann zur Berechnung der Neigung von Rutschen, Gleitbahnen usw. sowie des Schüttwinkels von Haufwerken dienen.

Introduction

The angle of friction of dry granular materials sliding down chutes, slides, etc., has often been measured and reported in the literature, but careful perusal of papers reveals no serious attempt to investigate the factors that affect the angle of friction. The term "angle of repose" is synonymous with "angle of friction," but in most engineering applications it is used only to designate the maximum slope taken up by heaps or beds of materials before sliding occurs [1].

At the beginning of this century a great deal of research was carried out into the effect of earth pressure on the angle of repose of soils by Wilson [2], Crossthwaite [3], Bell [4], Darwin [5] and Cain [6]. The main purpose of this work was to investigate the earlier theories of Rankine [7, 8, 9, 10]. Rankine does not appear to have measured angles of friction himself, as the figures he quotes are taken from a previous investigation by General Morin who was interested in trench embankments, etc., for military purposes. It appears, therefore, that the figures for angle of friction have been handed down by text books for at least a century without a check being applied. The table of angles of friction appearing in the *Handbook of Physics and Chemistry* [11] of 1953 is compiled from the data of Rankine in 1858, who obtained the figures from other earlier investigators.

Recent work on the angle of friction of sliding metal blocks has been carried out by Burwell and Rabinowicz [12], Parker and Hatch [13] and Bikerman [14, 15, 16], who have put forward theories based on Amonton's Law. In 1954 Richter [17] measured the static coefficient of friction for chopped grass, corn silage, hay and straw sliding on galvanized steel in order to obtain data for the design of chutes. His method of measurement was a variation of the original experiment of Coulomb for measuring the vertical and tangential forces applied to a frame containing the material. Holbrook and Fraser [18] obtained some interesting results on angle of friction while investigating the sizing of coal by screening. They found that the angle of friction for coal sliding on bright polished steel was less for round particles than for flat or wedge-shaped particles. They observed that for larger sizes of coal the angle of friction was less than for small sizes, and the angle increased rapidly as the size decreased and the specific surface increased.

The object of this investigation is to find the effect of particle and surface properties on the coefficient of friction. The properties considered are: shape factor, specific gravity and average diameter of the granular material, and roughness and specific gravity of the surface on which the granules slide. It was expected that an empirical dimensionless relationship of the form

$$\mu = \tan\theta = \phi\left[f_s \cdot \frac{\epsilon}{D} \cdot s_1 \cdot s_2\right] \qquad (1)$$

would be obtained.

Experimental Procedure and Results

A wooden chute was constructed of dimensions 18 in. × 6 in. × 6 in. pivoted at one end and raised at the other by a fine-threaded screw so that angles from the horizontal between 0° and 45° were obtainable. The angles of inclination were measured by means of a plumb-bob and graduated scale reading in half degrees but allowing estimation to the nearest quarter of a degree. The floor of the chute was interchangeable, so that surfaces of different roughness and specific gravity could be used.

Surfaces were made up by coating a base board with glue and sprinkling different materials over the glue so that, on drying, a surface of a suitable degree of roughness was obtained.

Different granular materials were used, the relevant physical properties being determined beforehand. The average shape factor of the particles was determined by permeability methods using a modified Lea and Nurse [19] apparatus, and by applying Carman's [20] equation. The materials used and their physical properties are shown in Table 1.

The roughness of the constructed surfaces was considered to be the average depth of the interstices between the particles making up the surface. This is analogous to the roughness measurement in pipes for friction loss determinations where the average depth of the pits and irregularities

VOL. 10 1959

Table 1. *Physical properties of granular materials*

Material	*Specific gravity at* 25°C s ($H_2O = 1$)	*Shape factor* f_s	*Average diameter* D (cm)
Lead shot	11·340	1·00	0·4026
Wheat	1·380	0·89	0·3134
Rice	1·434	0·82	0·2517
Rape seed	1·103	1·00	0·1924
Sugar	1·590	0·76	0·0592
Sand A	2·647	0·75	0·0981
Sand B	2·647	0·72	0·0661
Sand C	2·647	0·76	0·0508
Sand D	2·647	0·75	0·0372
Sand E	2·647	0·67	0·0272

in the surface are taken as a measure of roughness. The roughness index (ϵ) for the surfaces is therefore proportional to the average diameter of the particles making up the surface. Ten surfaces were prepared of differing roughness and specific gravity.

Each of the materials of Table 1 were tested on the prepared surfaces in an experiment of 100 runs suitably randomized to prevent bias due to wear of the surfaces and experimental error from affecting the statistical analysis.

The angle of friction was measured as the angle at which at least 50 per cent of a bed of granular materials slide freely down a prepared surface. It was found that the bed should be as thin as possible so that the maximum influence of the roughness of the surface could be exerted. If a thick bed was used it was found that the angle measured was an angle compounded of the angle of repose of the material and the sliding angle. The criterion that at least 50 per cent of the bed must be discharged at the sliding angle was adopted as it was found that some material was discharged at angles greater and less than the true angle, due to outside influences over which there was no control, e.g. accidental vibration due to the method of raising the chute.

The results obtained for angle of friction are tabulated in Table 2. Preliminary observation of the results in Table 2 indicated some relation between angle of friction and roughness of surface for each material tested, also for a given roughness of surface the angle of friction tended to increase as the particle size decreased.

It was considered that a relationship of the form

$$\mu = \tan\theta = \frac{a}{(f_s)^x} + b\left(\frac{\epsilon}{D}\right)^y + c \cdot s_1 + d \cdot s_2 + e \qquad (2)$$

Table 2. *Experimental results for sliding angle for different materials and surfaces*

Sliding surface	*Roughness* (cm)	*Sliding materials*									
		Lead shot	*Wheat*	*Rice*	*Rape*	*Sugar*	*Sand* A	*Sand* B	*Sand* C	*Sand* D	*Sand* E
Wheat	0·3134	32·0	38·5	41·5	35·0	40·0	41·5	42·0	41·5	41·0	39·0
Rice	0·2517	32·5	37·5	41·5	34·5	49·0	39·5	40·0	39·0	38·0	38·0
Rape seed	0·1924	25·0	34·0	39·5	33·0	41·0	39·5	39·5	39·0	37·5	37·5
Sugar	0·0592	25·0	39·0	39·0	34·5	40·0	39·5	40·0	39·0	38·0	38·0
Sand A	0·0981	17·5	31·5	37·0	32·5	42·0	39·0	39·0	39·0	37·5	38·5
,, B	0·0661	14·0	28·5	33·0	26·0	40·5	39·5	39·5	39·0	37·0	37·0
,, C	0·0508	15·5	28·5	34·0	25·5	40·0	38·0	39·0	39·5	37·5	37·5
,, D	0·0372	11·5	28·0	32·0	23·0	39·5	38·0	38·5	38·0	37·5	39·0
,, E	0·0272	11·5	25·5	31·0	19·5	39·0	37·0	38·5	37·0	37·5	39·0
Smooth plastic	0(approx.)	10·0	22·0	23·0	16·0	30·0	29·0	32·5	32·0	34·0	32·5

Note—Excessive humidity may cause sticking of the materials and consequent alteration of angle of friction. The materials were dried and the experiments were carried out with average atmospheric conditions of 70-75°F and relative humidity of 50-60 per cent. Due to the influence of the relative humidity, the effects of electrostatic attraction were considered to be negligible.

would explain the variations where x and y are exponents and so the data was analysed and the values of the exponents determined. Initial tests showed that the influence of the specific gravity of the surface was negligible. The statistical regression analysis was continued and the final equation derived was of the form

$$\mu = \tan\theta = \frac{0{\cdot}2110}{f_s^2} + 0{\cdot}3436\left(\frac{\epsilon}{D}\right)^{0{\cdot}5} - 0{\cdot}0171\, s_1 + 0{\cdot}1834 \qquad (3)$$

The equation was found to have a correlation coefficient of 0·92 with a standard deviation of 0·0836.

The value of ϵ/D was assumed to have a maximum value of unity as any increase above unity means that the particles of the flowing material are smaller than the interstices. When this occurs the flowing material will fill the interstices and alter the surface so that the material flowing is sliding over a surface of the same characteristics,

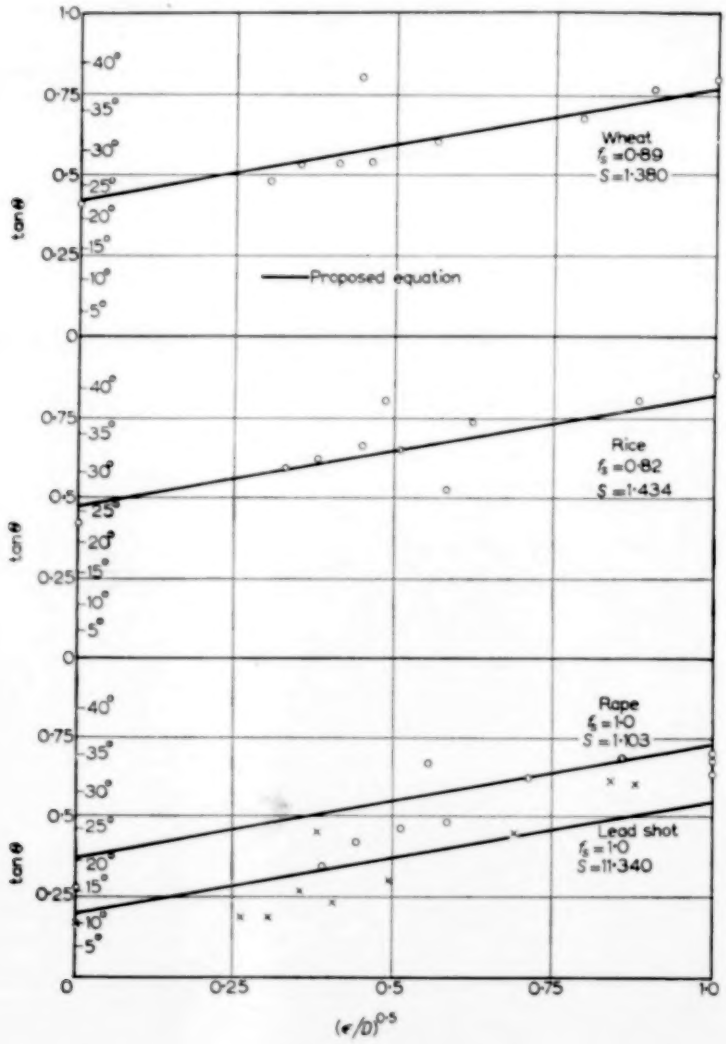

Fig. 1.

Fig. 2.

Fig. 3.

Figs. 1, 2 and 3. A plot of $\tan\theta$ against $\left(\frac{\epsilon}{D}\right)^{0·5}$ for wheat rice, rape seed and lead shot.

and the angle of friction is equal to the angle of repose of the material.

Discussion and Conclusions

Analysis of the results indicates that the correlation is highly significant and that the angle of friction of the materials considered depends on the shape factor, specific gravity and average diameter of the flowing particles, and on the roughness of the surface upon which the particles are sliding.

The value of ϵ may be considered as a relative roughness term and can have values between 0 and 1. Values of zero are to be expected if the surfaces are smooth, as in polished steel, etc., and values of unity are to be expected when the material flows over a surface composed of materials identical to itself, i.e. that the angle of friction is equal to the angle of repose.

The results for wheat, rice, rape seed and lead shot are plotted against $(\epsilon/D)^{0.5}$ and are shown in Fig. 1, 2, and 3. The values for wheat and rice fall close to the curve as given by equation (3), but the values for rape seed and lead shot are lower than predicted due to the probability of rolling of the particles rather than sliding.

The equation predicts variations of sliding angle in accordance with variations as stated by other investigators in the following manner.

(1) Materials of the same average diameter and specific gravity sliding down a surface of known roughness will have a higher angle of friction as the particle shape factor decreases from unity, i.e. irregular shaped particles slide less freely than spherical particles of the same average diameter.

(2) Materials of the same shape factor and average diameter sliding down a surface of known roughness have angles of friction that decrease as the specific gravity increases, i.e. heavier particles slide easier than lighter particles of the same average diameter.

(3) Materials of same shape factor, average diameter and specific gravity sliding down a surface of known roughness have angles of friction that increase as the roughness of the surface increases, i.e. the rougher the surface, the greater the angle for sliding until the relative roughness equals unity and the material then slides over itself.

(4) Angles of friction of sliding materials are independent of the composition of the surface, except for its physical state. It is not possible to compare the results obtained in this investigation with the results of other investigators due to the dearth of information on how the results were obtained. Rankine (7) publishes angles of friction for sand without specifying either its properties or method of measurement.

The equation derived in this experiment indicates the influence of the variables only, and it is not expected that equation (3) will be applicable to prediction of angles of friction for cases other than materials with the property ranges quoted or by other methods of measurement of the angle of friction. It must also be noted that the experiments were carried out using dry materials and that the presence of water can appreciably affect the angle of friction.

Alternative methods of measuring the angle of friction of materials are being considered and tested and it is hoped that, with the new data obtained, equation (2) can be rechecked.

Notation

D = average particle diameter of granules

ϵ = roughness index of surface

f_s = average shape factor of granules

$\mu = \tan\theta$ = coefficient of friction where θ = angle of friction

s_1 = specific gravity of granules [relative to $H_2O = 1$]

s_2 = specific gravity of surface [relative to $H_2O = 1$]

References

[1] Brown G. G. (Editor) *Unit Operations* Wiley, New York 1950

[2] Wilson G. *Proc. Inst. Civil Engrs.* 1902 **149** 210.

[3] Crossthwaite P. M. *Proc. Inst. Civil Engrs.* 1916 **203** 124.

[4] Bell A. L. *Archit. Contract Reporter* 1915 March 262.

[5] Darwin G. H. *Proc. Inst. Civil Engrs.* 1883 **71** 350.

[6] Cain W. *Trans. Amer. Soc. Civil Engrs.* 1911 **72** 403.

[7] Rankine W. J. M. *Applied Mechanics* (4th Ed.) Griffin, London 1868.

[8] Rankine W. J. M. *Manual of Civil Engineering.* Griffin, London 1862.

[9] Rankine W. J. M. *Miscellaneous Scientific Papers.* Griffin, London 1881.

[10] Rankine W. J. M. *Rules and Tables.* (2nd Ed.) Griffin, London 1867.

[11] *Handbook of Physics and Chemistry* (39th Ed.) p. 2014. Chemical Rubber Publishing Co., Cleveland, Ohio 1957-58.

[12] Burwell J. T. and Rabinowicz E. *J. Appl. Phys.* 1953 **24** 136.

[13] Parker R. C. and Hatch D. *Proc. Phys. Soc.* 1950 **63** 185.

[14] Bikerman J. *J. Appl. Phys.* 1949 **20** 971.

[15] Bikerman J. *Rev. Mod. Phys.* 1944 **16** 53.

[16] Bikerman J. *Lubric. Engng.* 1948 **4** 208.

[17] Richter D. W. *Agric. Engr.* 1954 **35** 411.

[18] *Bull. U.S. Bureau Mines* 1925 234.

[19] Lea F. M. and Nurse R. W. Particle size analysis symposium. *Trans. Inst. Chem. Engrs.* (Suppl.) 1947 **25** 47.

[20] Carman P. C. *Trans. Inst. Chem. Engrs.* 1937 **15** 150.

Chemical Engineering Science, 1959, Vol. 10 pp. 163 to 170. Pergamon Press Ltd. London Printed in Great Britain.

The influence of various factors upon the effectiveness of separation of a finely divided solid by a vibrating screen

R. T. Fowler and S. C. Lim

Chemical Engineering Department, University of Sydney, N.S.W.

(*Recieved* 20 *March* 1958)

Abstract—The effect of feed rate, frequency of vibration, angle of inclination and screen aperture on the effectiveness of a single deck vibrating screen was investigated by a statistically planned experiment of 256 runs using clean sand.

It was found that in order to get a high effectiveness it was necessary to select proper combinations of feed rate and screen aperture as main variables and to control angle of inclination and frequency of vibration as the main interaction, but it has been shown that certain combinations of these factors are more important than others. It has been found that all things being constant the effectiveness of separation increases with :

(a) an increase in screen aperture
(b) an increase in angle of inclination up to maximum of about 15° and then progressive decrease in effectiveness with higher angles
(c) a decrease in the feed
(d) an increase in frequency of vibration to a certain maximum and then a decrease in effectiveness with higher frequencies.

The influence of these factors upon the attrition of the sand particles showed that for sand the amount of " fines " produced is negligible, indicating no change in the size of the product.

Résumé—Les auteurs ont étudié les différents effets de la vitesse d'alimentation, la fréquence de vibration, l'angle d'inclinaison et le nombre de mailles du tamis, sur l'efficacité d'un simple tamis vibrant, par une expérience de 256 essais avec du sable propre. Ils ont montré que, pour avoir un bon rendement il faut ajuster la vitesse d'alimentation au nombre de mailles du tamis comme principales variables et l'angle d'inclinaison à la fréquence de vibration, dont l'interaction est importante. Certaines combinaisons de ces facteurs sont plus importantes que d'autres. Les auteurs ont montré que tous les paramètres étant constants l'efficacité de la séparation croît avec :

(a) une augmentation de l'ouverture du tamis.
(b) une augmentation de l'angle d'inclinaison jusqu'à un maximum d'environ 15°, après quoi le rendement décroît pour des angles plus grands.
(c) une alimentation plus faible.
(d) une augmentation de la fréquence de vibration jusqu'à un maximum, car ensuite la séparation décroît avec des fréquences plus élevées.

L'influence de ces facteurs sur l'usure des particules de sable a montré que la quantité de " fines " produites est négligeable ce qui prouve qu'il n'y a pas de variation de dimension du produit.

Zusammenfassung—Der Einfluss der Aufgabemenge, Schwingungsfrequenz, Neigungswinkel und Maschenweite auf die Wirkung eines einfachen Schwingungssiebes wurde durch einen statistisch geplanten Versuch von 256 Messungen an reinem Sand untersucht.

Um einen hohen Wirkungsgrad zu erzielen, musste man geeignete Kombinationen von Aufgabemenge und Maschenweite als Hauptvariable auswählen und Neigungswinkel und Schwingungsfrequenz als wichtigste Einflussgrössen regeln, aber es wurde gefunden, dass bestimmte Kombinationen dieser Kaktoren wichtiger waren als andere. Leiss man alles übrige konstant, so stieg die Trennwirkung an mit :

(a) steigender Maschenweite,
(b) steigendem Neigungswinkel bis zu einem Maximum von 15°, um bei höheren Winkeln progressiv abzufallen,
(c) fallender Aufgabemenge
(d) steigender Schwingungsfrequenz bis zu einem Maximum, um bei höheren Frequenzen wieder abzufallen.

Der Einfluss dieser Grössen auf den Abrieb der Sandteilchen zeigte, dass für Sand die Erzeugung feinster Teilchen vernachlässigbar blieb, dass also die Korngrösse des Produkts nicht verändert wurde.

Introduction

Screening is one of the most commonly used methods for separation of finely divided solids in industry. Among the various types of screens used, the vibrating screen is the most important having made great progress since 1920 after successful manufacture of the constructional materials to withstand the vibration stresses set up in its operation (1).

The effectiveness of separation of solid particles by a vibrating screen can be affected by many different variables, and it is due to the large number of these variables that progress so far has been restricted in defining optimum operating conditions for these screens. The variables that can affect the effectiveness of separation are as follows, as proposed by many different workers [1, 2, 3, 4, 5, 6, 7, 8 and 11].

(1) *Variables due to the material being screened*
- (a) Bulk specific gravity of feed.
- (b) Particle shape.
- (c) Percentage of near size (0·7–1·5 times the screen aperture) material in the feed.
- (d) Moisture content of the feed.
- (e) Static charge generation.
- (f) "Stickiness" of the material.
- (g) Abrasion resistance to attrition.

(2) *Mechanical variables due to the type of screen used*
- (a) Length and width of screen.
- (b) Amplitude of vibration.
- (c) Frequency of vibration.
- (d) Angle of inclination of screen.
- (e) Direction of vibration.
- (f) Capacity of the screen, i.e. feed rate.

(3) *Variables due to the screen cloth*
- (a) Mesh aperture.
- (b) Free area available in cloth.
- (c) Type of screen, i.e. square, circular, rectangular aperture, etc.
- (d) Feed rate to prevent "blinding."
- (e) Material of construction, i.e. copper, steel etc. to withstand distortion of mesh with time.
- (f) Uniformity of mesh size over area of screen.

It is due to this large number of variables that for 30 years workers have been prevented from evolving a general relationship that would allow the prediction of effectiveness of a screen. However, some general rules have been proposed by several workers and these may be summarized as follows:

- (a) A wet, sticky material should be dried as much as possible before dry screening, although under certain circumstances excess water can be used in wet screening.
- (b) The frequency and amplitude of vibration depends on the median size of the particles in the feed and there are optimum values that give the maximum effectiveness of screening [5] [9], but these factors work in opposition.
- (c) The angle of inclination of a screen should be such that "blinding" is prevented with too low an angle, but time of residence shall be as long as possible before discharge [5].
- (d) The direction of vibration of the screen should be counter-flow to the

VOL. 10 1959

material flowing down the screen in order to get maximum agitation and residence time (5).

(e) The screen length has an optimum value of about 2–2½ times its width. Square-aperture screen cloths have a greater free area than screen cloths with circular apertures (1).

(f) The capacity of a screen, defined as lb of feed/ft² of screen area/hr/mm screen aperture, should be kept constant for any particular screen to prevent "blinding" and loss of effectiveness.

It is the intention of this paper to present results of effectiveness of screening of dry sand on altering the four variables of feed rate, angle of inclination, frequency of vibration and screen aperture and to estimate the amount of attrition that may be produced as the sand passes through the screener.

Experimental Appartus

The vibrating screen used in the experiments was a single deck Denver-Dillon screen vibrated by an off-balance flywheel. The speed of vibration could be varied by the use of various diameter pulley wheels driven from ½ h.p. electric motor. The off-balance flywheel gave a fixed amplitude at all speeds. The angle of inclination of the screen could be varied from 0° to 20°. The screen over-all size was fixed at 10 in. width and 24 in. length giving an effective screening area of 1·76 ft². The feed rate to the screen was controlled by varying the orifice diameter of a bottom discharge conical hopper which had been previously calibrated. Screens of various apertures were selected made of copper woven mesh giving square openings.

Clean, dry river sand was used in the tests of a size distribution covering the range of screen apertures selected so that measurable amounts of oversize and product could be obtained.

Experimental Procedure

Clean river sand in 5 ton lots was obtained and air dried. A screen analysis on this sand showed that reasonable proportions of oversize and undersize could be obtained if screens of aperture 30, 40, 50 and 60 mesh were used in the experiments. The speed of vibration was fixed at 952, 1130, 1326 and 1498 rev/min by the use of various diameter pulleys on the driving motor. The machine had a fixed amplitude of 7/64 in. at all speeds. The angle of inclination of the screens were fixed at 6°, 11°, 15° and 19° while the feed rate to the screens could be controlled at 5·5, 7·25, 10·0 and 15·45 lb/min.

A statistically planned experiment of $4 \times 4 \times 4 \times 4 = 256$ runs was developed in which the four levels of each of the four factors were split arbitrarily into pseudo-factors giving 2^8 full factorial design. This design was split into 4 blocks of 64 runs with the block differences compounded with the third order interaction. This ensured that any differences in sand quality being used for the individual blocks did not cause a bias to the results. The runs in each block were suitably "randomized."

The values of the factors and levels used are given in Table 1.

Table 1. *Table of levels and factors used in the statistical design*

Level	*Factors*					
	Feed rate A		*Speed of vibration B*	*Angle of inclination C*	*Screen aperture D*	
	(lb/min)	(g/sec)	(rev/min)	(°)	*Mesh No.*	*Aperture* (μ)
00	5·5	41·5	952	6	60	276
01	7·25	54·8	1130	11	50	318
10	10·0	83·9	1326	15	40	447
11	15·45	116·7	1489	19	30	596

Table 2. Analysis of variance for effectiveness

Nature of effect	*Source*	*Sum of squares*	*D.F.*	*Variance estimate*	*Variance ratio*	
Main factors	*A*	4640·749	3	1546·916	*A/AD*	6·419*
	B	1048·889	3	349·630	*B/BC*	0·265
	C	3267·429	3	1089·143	*C/BC*	0·825
	D	22,240·029	3	7413·343	*D/AD*	30·763†
Interaction between pairs of factors	*AB*	723·441	9	80·382	*AB/ABC*	0·943
	AC	460·601	9	51·178	*AC/ABCD*	0·601
	AD	2168·821	9	240·980	*AD/ABCD*	5·766†
	BC	11,887·591	9	1320·843	*BC/BCD*	14·053†
	BD	169·451	9	18·828	*BD/BCD*	0·200
	CD	593·951	9	65·995	*CD/BCD*	0·702
Interaction between triplets of factors	*ABC*	2300·359	27	85·198	*ABC/ABCD*	2·039†
	ABD	596·003	27	22·074	*ABD/ABCD*	0·528
	BCD	2537·772	27	93·992	*BCD/ABCD*	2·249†
	CDA	1296·089	27	48·003	*CDA/ABCD*	1·149
Residual	*ABCD*	3385·173	81	41·792		
Total		57316·348	255			

* significance level of 1 in 20 † significance level of 1 in 1000

Standard error of estimate of effectiveness $= \sqrt{\left(\frac{41{\cdot}792}{256}\right)} = 0{\cdot}4$ per cent.

The screener was set to the particular conditions required and sand allowed to flow onto the screen until steady conditions were obtained. When this occured two samples of both oversize and undersize were collected in 10 sec and weighed. The samples were reduced in size and then test screened on Tyler standard screens in a vibrating shaker. The size distribution was then obtained for each sample. Since the aperture of the screens in the machine differed slightly from the corresponding test sieve the actual mass in the undersize was interpolated from the assumption that the cumulative mass fraction retained on the test screens of apertures above and below the actual screen was a linear relationship. This assumption was tested and found to be a good approximation and obviated the necessity of graphically representing the cumulative mass

VOL. 10 1959

fraction retained against aperture for every sample taken.

The effectiveness [10] of the screen was calculated from the relationship defined as the product of recovery and rejection of material of the desired mesh size.

$$\text{Recovery} = \frac{x_u U}{x_u U + x_o O}$$

$$\text{Rejection} = 1 - \frac{(1 - x_u) U}{F - (x_u U + x_o O)}$$

Thus effectiveness % =

$$\text{Recovery} \times \text{Rejection} \times 100 \qquad (1)$$

The mean mesh size of the material leaving the screen was calculated as the sum of the mean mesh sizes of the undersize and oversize with respect to their individual mass flow rates as in equation (2).

$$M = \frac{M_o O + M_u U}{O + U} \qquad (2)$$

The value of M was calculated from the screen analyses of the undersize and oversize by the relationship

$$M = \frac{\Sigma (mD)}{\Sigma (m)} \qquad (3)$$

Results and Conclusions

The complete results for the 256 runs for replicate runs are available on request to the authors. A statistical analysis of these results yielded the analysis of variance given in Table 2.

The analysis of variance for the total mean mesh size expressed in μ is given in Table 3.

Examination of the results for the effect of the various factors upon the per cent effectiveness of the screens showed that only two main factors of screen aperture and feed rate were important, with aperture considerably more significant than feed rate. Two significant first order interactions of feed rate with aperture and frequency of vibration and angle of inclination were obtained.

Table 3. Analysis of variance for mean mesh size

Nature of effect	*Source*	*Sum of squares*	*D.F.*	*Variance estimate*
Main factors	*A*	739	3	246
	B	376	3	125
	C	264	3	88
	D	1459	3	486
Interaction between pairs of factors	*AB*	4556	9	506
	AC	2311	9	257
	AD	1679	9	187
	BC	4464	9	496
	BD	3428	9	381
	CD	2231	9	248
Interaction between triplets of factors	*AABC*	10,358	27	384
	BD	7880	27	292
	BCD	9780	27	362
	CDA	3429	27	127
Residual	*ABCD*	24,569	81	303
Total		77,523	255	

No factor or interaction proved to be significant.

Standard error of estimate of mean mesh size $= \sqrt{\left(\frac{303}{256}\right)} = 1{\cdot}1\ \mu$

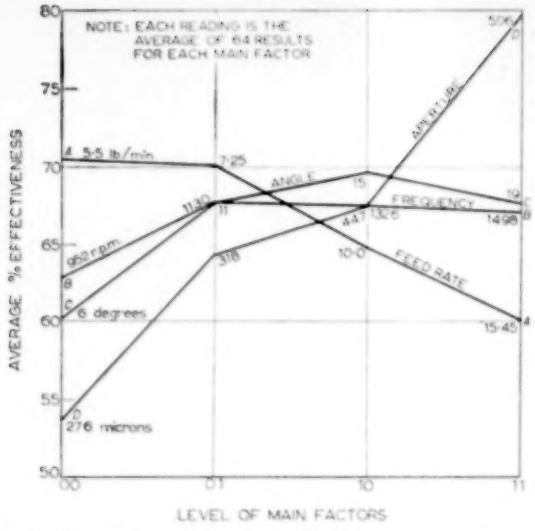

Fig. 1. Graph showing the trend of the average per cent effectiveness of a screen with increasing level of the main variable.

while the only significant second order interactions were feed rate, frequency of vibration with angle of inclination and frequency of vibration, angle of inclination and aperture. Since the design of the experiment was such that the third order interaction *ABCD* was confounded with the residual, the above conclusions must be regarded as relative as it may well be shown that a combination of all four factors could affect the effectiveness of the screen.

A clearer interpretation of the results can be seen from Fig. 1, 2 and 3. Fig. 1 shows the effect of the four factors with increasing level on the average per cent effectiveness if operating conditions are regarded as constant. Fig. 2 shows the effect on the effectiveness with an alteration in both feed rate and aperture while Fig. 3 shows the effect of angle of inclination and frequency of vibration on the effectiveness.

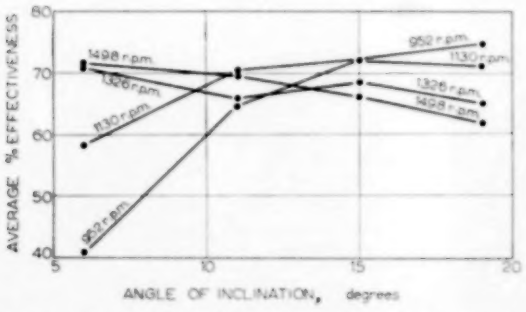

Fig. 2. Graph showing the effect of angle of inclination and frequency of vibration on the per cent average effectiveness.

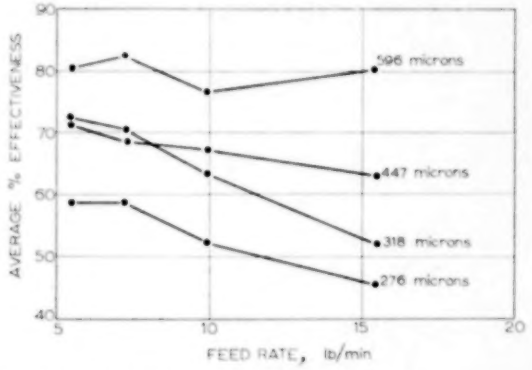

Fig. 3. Graph showing the effect of feed rate and aperture of screen on the per cent average effectiveness.

As a check to the findings of the main experiment and to estimate the standard error, a set of duplicate runs was performed. The 9 runs were performed on 3 levels of frequency of vibration and angle of inclination, with the feed rate and aperture fixed at 7·25 lb/min and 30 mesh respectively. The analysis of variance for both effectiveness and mean mesh are shown in Tables 4 and 5.

The results of Tables 4 and 5 confirm the conclusions obtained from Tables 2 and 3. The estimate of the standard error from Table 2 is 0·4 per cent for the per cent effectiveness which is higher than that of Table 4 of 0·24 per cent, but this may be due to the fact that Table 2 is based on 256 runs while Table 4 is based on 18 and block differences are included in the residual for Table 2. The estimate of the standard error in mean size for Table 3 and Table 5 are 1·1 μ and 1·8 μ respectively. This is indicative of the fact that the amount of attrition is negligible and the change in mean mesh size of the material passing the screen is not significant. This conclusion only applies to the sand used in the experiment and it is obvious that this will not be true for all materials.

VOL. 10 1959

Table 4. Analysis of variance for effectiveness for 18 *runs*

Nature of effect	*Source*	*Sum of squares*	*D.F.*	*Variance estimate*	*Variance ratio*	
Main factors	*B*	237·23	2	118·62	$\frac{B}{BC}$	5·01
	C	42·58	2	21·29	$\frac{C}{BC}$	0·90
Interaction between B and C	*BC*	94·63	4	23·66	$\frac{BC}{\text{Residual}}$	23·66*
Replications	Residual	9·01	9	1·00		
	Total	383·45	17			

*Significance level 1 in 1,000.

Standard error of estimates of effectiveness $= 1{\cdot}00/\sqrt{18} = 0{\cdot}24$ per cent.

Table 5. Analysis of variance for mean mesh size for 18 *runs*

Nature of effect	*Source*	*Sum of squares*	*D.F.*	*Variance estimate*	*Variance ratio*	
Main factors	*B*	129	2	64·5	$\frac{B}{\text{Residual}}$	1·05
	C	225	2	112·5	$\frac{C}{\text{Residual}}$	1·83
Interaction between B and C	*BC*	803	4	200·8	$\frac{BC}{\text{Residual}}$	3·27
Replications	Residual	553	9	61·4		
	Total	1710	17			

No factor or interaction proved to be significant.

Standard error of estimate of mean mesh size $= \sqrt{61{\cdot}4}/\sqrt{18} = 1{\cdot}8\ \mu$.

In the runs performed the percentage effectiveness of the screen using sand varied from a high value of 94·5 per cent for a feed rate of 7·25 lb/min, 952 rev/min, 15° angle of inclination and an aperture of 30 mesh (run No. 231) to a low value of 22·5 per cent with identical conditions except that the angle of inclination was 6 degrees (run No. 67). This is probably due to " blinding " of the screen as at low angles the oversize material cannot escape quickly enough from the screen surface. Examination of Fig. 1 shows that, for all conditions being kept constant, the per cent effectiveness of a screen increases as:

(a) the feed rate decreases
(b) the angle of inclination increases to a certain value of the angle when the effectiveness decreases with further increase in angle
(c) the frequency of vibration increases and then decreases as the frequency increases
(d) the screen aperture increases.

The main conclusions developed from this paper were used as a basis for a set of new experiments using different materials and varying the amplitude of vibration. It is hoped to present these results in a later paper.

Notation

D = aperture of screen which just prevents passage of material
F = feed rate of material
m = mass of material retained on screen of aperture D
M = mean mesh size of material
M_o = mean mesh size of oversize material leaving screen
M_u = mean mesh size of undersize material leaving screen
O = oversize rate of material
U = undersize rate of material
x_o = mass fraction of desired mesh material in oversize
x_u = mass fraction of desired mesh material in undersize

References

[1] Dunn J. E. *Coal Age* 1942 **47** (Dec.) 135.
[2] Richards R. H. and Locke C. E. *Textbook of Ore Dressing* (3rd Ed.) p. 104. McGraw-Hill, New York 1940.
[3] Bullock H. L. *Chem. Engng.* 1947 **54** 97.
[4] Caler W. R. *J. Mining Congr.* 1949 **35** 66.
[5] Perry J. H. *Chemical Engineers Handbook* (3rd Ed.) p. 955. McGraw-Hill, New York 1950.
[6] Taggart A. F. *Handbook of Mineral Dressing* Section 7. Wiley, New York 1945.
[7] Shira W. S. and Hahn M.P. *Rock Products* 1953 **56** 81.
[8] Wolff E. R. *Industr. Engng. Chem.* 1954 **46** 1778.
[9] Davis R. F. *Trans. Inst. Chem. Engrs, Lond.* 1940 **18** 76.
[10] Brown G. G. *Unit Operations* (2nd Imp.) p. 15. Wiley, New York 1950.
[11] Dallavalle J. M. *Micromeritics.* Pitman, New York 1948.

VOL. 10 1959

Chemical Engineering Science, 1959, Vol. 10, pp. 171 to 189. Pergamon Press Ltd. London. Printed in Great Britain.

Research on ion exchangers by means of the percolation technique

C. J. H. WEVERS*
Activit, Amsterdam.

(*Received* 8 *August* 1958 ; *in revised form* 10 *October* 1958)

Abstract—In ion exchange important process characteristics are the equilibrium curve, relating the concentrations in the two phases, when they are in equilibrium, and the kinetic data, governing the mass transfer, when both phases are not in equilibrium. It is shown, that these data can be determined by simple percolation experiments.

The first part of this paper describes a method to determine the equilibrium relation graphically, that is generally valid if the equilibrium curve shows no inflexion point. For exchange of ions of equal valency a numerical method is deduced, which also gives the bed capacity. These methods are applied to a number of systems. It is shown that the anion species exerts a strong influence on the exchange if hydrogen is one of the exchanging species. This phenomenon is explained semi-quantitatively.

The second part describes a method to determine the mass transfer characteristics graphically from a sharp break-through curve and the equilibrium curve. The break-through curve is of the stationary type, in which case the relative concentrations in the two phases on one cross-section are equal.

This method is applied to a number of systems with varying flow rate and particle diameter.

Résumé—Les caractéristiques importantes des processus d'échanges ioniques sont la courbe d'équilibre reliant les concentrations dans les deux phases et les données cinétiques qui gouvernent le transfert de masse quand les deux phases ne sont pas en équilibre. Ces données sont déterminées dans une simple expérience de percolation. Dans une première partie, l'auteur donne une méthode graphique de détermination de courbe d'équilibre qui est généralement valable lorsque la courbe ne présente pas de point d'inflexion. Pour les échanges d'ions de même valence l'auteur déduit une méthode numérique qui donne la capacité du lit. Ces méthodes ont été appliquées à un certain nombre de systèmes. Les anions exercent une grande influence sur l'échange surtout en présence d'ions hydrogènes. Ce phénomène a été expliqué semi quantitativement.

Dans une 2e partie l'auteur décrit une méthode de détermination graphique du transfert de masse à partir de la courbe d'équilibre et d'une courbe nettement brisée. La courbe brisée est du type stationnaire, et dans ce cas les concentrations relatives dans les deux phases pour une section sont égales.

Cette méthode est appliquée à un certain nombre de systèmes en utilisant des écoulements et des diamétres particules variables.

Zusammenfassung—Wichtige Einflussgrössen für den Ionenaustausch sind die Gleichgewichtskurve, die die Konzentrationen in den beiden Phasen im Gleichgewicht enthält, und die kinetischen Daten, die den Stoffübergang im Ungleichgewicht wiedergeben. Es wird gezeigt, dass man diese Werte aus einfachen Perkolationsversuchen erhalten kann.

Der erste Teil dieser Arbeit beschreibt eine Methode zur graphischen Bestimmung der Gleichgewichtsbeziehung, die allegemein gültig ist, wenn die Gleichgewichtskurve keinen Biegepunkt aufweist. Für den Austausch von Ionen gleicher Valenz ist eine numerische Methode abgeleitet, die auch die Bettkapazität ergibt. Diese Methoden werden auf eine grosse Zahl von Systemen angewandt. Es wird gezeigt, dass die Anionenart einen grossen Einfluss auf den Austausch ausübt, wenn Wasserstoff eine der austauschenden Arten ist. Diese Erscheinung wird halb quantitativ erklärt.

*Present address: Dorther Weg 16, Epse, Near Gorssel, Netherlands.

Der zweite Teil beschreibt eine Methode zur graphischen Bestimmung der Stoffübergangsgrössen mit Hilfe einer scharfen Durchbruchskurve und der Gleichgewichtskurve. Diese Durchbruchskurve ist stationär, in welchem Falle die relativen Konzentrationen in den beiden Phasen auf einem Querschnitt gleich sind.

Diese Methode wird auf eine grosse Zahl von Systemen mit veränderlichem Durchfluss und Teilchendurchmesser angewendet.

1. INTRODUCTION

IN ion exchange, as in all mass transfer processes, both the equilibrium and the kinetic characteristics of the process are of interest. As a consequence, it is important to be able to determine these characteristics in a simple way.

The equilibrium relation of ion exchange processes is mostly determined by means of batch experiments. A modification of this method exists in which a column technique is used. Here a column of ion exchange particles is equilibrated (by percolation) with a solution in which the concentration ratio of ions A^+ and B^+ is known.

By regenerating the column contents one can determine the concentration ratio of these ions in the resin phase. Then one point of the equilibrium curve of ion pair $A^+ - B^+$ is known.

The kinetic characteristics of an ion exchange process are usually determined by measuring the slope of the break-through curve resulting from a percolation experiment, in which the displacing ions show greater affinity towards the resin phase than the ions, originally bound by the ion exchanger. Although this method is used almost exclusively, there exists some confusion in the interpretation of the measured break-through curves.

In this paper it will be shown, that for monofunctional exchangers the binary equilibrium relation can be determined from one break-through curve. Further the determination of the mass transfer coefficients from the equilibrium relation and a break-through curve will be treated.

2. THEORY

The following assumptions are made concerning the packed bed and the flow through it.

(a) The ion exchange particles are supposed to be uniformly packed;

(b) Swelling and shrinking of the particles is neglected at present;

(c) Longitudinal mixing is supposed to be negligible.

With these assumptions a material balance around an infinitesimal slab of the bed gives the equation:

$$R\frac{\partial C}{\partial z} + \epsilon F\frac{\partial C}{\partial t} + F\frac{\partial q}{\partial t} = 0 \qquad (1)$$

Introducing $x = C/C_0$ and $y = q/q_0$, the relative concentrations in the liquid and resin phase respectively, and $v_0 = R/F$, the superficial flow velocity, equation (1) becomes:

$$v_0\frac{\partial x}{\partial z} + \epsilon\frac{\partial x}{\partial t} + \frac{q_0}{C_0}\frac{\partial y}{\partial t} = 0 \qquad (2)$$

Instead of the independent variable t one can introduce $t - (\epsilon z/v_0)$; the term $\epsilon z/v_0$ is the time necessary to fill the voids between the resin particles with the incoming solution. So $[t - (\epsilon z/v_0)]\,C_0R$ is the total number of equivalents that has flown out of the column since $t = 0$.

After the following substitutions:

$$\tau = \left(t - \frac{\epsilon z}{v_0}\right)C_0R, \text{ and}$$

$$s = q_0 F z = \text{ total bed capacity,}$$

there results:

$$\left(\frac{\partial x}{\partial s}\right)_\tau + \left(\frac{\partial y}{\partial \tau}\right)_s = 0 \qquad (3)$$

When for $t \leqslant 0$ the bed is completely charged with B^+ ions and washed with pure water, and if the incoming solution contains A^+ ions only, in concentration C_0 the boundary conditions for equation (2) are:

$$t = 0\,;\, z > 0 : x = 0,$$

$$t > 0\,;\, z = 0 : x = 1.$$

VOL. 10 1959

3. Determination of the Equilibrium Relation from Percolation Experiments General Solution

When in an ion exchange reaction only two ion species, A^+ and B^+ are present, then x and y are a direct measure of the composition of the two phases.

It is assumed that the equilibrium relation is given by:

$$y = \mathrm{f}(x), \tag{5}$$

and that $\mathrm{f}''(x)\,(= d^2\mathrm{f}(x)/dx^2)$ is nowhere equal to zero.

The latter is generally the case with monofunctional exchangers.

It is well known from literature, [8, 18], that under suitable conditions the experimental break-through curve is nearly indiscernible from an "equilibrium" break-through curve, that would result from a percolation experiment, in which the two phases on a cross-section are in equilibrium.

It can be shown [20], that this situation applies, if (for $\mathrm{f}''(x) > 0$):

$$\frac{z\,\mathrm{f}''(x)\,K_L S}{v_0\,\mathrm{f}'(x)} \geqslant 1 \tag{6}$$

The condition $\mathrm{f}''(x) > 0$ means that the displaced ions have a stronger affinity towards the resin phase than the displacing ions. It can be shown that the actual and the "equilibrium" break-through curves differ most for very low and very high values of x.

This criterion (6) and another one (39), to be given later on, are easily deduced from the material balance (2).

For a complete description of this deduction the reader is referred to [20].

When the criterion (6) is fulfilled it is allowed to substitute the equilibrium relation (5) in the material balance (3). This gives:

$$\left(\frac{\partial x}{\partial s}\right)_\tau + \mathrm{f}'(x)\left(\frac{\partial x}{\partial \tau}\right)_s = 0 \tag{7}$$

Now a new variable is introduced, $l = \tau/s$; l is the dimensionless ratio of the number of equivalents, that has passed through the column and the total bed capacity.

Introduction of l in (7) results in:

$$\frac{dx}{dl}\{\mathrm{f}'(x) - l\} = 0 \tag{8}$$

This formula has already been given by Sillén [17].

In (8) dx/dl is the slope of the break-through curve in an $x - l$ graph. Since $dx/dl \neq 0$, we have from (8)

$$\mathrm{f}'(x) = l \tag{9}$$

and

$$\mathrm{f}(x) = \int l\,dx \tag{10}$$

The meaning of this equation is clear from Fig.1, where the hatched area corresponds to $y_1 = \mathrm{f}(x_1)$.

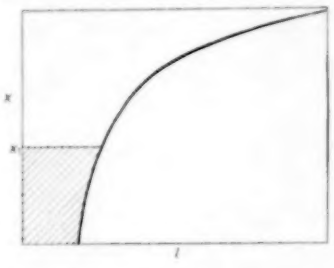

Fig. 1. Determination of $f(x)$ from an "equilibrium" break-through curve.

Thus equation (10) provides a simple way to determine the equilibrium relation, either by numerical or mechanical integration of the "equilibrium" break-through curve according to Fig. 1.

In using this method it is necessary to know the total bed capacity, in order to be able to determine the value of

$$l = \frac{[t - (\epsilon z/v_0)\,C_0\,R]}{\text{total bed capacity}}$$

In principle it is possible to determine the bed capacity from the same break-through curve by integrating it from $x = 0$ to $x = 1$. A much more accurate determination is based upon the sharp break-through curve resulting from a percolation experiment in which the displacing ions show greater affinity to the exchanger than the displaced ions ($\mathrm{f}''(x) < 0$).

This method is generally valid (provided $f''(x) > 0$), also for reactions where ions of inequal valency exchange.

Numerical solution

If two ion species of equal valency exchange on a monofunctional exchanger, it is possible to describe the reaction:

$$A^+_L + B^+_R \rightleftharpoons A^+_R + B^+_L \qquad (11)$$

with an equilibrium constant K_1, defined by:

$$K_1 = \frac{[A^+_R]\,[B^+_L]}{[A^+_L]\,[B^+_R]} \qquad (12)$$

Here the square brackets indicate the ion activities. If, as an approximation, concentrations are used instead of activities, (12) reduces to:

$$K_1 = \frac{y\,(1-x)}{x\,(1-y)} \qquad (13)$$

where x and y are the relative concentrations of the displacing ions.

In this case the general equilibrium relation (5) takes the following shape:

$$y = f(x) = \frac{K_1 x}{K_1 x + 1 - x} \qquad (14)$$

and

$$f'(x) = \frac{K_1}{(K_1 x + 1 - x)^2} \qquad (15)$$

Substitution of (15) in (9) gives:

$$x = \frac{\sqrt{K_1} - \sqrt{l}}{K_1\sqrt{l} - \sqrt{l}} \qquad (16)$$

This equation was also arrived at by HIESTER and VERMEULEN [10]. By means of equation (16) it is possible to determine the equilibrium constant K_1, as well as the bed capacity numerically from one break-through curve, for which $f''(x) > 0$.

Equation (16) is quadriatic in $\sqrt{K_1}$:

$$\phi(x, \sqrt{K_1}, l) = K_1 x\sqrt{l} - \sqrt{K_1} + (1-x)\sqrt{l} = 0, \qquad (17)$$

with

$$\sqrt{K_1} = \frac{1 \pm \sqrt{1 - 4lx\,(1-x)}}{2x\sqrt{l}} \qquad (18)$$

If the discriminant in (18) is put equal to zero, it is clear that $\phi = 0$ leads to the condition:

$$\left(\frac{\partial \phi}{\partial \sqrt{K_1}}\right)_{x,l} = 0 \qquad (19)$$

From $\phi = 0$ it follows that:

$$d\phi = \left(\frac{\partial \phi}{\partial x}\right)_{\sqrt{K_1},l} dx + \left(\frac{\partial \phi}{\partial \sqrt{K_1}}\right)_{x,l} d\sqrt{K_1} + \left(\frac{\partial \phi}{\partial l}\right)_{x,\sqrt{K_1}} dl = 0 \qquad (20)$$

For constant l, (20) can be written as:

$$\left(\frac{\partial \phi}{\partial \sqrt{K_1}}\right) = \left(\frac{\partial \phi}{\partial x}\right)_{\sqrt{K_1},l}\left(\frac{\partial x}{\partial \sqrt{K_1}}\right)_l + \left(\frac{\partial \phi}{\partial \sqrt{K_1}}\right)_{x,l} = 0. \qquad (21)$$

Combination of (21) and (19) results in

$$\left(\frac{\partial x}{\partial \sqrt{K_1}}\right)_l = 0$$

or

$$\left(\frac{\partial x}{\partial K_1}\right)_l = 0. \qquad (22)$$

This equation locates a minimum of x as a function of K_1 with constant l. This means that for each value of $l\ (> 1)$ there is one value of K_1 for which x is smaller than for any other value K_1: for another value of l there is also another value of K_1 for which x is a minimum.

Apparently there exists an envelope that is tangent to all equilibrium break-through curves in an $x-l$ graph.

The envelope is given by the equation:

$$l = \frac{1}{4x\,(1-x)} \qquad (23)$$

An experimental break-through curve gives x as a function of the volume of solution that has passed through the column, V_{ex}; in order to calculate K_1 from (18) one should know x as a function of l. So a relation between V_{ex} and l has to be found.

The following symbols are introduced here:

l_m = the value of l, where the equilibrium curve is a tangent to the envelope; there $l = [4x\,(1-x)]^{-1}$.

V_C = value of V_{ex}, where $l = 1$.

VOL. 10 1959

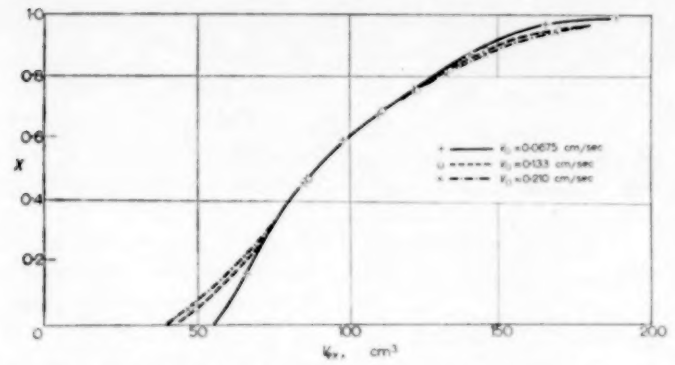

FIG. 2. Influence of the flow rate on the "equilibrium" break-through curve.

So V_C is the factor that links V_{ex} and l by the equation:

$$\frac{V_{ex}}{l} = V_C \tag{24}$$

Now $\sqrt{K_1}$ and K_1 are real, so from (18):

$$1 - 4l\,x\,(1-x) \geqslant 0 \qquad \text{or}$$

$$\left.\begin{aligned} l &< \frac{1}{4x\,(1-x)} && \text{for } l \neq l_m \\ l &= \frac{1}{4x\,(1-x)} && \text{for } l = l_m \end{aligned}\right\} \tag{25}$$

Combination of (24) and (25) gives:

$$\left.\begin{aligned} V_{ex}\,4\,x\,(1-x) &< V_C \text{ for } l \neq l_m \\ V_{ex}\,4\,x\,(1-x) &= V_C \text{ for } l \neq l_m \end{aligned}\right\} \tag{26}$$

From (26) it is apparent that the function $V_{ex}\,4\,x\,(1-x)$, which can be calculated from the measurements, shows a maximum, and the value of that maximum is V_C. The bed capacity is $V_C \cdot C_0$.

It is then possible to calculate a value of K_1 for every measured point of the break-through curve.

Relation (18) gives two values for $\sqrt{K_1}$ (and for K_1). The highest value should be taken for $l > l_m$, the smallest one for $l < l_m$.

Another procedure to determine the equilibrium relation from a break-through curve, for which $f''(x) > 0$, was described and used by GLUECKAUF [8] and by DUNCAN and LISTER [5].

4. RESULTS OF EQUILIBRIUM MEASUREMENTS

In this section some equilibrium data are presented which were obtained with methods described earlier in this paper.

The break-through curves from which the equilibrium data were calculated sufficiently approached condition (6) of "equilibrium" between the two phases. The reader is referred to the end of this paper for some remarks on the experimental technique used.

The system $H^+ - Na^+$ (Cl^-) – *Dowex* 50 × 8.

To show the influence of the fluid flow rate on the shape of the break-through curve, Fig. 2 gives the curves for three different rates. It is evident that the deviations from the equilibrium break-through curve are the most serious in the beginning and in a smaller degree in the end of the curve.

In Fig. 3 the equilibrium curve of this system is given in a y–x diagram. K_1 was calculated with

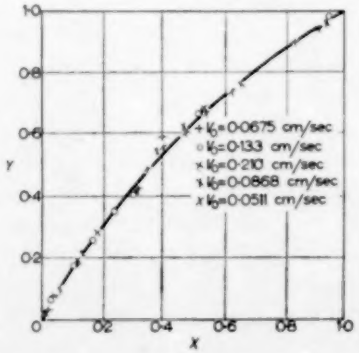

FIG. 3. Equilibrium curve of the system $Na^+ - H^+$ (Cl^-) – Dowex 50 × 8.

the method, described in the foregoing paragraph; y was determined from (13).

The value of K_1, calculated from the equilibrium break-through curve is always < 1; the equilibrium curves are normally given for $K_1 > 1$; therefore the equilibrium diagrams determined using the theory given above, are turned over an angle of 180°. This has been done with the diagram of Fig. 3 and with all the equilibrium diagrams to come.

From this graph the following conclusions can be drawn:

(a) The shape of the equilibrium curve is influenced only slightly by the flow rate.

(b) The spread of the observation points is acceptably small except in the vicinity of $x = 0{\cdot}4$; the latter phenomenon is caused by the fact, that the discriminant of (17) is zero there. As a consequence, small experimental errors produce large variations in the equilibrium constant.

The system $H^+ - Na^+ (SO_4^{2-})$ – *Dowex* 50 × 8

The equilibrium curve is again calculated from the "equilibrium" break-through curve and compared with the curve, determined from batch experiments, in which a known quantity of the exchanger is equilibrated with a known quantity of solution. Fig. 4 gives the results for this system.

From this graph the following conclusions can be drawn:

(a) The percolation experiments give equilibrium curves which coincide very well; the flow rate was varied a factor 2 and the experiments were performed by three different observers.

(b) The equilibrium curve is asymmetrical, which means that K_1 is not a true constant but depends on x. The question arises, whether it then is allowed to use the numerical method to calculate K_1; in the derivation of this method K_1 was assumed to be constant. Comparison with the results of the batch experiments shows, that for the (small) variations in K_1, encountered here, the numerical method gives results which are equivalent to those of batch experiments. As a consequence, it is concluded that the numerical method may be used for a variable K_1, if the variations are not excessive.

(c) The equilibrium curve for the SO_4^{2-} system lies at a greater distance from the diagonal $y = x$ than the Cl^- curve (Fig. 3). This difference is caused by the fact that HCl is a stronger acid than H_2SO_4. This effect will be discussed more quantitatively below.

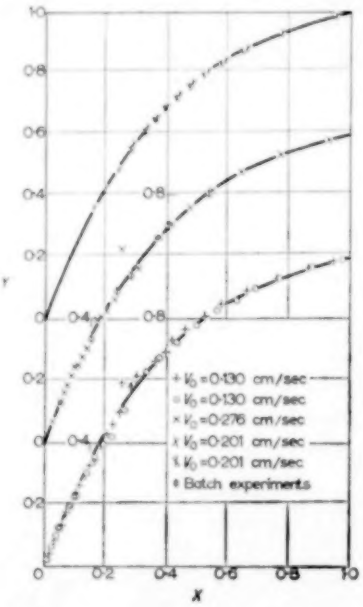

FIG. 4. Equilibrium curve of the system $Na^+ - H^+ (SO_4^{2-})$ – Dowex 50 × 8.

The system $H^+ - Ag^+ (NO_3^-)$ – *Dowex* 50 × 8

In Fig. 5 the equilibrium curve of the above mentioned system is given. In the three runs the concentration and the flow rate were slightly varied. Further it is apparent that this curve is also asymmetrical.

The influence of the anion on cation exchange

If the anion present in the solution (Z^-) forms a weak acid with H^+ ions, then two reactions occur at the same time:

$$M_L^+ + H_R^+ \rightleftharpoons M_R^+ + H_L^+ \qquad (27)$$

$$H_L^+ + Z_L^- \rightleftharpoons HZ \qquad (28)$$

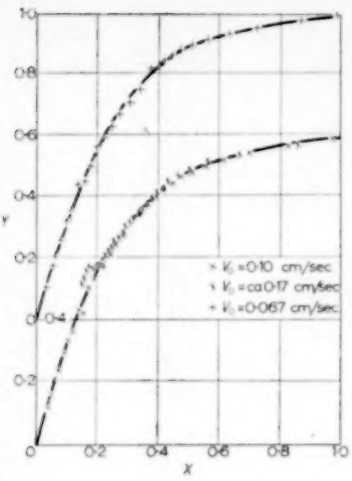

FIG. 5. Equilibrium curve of the system $Ag^+ - H^+$ (NO_3^-) – Dowex 50 × 8.

If HZ is weakly dissociated, reaction (28) will withdraw H^+ ions from the solution and reaction (27) will be drawn to the right-hand side. That means that in this case the charging of the ion exchanger with M^+ ions will proceed further than if HZ is completely dissociated.

This effect will be demonstrated quantitatively in the first place for the exchange of Na^+ and H^+ ions on Dowex 50 × 8 with either Cl^- or SO_4^{2-} anions.

It is assumed, that there occurs complete dissociation of HCl and of the first H^+ ion of sulphuric acid. For the dissociation reaction of the second H^+ ion.

$$HSO_4^- \rightleftharpoons H^+ + SO_4^{2-}$$

the equilibrium constant is given by [15]

$$K_d = \frac{[H^+]\,[SO_4^{2-}]}{[HSO_4^-]} = 2 \cdot 10^{-2} \text{ kg mol/m}^3 \qquad (29)$$

After the introduction of concentrations instead of activities, (29) becomes:

$$\frac{[H^+]\,[SO_4^{2-}]}{[HSO_4^-]} = \frac{\gamma HSO_4^-}{\gamma SO_4^{2-}\,\gamma H^+}\, 2 \cdot 10^{-2} \text{ kg mol/m}^3 \qquad (30)$$

in which γ_{A+} is the activity coefficient of ion A^+. The activity coefficients of the univalent ions are taken to be equal and γSO_4^{2-} is found by extrapolating the values given by LEWIS and RANDALL [14] to higher ionic strengths corresponding to 0·4 N solutions; in so doing one finds $\gamma SO_4^{2-} \approx 0{\cdot}2$. So

$$\frac{[H^+]\,[SO_4^{2-}]}{[HSO_4^-]} \approx 0{\cdot}1 \text{ kg mol/m}^3 \qquad (31)$$

With (31) it is possible to calculate the true value of $[H^+]$ instead of the value $[H^+ + HSO_4^-]$ found by titration. Then it is possible to make a graph of y against the true value of $x = Na_L^+/(Na_L^+ + H_L^+)$ instead of the fictitious value $Na_L^+/(Na_L^+ + H_L^+ + HSO_{4L}^-)$ which is directly based on the titration. The result of this correction is given in Fig. 6. It is seen that the corrected SO_4^{2-} curve coincides very well with the measured Cl^- curve. In the same Fig. the equilibrium curves for $Na^+ - H^+$ exchange are given for the anions CH_2ClCOO^- and CH_3COO^-. For the correction of these curves the following values of the dissociation constants were taken [15]:

Monochloracetic acid $K_d = 1{\cdot}55.10^{-3}$ kg mol/m³
Acetic acid $K_d = 1{\cdot}75.10^{-3}$ kg mol/m³

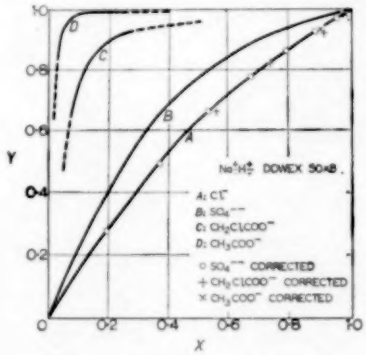

FIG. 6. Equilibrium curve of the system $Na^+ - H^+$ – Dowex 50 × 8 with different anions.

The author could not find data concerning the activity coefficients of the anions used here. So it was assumed that the influence of the activity coefficients were the same in both cases.

Then this influence was chosen at such a value that the curve for CH_2ClCOO^- coincided approximately with the Cl^- curve and then the same value was used for correcting the CH_3COO^- curve.

It is seen that this last correction fits the CH_3COO^- curve reasonably well to that for Cl^-.

Although the latter procedure is not exact, the following conclusions can be drawn here:

(a) In cation exchange the type of the anion can exert a strong influence upon the equilibrium curve, if H^+ is one of the exchanging ion species.

(b) It is possible to explain and predict this influence by taking the dissociation of the acid into consideration.

These conclusions are a direct contradiction of those of DRANOFF and LAPIDUS [4].

The exchange of divalent against univalent ions on Dowex 50 × 8

The exchange of reaction of a divalent cation against for instance H^+ ions

$$Me_L^{2+} + 2\,H_R^+ \rightleftharpoons Me_R^{2+} + 2\,H_L^+ \qquad (32)$$

can, analogous to (12) and (13), be described with an equilibrium constant K_2, defined by:

$$K_2 = \frac{[Me_R^{2+}][H_L^+]^2}{[Me_L^{2+}][H_R^+]^2} \quad \text{or}$$

$$K_2 = \frac{C_0}{q_0}\,\frac{y}{x}\,\frac{(1-x)^2}{(1-y)^2} \qquad (33)$$

It is impossible to solve (9) analytically with the equilibrium relation (33) as has been done for uni-univalent exchange. Therefore HIESTER and VERMEULEN [9] try to describe reaction (32) with an equilibrium relation of the form of (13). If this would be allowed, one could again calculate the equilibrium relation from a break-through curve.

If, on the other hand, such a procedure is not allowed, the equilibrium curve can be determined by (for instance mechanical) integration, as pointed out in Fig. 1.

A third method to obtain the equilibrium curve, is provided by batch experiments.

These three methods have been applied to the system $H^+ - Zn^{2+}$ (SO_4^{2-}) – Dowex 50 × 8.

The results are shown in Fig. 7.

The drawn line in Fig. 7 is a graphical representation of the equation:

$$\frac{y\,(1-x)^2}{x\,(1-y)^2} = 40$$

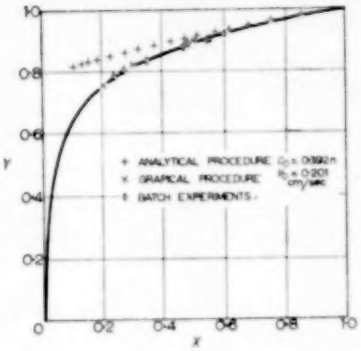

FIG. 7. Equilibrium curve of the system $Zn^{2+} - H^+$ (SO_4^{2-}) – Dowex 50 × 8.

From Fig. 7 the following conclusions can be drawn:

(a) It is not allowed, to describe the exchange of divalent against univalent ions by an equilibrium constant according to (13).

(b) The equilibrium curve found by the graphical procedure agrees well with the results from the batch experiments.

(c) If this equilibrium is described by relation (33) there results a reasonably constant K_2. In this case ($C_0 = 0{\cdot}392$ kg eq./m³; $q_0 = 2{\cdot}1$ kg eq./m³ bed volume) $K_2 \approx 7{\cdot}5$.

Some other di-univalent systems on Dowex 50 × 8

Of three other systems the equilibrium curves were determined graphically. Those systems were: $H^+ - Zn^{2+}$ (Cl^-) – Dowex 50 × 8; $H^+ - Ba^{2+}$ (Cl^-) – Dowex 50 × 8 and $H^+ - Mg^{2+}$ (Cl^-) – Dowex 50 × 8. The Mg^{2+} system was measured at two different concentrations.

The results are given in Figs. 8, 9 and 10. The lines drawn in these diagrams correspond to the following values of K_2.

$H^+ - Zn^{2+}$ (Cl^-) – Dowex 50 × 8:
$K_2 = 3{\cdot}28$ at $C_0 = 0{\cdot}422$ kg eq./m³.

$H^+ - Ba^{2+}$ (Cl^-) – Dowex 50 × 8:
$K_2 = 19{\cdot}6$ at $C_0 = 0{\cdot}592$ kg eq./m³.

$H^+ - Mg^{2+}$ (Cl^-) – Dowex 50 × 8:
$K_2 = 2{\cdot}90$ at $C_0 = 0{\cdot}386$ kg. eq./m³.
$K_2 = 3{\cdot}50$ at $C_0 = 0{\cdot}656$ kg. eq./m³.

VOL. 10 1959

From the Figs. 8, 9 and 10 it is apparent, that the value of K_2 defined by (33) is independent of x for the systems studied here but slightly dependent on the total concentration.

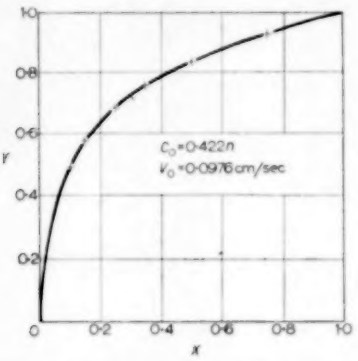

FIG. 8. Equilibrium curve of the system $Zn^{2+} - H^+ (Cl^-)$ – Dowex 50 × 8.

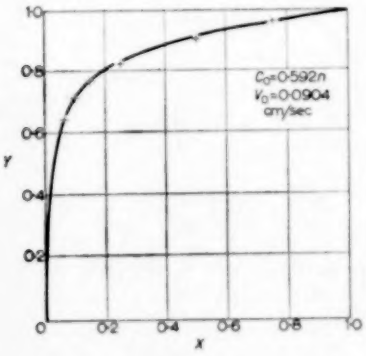

FIG. 9. Equilibrium curve of the system $Ba^{2+} - H^+ (Cl^-)$ – Dowex 50 × 8.

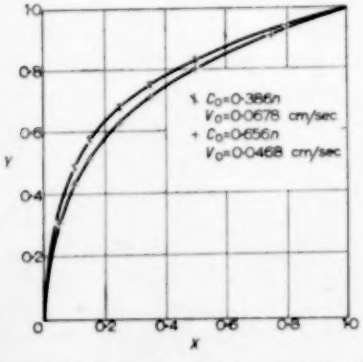

FIG. 10. Equilibrium curve of the system $Mg^{2+} - H^+ (Cl^-)$ – Dowex 50 × 8.

RELATIONSHIP BETWEEN KINETIC PROPERTIES AND SHAPE OF THE SHARP BREAK-THROUGH CURVES

In paragraph 2 a material balance (2, 3) was deduced and the boundary conditions (4) were given.

To completely describe the percolation process one further equation is needed. This relation is provided by the kinetic equation, giving the rate of mass transfer, if there exists no equilibrium between the two phases.

GILLILAND and BADDOUR [6] and HIESTER and VERMEULEN [9] have used the following equation:

$$\frac{\partial y}{\partial t} = k C_0 \left\{ (1-y)\, x - \frac{1}{K_1} (1-x)\, y \right\} \qquad (37)$$

It is analogous to rate equations of chemical reactions, and as such it is not very satisfactory. It is to be expected, and also borne out by experiments, that the rate of exchange is not determined by the very fast ionic reactions, but by diffusion phenomena in both the liquid and the resin phase. On the other hand (37) is the only rate equation for which it is possible to solve the set of equations (3) and (37) exactly [9].

It can be shown that the asymptotic solution (e.g. for infinite rate of mass transfer, or infinite bed length) for $K_1 > 1$ gives a symmetric break-through curve. In view of the fact that such a break-through curve is more the exception than the rule, one may conclude, that (37) does not describe the mass transfer adequately.

Another rate relation, based on the diffusional character of the mass transfer, is the following:

$$\left.\begin{aligned} \Phi'' &= \frac{1}{S}\left(\frac{\partial q}{\partial t}\right) = k_L (C - C_i) = k_R (q_i - q) \\ \text{or} \\ \Phi'' &= \frac{q_0}{S}\left(\frac{\partial y}{\partial t}\right) = k_L C_0 (x - x_i) = k_R q_0 (y_i - y) \end{aligned}\right\} \qquad (38)$$

Φ'' = mass transfer per unit area (kg aq/m² sec).

S = specific surface of the ion exchange particles in the bed (m²/m³).

If the bed consists of equal spheres $S = 6\,(1-\epsilon)/d$.

k_L = mass transfer coefficient in the liquid phase (m/sec).

k_R = mass transfer coefficient in the resin phase (m/sec).

In (38) C and q (or x and y) are the mean concentrations in the liquid or resin phase. The index i indicates the situation at the interface between the two phases.

There are some objections against the use of relation (38) too. This type of relation is mostly and very successfully used for those heat or mass transfer processes, where the temperature or the concentration changes very rapidly in a thin boundary layer adjacent to the interface and becomes constant at a greater distance. This situation does not occur in an ion exchange process.

In the resin phase the exact description of the unsteady state diffusion phenomena gives a solution which is totally intractable [1].

In the liquid phase the flow rates used here are so low that the flow through the bed is essentially laminar; consequently, the concentration will change gradually in a direction perpendicular to the direction of flow.

However, the fact that the use of (38) results in consistent values of the coefficients k_R and k_L makes it attractive for practical purposes.

Glueckauf [7] has proposed other rate relations; these empirical equations will not be applied here because they lack any theoretical back-ground and—being non-linear—are more difficult to use.

Hiester and Vermeulen [9] have tried to adapt the exact solution, valid for relation (37), to relation (38). There are two objections against this procedure: (a) it is not exact; (b) it is only relatively simple if the mass transfer resistance lies mainly in one of the two phases. If both phases show comparable resistances their procedure becomes very cumbersome.

To be able to solve the set of equations (3) and (38) Klamer [10], [11] and [12] proposed to use the stationary sharp front; that occurs (for $K_1 > 1$) for:

$$\frac{q_0/C_0\, z\, (\partial x/\partial t)_z}{v_0} \gg 1, \qquad (39)$$

so for high values of the residence time v_0/z [20].

This front is characterized by the fact that its shape does not change any more, once it has been established. This means that the speed, with which the front passes through the column $(\partial z/\partial t)_x$, is independent of the concentration x. This speed is given by:

$$v_x = \left(\frac{\partial z}{\partial t}\right)_x = \frac{v_0}{\epsilon + q_0/C_0(\partial y/\partial x)_z} \qquad (40)$$

which is easily deduced from (2).

The front is stationary if $(\partial v_x/\partial x) = 0$ or if $(\partial y/\partial x)_z$ = constant.
From $(\partial y/\partial x)_z = C_1$ follows:

$$y = C_1 x + C_2 \qquad (41)$$

Insertion of the boundary values $x = 0 : y = 0$
$x = 1 : y = 1$
results in:

$$y = x \qquad (42)$$

So if a stationary sharp front exists, the relative concentrations in both phases of a cross-section are equal. A similar relation has been deduced by Klamer [10], [11].

Combination of (42) with (3) provides another way of writing this condition for the occurrence of this type of front:

$$\left(\frac{\partial \tau}{\partial s}\right)_x = 1 \qquad (43)$$

By means of this relation, it is easy to show that the asymptotic form of the analytical solution, given by Hiester and Vermeulen [9]:

$$x = \frac{1}{1 + \exp\left[k/K_1 R\,(1 - K_1)\,(\tau - s)\right]} \qquad (44)$$

describes the stationary sharp break-through curve. Also Gilliland and Baddour [6] use essentially this type of front.

When the stationary front is used, the relations describing the mass transfer, are greatly simplified by equation (42). From (38) and (42) follows:

$$\left(\frac{\partial x}{\partial t}\right)_z = \frac{C_0}{q_0} k_L S\,(x - x_i) = k_R S\,(y_i - y) \qquad (45)$$

where $(\partial x/\partial t)_z$ is the slope of the break-through curve.

It is easily seen that (45) is still further simplified if the mass transfer resistance lies mainly in one of the two phases.

VOL. 10 1959

If the liquid phase resistance predominates

$$\left(\frac{\partial x}{\partial t}\right)_z = \frac{C_0}{q_0} k_L S (x - x^*) \qquad (46)$$

[x^* from $y = \mathrm{f}(x^*)$] and if the resin phase resistance prevails

$$\left(\frac{\partial x}{\partial t}\right)_z = k_R S \{\mathrm{f}(x) - y\} \qquad (47)$$

In Figs. (11) and (12) it is clear that AA′ represents the driving force in (46) and (47); further it is apparent that the inflexion point in the break-through curve will have concentration x_b (see Figs. 11 and 12) if the tangent in B is parallel to the diagonal.

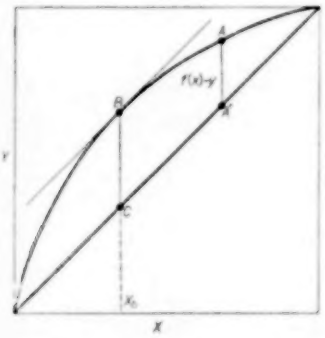

Fig. 11. Resistance in the resin phase.

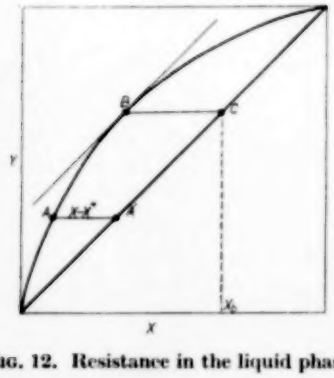

Fig. 12. Resistance in the liquid phase.

The procedure given above has been described earlier by Klamer [10].

If the resistance is in both phases of comparable magnitude, it is advantageous to introduce the slope m of the line connecting the origin with the point A (x_i, y_i) which indicates the concentrations at the interface. So $m = y_i/x_i$.
Introduction of m in (38) results in;

$$\Phi'' = \frac{q_0}{S}\left(\frac{\partial y}{\partial t}\right) = C_0 K_L \left(x - \frac{y}{m}\right) = q_0 K_R (mx - y) \qquad (48)$$

if $K_L = \left(\frac{1}{k_L} + \frac{C_0}{m q_0 k_R}\right)^{-1}$

= over-all mass transfer coefficient based on the liquid phase (m/sec).

and $K_R = \left(\frac{m q_0}{C_0 k_L} + \frac{1}{k_R}\right)^{-1}$

= over-all mass transfer coefficient based on the resin phase (m/sec).

In Fig. (13) it is seen that the driving forces occurring in (48) are indicated by BC $= x - (y/m)$ and by DB $= mx - y$. Further the ratio of the resistances R_L and R_R in the two phases

$$\frac{R_L}{R_R} = m \frac{k_R q_0}{k_L C_0} = m \operatorname{cotg} \delta \qquad (49)$$

is given by EB/CE = FD/BF in Fig. (13).

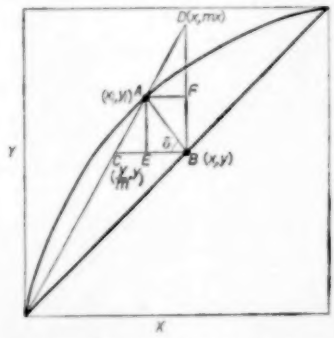

Fig. 13. Resistance in both phases.

From the foregoing one may conclude:

(a) the concentration x_b of the inflexion point of stationary sharp break-through curve, gives an indication what phase causes the biggest mass transfer resistance;

(b) since in (49) δ is nearly independent of x and m varies with x, the ratio of resistances changes when during an experiment x varies from 0 to 1.

If the equilibrium curve can be represented by relation (13), m varies from K_1 for $x = 0$, to $\sqrt{K_1}$ for $x = 1 - y$ and to 1 for $x = 1$. So, for a large value of K_1 (both ions differ greatly in their affinity towards the resin) it is quite well possible that at first (low x, $m \approx K_1$) the fluid phase resistance predominates, and later on (high x, $m \approx 1$) the resin phase resistance.

For extreme values of K_1 the equilibrium curve lies near to the sides of the quadrangle, and can be approximated by two right lines; one from the origin to $x = 0, y = 1$, and one from there to $x = 1, y = 1$. From Fig. (14) it is clear that (47) and (48) can then be written:

$$\frac{\partial x}{\partial t} = \frac{C_0}{q_0} k_L S x \quad (50) \quad \text{and} \quad \frac{\partial x}{\partial t} = k_R S (1 - x), \quad (51)$$

since at first $x^* = 0$ and later $f(x) = 1$ (and $y = x$).

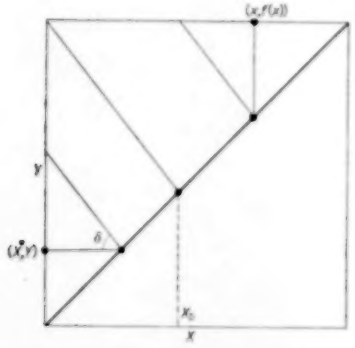

FIG. 14. Extremely high equilibrium constant.

Equations (50) and (51) will give linear relations between t and $ln\ x$ or $ln(1 - x)$. Then, from a graph of $ln\ x$ and $ln(1 - x)$ against t, one can calculate k_L and k_R from the slopes of the two lines.

For normal equilibrium curves, where (50) and (51) can not be applied, the main difficulty in the interpretation is the fact, that the point (x_i, y_i) (or the angle δ) is unknown. In principle the inflexion point concentration x_b together with the shape of the equilibrium curve could give the magnitude of δ, which is sufficient to solve the problem. However, it is difficult to estimate the place of an inflexion point accurately; still, combining the information provided by the estimated value of x_b, with data from analogous experiments [e.g. interpreted with (50) and (51)], it is possible to make a reasonable estimate of δ.

Then $(x - x_i)$ and $(y_i - y)$ from (45) are known and k_R and k_L can be calculated from the slope of the break-through curve.

6. KINETIC DATA FROM EXPERIMENTS

In Table 1 a summary is given of the systems used for kinetic experiments.

Table 1.

Ion exchanger	*Ion pair*	*Anion*
Amberlite IRC 50	$Na^+ - H^+$	$H_2BO_3^-$
	$Na^+ - H^+$	OH^-
	$H^+ - Na^+$	SO_4^{2-}
Dowex 50 × 8	$Na^+ - H^+$	Cl^-
	$Na^+ - H^+$	SO_4^{2-}
	$Ag^+ - H^+$	NO_3^-

Nearly all the experiments were performed in "plastic" columns; only those with systems $Na^+ - H^+$ (SO_4^{2-}) – Dowex 50 × 8 and $Ag^+ - H^+$ (NO_3^-) – Dowex 50 × 8 were done in glass columns.

The equilibrium curves of the systems used with Dowex 50 × 8 were taken from the first part of this paper. The dissociation constants of HOH, H_3BO_3 and H_2SO_4 were so far different from that of the — COOH groups in the resin that the three Amberlite IRC 50 systems could be interpreted with relations (50) and (51).

From the values found for k_R a diffusion coefficient in the resin phase $\mathfrak{D}_R$ was calculated with

$$\mathfrak{D}_R = \frac{k_R S d^2}{60} = \frac{k_R (1 - \epsilon) d}{10} \quad (52)$$

It has been argued already that the rate relation

(38) cannot describe the real phenomena accurately. That is the reason why a number of authors has used other constants in (52); the following numerical values are used: 60 or $4\pi^2$ [7, 10], $4\pi^2$ or 48 [6] and 30 [13]. The choice is rather arbitrary and not very important, since from the simplified description [by (38)] one should not expect more than an order of magnitude of $\mathfrak{D}_R$.

Criterion (39) was sufficiently fulfilled for all kinetic experiments to be described.

Kinetic experiments with Amberlite IRC 50

Table 2 gives a summary of the particle diameters and specific surfaces used.

Table 2.

Mesh no. (ASTM)	*Effective diameter* (mm)	$S.10^{-2}$ (m^{-1})
Unscreened	0·42	89 (indicatedwith + in following tables)
30	0·64	58
35-45	0·42	89

The results of the experiments are given in Tables 3, 4 and 5 for the resin phase resistance for $H_2BO_3^-$, OH^- and SO_4^{2-} anions and in Tables 6 and 7 for the liquid phase resistance for SO_4^{2-} and $H_2BO_3^-$ anions.

Table 3. Results of experiments with $Na^+ - H^+$ ($H_2BO_3^-$) – *Amberlite IRC 50 (resin phase);* $Co = 0{\cdot}134 - 0{\cdot}137$ kg eq./m³.

Experiment no.	*Column diameter* (mm)	$S.10^{-2}$ (m^{-1})	$\mathfrak{D}_R.10^{12}$ (m^2/sec)
43+	6	89	1·31
47+	6	89	1·31
51+	6	89	1·36
53+	6	89	1·43
55+	6	89	1·53
59+	6	89	1·45
61	10	89	1·26
65	10	89	1·14
73	10	58	1·06
81	10	58	1·01
		Mean	1·3

Table 4. Results of kinetic experiments with $Na^+ - H^+(OH^-)$ – *Amberlite IRC 50 (resin phase);* $Co = 0{\cdot}31 - 0{\cdot}51$ kg eq./m³.

Experiment no.	*Column diameter* (mm)	$S.10^{-2}$ (m^{-1})	$\mathfrak{D}_R.10^{12}$ (m^2/sec)
29+	10	89	5·03
33+	10	89	5·61
88	10	89	4·38
93	10	89	3·81
97	10	89	4·71
101	10	89	3·44
		Mean	4·5

Table 5. Results of kinetic experiments with $H^+ - Na^+ (SO_4^{2-})$ – *Amberlite IRC 50 (resin phase).*

Experiment no.	*Column diameter* (mm)	$S.10^{-2}$ (m^{-1})	$\mathfrak{D}_R.10^{12}$ (m^2/sec)	*Co* (kg eq./m³)
31+	10	89	29·1	0·757
37+	6	89	38·5	0·39 – 0·41
41+	6	89	37·9	
45+	6	89	42·3	
57+	6	89	29·8	
75	6	58	38·7	
89	10	89	42·1	

Table 6. Results of kinetic experiments with $H^+ - Na^+$ (SO_4^{2-}) – *Amberlite IRC 50 (liquid phase;* Co = *ca.* 0·4 kg eq./m³, $S = 89.\ 10^2 m^{-1}$).

$k_L.10^6$ m/sec	$v_0.10^2$ m/sec	*Sh*	*Re*
8·8	7·73	1·28	0·087
8·5	6·64	1·24	0·075
11·1	13·31	1·62	0·150
7·4	5·95	1·09	0·067
7·2	7·31	1·04	0·082
6·1	5·51	0·89	0·062
3·9	3·45	0·56	0·039

Not all experimental break-through curves could be used for the determination of both k_L and k_R. That depended on the number of observation points either in the beginning (for k_L) or the end (for k_R) of the break-through curve.

Table 7. Results of kinetic experiments with $Na^+ - H^+$ $(H_2BO_3^-)$ *– Amberlite IRC 50 (liquid phase ;* $Co = 0{\cdot}134 - 0{\cdot}137$ kg eq./m³, $S = 89.\ 10^2$ m^{-1})

$k_L.10^6$	$v_0.10^4$	*Sh*	*Re*
8·5	15·70	1·00	0·176
6·8	11·98	0·80	0·135
3·5	6·36	0·42	0·072
4·8	7·25	0·56	0·082

In Tables 6 and 7 values for the numbers of Reynolds and Sherwood are given, defined according to :

$$Sh = \frac{k_L}{S\,\mathfrak{D}_L} \qquad Re = \frac{v_0}{Sv}$$

Here $\mathfrak{D}_L$ = diffusion coefficient in the liquid phase (m²/sec),

ν = kinematic viscosity of the liquid (m²/sec).

For ν the value of 10^{-6} m²/sec was always taken (= viscosity of water at 20°C), because all experiments were performed at around 20°C. Less simple is the choice of a value for $\mathfrak{D}_L$ since different ions are diffusing in opposite directions. In general the smallest diffusion coefficient of the two substances present was chosen.

For the $Na^+ - H^+$ $(H_2BO_3^-)$ system the value for boric acid was taken, that for borax being unknown. Table 8 gives the values used (I.C.T.)

Table 8.

System	$\mathfrak{D}_L.10^9$ (m²/sec)
$Na^+ - H^+$ (SO_4^{2-})	0·77
$Na^+ - H^+$ $(H_2BO_3^-)$	0·95
$Na^+ - H^+$ (Cl^-)	1·2
$Ag^+ - H^+$ (NO_3^-)	1·3

In Fig. 15 a double logarithmic graph is given, representing the experimental results of Tables 6 and 7. The drawn lines in this Fig. can be represented by :

$$Sh = C\,Re^n$$

with $n = 0{\cdot}8$.

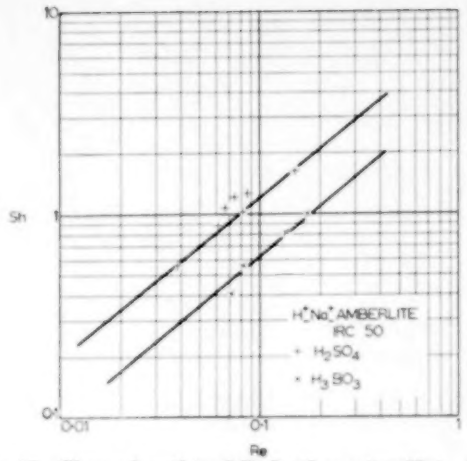

FIG. 15. *Sh* as a function of *Re* for the system $Na^+ - H^+$ Amberlite IRC 50.

Kinetic experiments with Dowex 50 × 8

In view of these results it is assumed for the $Na^+ - H^+$ (Cl^-) experiments with Dowex 50 × 8, that could not be interpreted with (50) and (51), that k_L and $tg\delta = C_0\,k_L/q_0 k_R$ varied proportional to $v_0^{0{\cdot}8}$. Further it was apparent from experiments summarized in Table 9, that the break-through curve at a medium flow rate was practically symmetrical. Therefore δ was taken to be 45° for experiment number 31.

Then it is possible to determine k_L and k_R from the break-through curves and the equilibrium curve given in Fig. 3.

The results are given in Table 9.

From the mean value of k_R follows with (52) $\mathfrak{D}_R = 1{\cdot}2.10^{-10}$ m²/sec, comparing reasonably well with the value $1{\cdot}6.10^{-10}$ m²/sec of GILLILAND and BADDOUR [6] and $8{\cdot}10^{-11} - 1{\cdot}10^{-10}$ m²/sec of BOYD and SOLDANO [2].

From two other experimental break-through curves mass transfer coefficients were determined ; the systems involved were $Na^+ - H^+$ (SO_4^{2-}) – Dowex 50 × 8 and $Ag^+ - H^+$ (NO_3^-) – Dowex 50 × 8. The inflexion point concentrations x_b combined with the equilibrium curves (Figs. 4 and 5) show that in the first mentioned case the liquid side resistance predominates ($\delta \approx 0°$) while in the second case $\delta \approx 45°$. The slope of the break-through curves was determined graphically for a few values of x. The results are given in Tables 10 and 11.

VOL. 10 1959

Table 9. *Results of experiments with the system* $Na^+ - H^+ (Cl^-)$ – *Dowex* 50 × 8

Experiment no.	$v_0 .10^4$ (m/sec)	$\left(\frac{\partial x}{\partial t}\right)_{x=0.5} .10^3$ (sec^{-1})	$k_R .10^6$ (m/sec)	$k_L .10^5$ (m/sec)	*Re*	*Sh*
27	21·1	8·06	7·25	5·28	0·155	3·24
31	12·8	6·25	6·70	3·34	0·094	2·05
35	5·8	3·90	5·98	1·62	0·042	0·99
45	22·6	6·80	5·91	4·69	0·166	2·88
47	28·1	8·89	7·35	6·77	0·206	4·15
53	2·2	2·71	7·66	0·92	0·016	0·56
55	26·8	8·71	7·24	6·57	0·197	4·03
57	34·3	9·44	7·41	8·11	0·252	4·97

Table 10. *Results of kinetic experiment with the system* $Na^+ - H^+ (SO_4^{2-})$ – *Dowex* 50 × 8. $S = 99.10^2\ m^{-1}$; *glass column, diameter* = 14 mm; $v_0 = 1{\cdot}3.10^{-3}$ m/sec; $Re = 0{\cdot}131$; $C_0 = 0{\cdot}392$ kg eq./m^3.

x	$\left(\frac{\partial x}{\partial t}\right) .10^3$ (sec^{-1})	$(k_L .10^5$ (m/sec)
0·25	5·15	1·97
0·40	6·97	1·81
0·50	8·04	1·72
0·60	10·9	2·06
		—
		Mean 1·9

Table 11. *Results of kinetic experiment with the system* $Ag^+ - H^+ (NO_3^-)$ – *Dowex* 50 × 8. $S = 192.10^2\ m^{-1}$; *glass column, cross-section* = 1 cm^2; $v_0 = 4{\cdot}78.10^{-4}$ m/sec; $Re = 0{\cdot}0249$; $C_0 = 0{\cdot}292$ kg eq./m^2.

x	$(dx/dt) .10^3$ (sec^{+1})	$k_L .10^3$ (m/sec)	$k_R .10^6$ (m/sec)	
0·40	3·91	1·1	1·5	
0·50	4·85	1·2	1·7	$\mathfrak{D}_R = 1{\cdot}7.10^{-11} m^2/sec$
0·75	3·64	0·8	1·1	

7. Discussion of the Results

Resin phase resistance

From Tables 3, 4 and 5 it is seen that the resin phase diffusion coefficients $\mathfrak{D}_R$ differ rather much for the three systems studied, that for borax being the lowest, and sulphuric acid the highest. A qualitative explanation of this phenomenon can be given as follows.

Upon exchange of Na^+ and H^+ ions with SO_4^{2-} as the anion, only the small mobile cations are diffusing. The anions need not diffuse simultaneously with the cations, the salt Na_2SO_4 being totally and the acid H_2SO_4 practically dissociated. If, however, OH^- is the anion, the acid formed, HOH, is very weakly dissociated. Consequently, the OH^- ions must enter the resin together with the Na^+ ions against a stream of undissociated H_2O.

The same applies to the borax experiments where Na^+ and $H_2BO_3^-$ ions diffuse countercurrently with practically undissociated boric acid; only in this case the ions involved are bigger and less mobile than with OH^- anions, resulting in a lower value for $\mathfrak{D}_R$.

Conway *et al.* [3] found a value of $0{\cdot}4.10^{-12}$ m^2/sec for the $Na^+ - H^+ (OH^-)$ – Amberlite IRC 50 system; that is an order of magnitude smaller than the value from Table 4. They calculated $\mathfrak{D}_R$ from batch experiments in which they measured the progress of this exchange in a stirred vessel. In their interpretation they supposed that no liquid side resistance was present. However, the value of m for this exchange will be extremely high in the beginning of the experiment; therefore the liquid phase resistance is bound to predominate in the first stages of the experiment. That means that the results of Conway *et al.* are not reliable since the specific properties of the resin make it unsuited for their method of measuring.

Liquid phase resistance

In Fig. 16 all liquid side kinetic measurements are summarized in one graph, giving *Sh* as a function of *Pé* ($Pé = v_0/S\mathfrak{D}_L$).

The following points are evident from this Fig.

(a) The points do not fall on one line as was to be expected. An important reason for this spread is probably the fact that the values taken for $\mathfrak{D}_L$ were wrong. The same reasoning explaining the difference in $\mathfrak{D}_R$ applies here too. As a consequence the diffusion coefficient for the borax system—and to a smaller extent for the sulphuric acid system too—should be much smaller relative to that for the chloride system. The effect of this is that the points in Fig. 16 are drawn together considerably.

(b) Notwithstanding the spread in the results, it is clear from the graph that the exponent n of the Reynolds, or Péclet, numbers, is decidedly higher than 0·5 [14, 19] and more nearly 0·8. The latter value agrees with that found by other authors, who performed kinetic experiments with ion exchangers [6, 18].

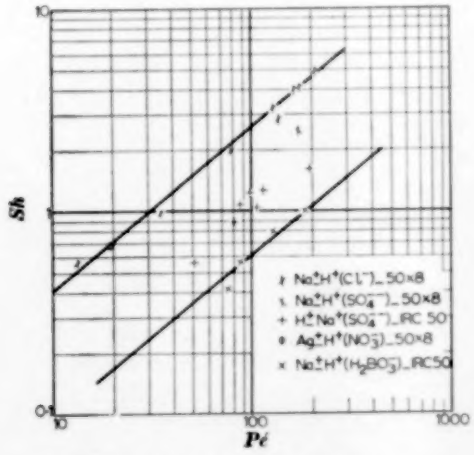

FIG. 16. *Sh* as a function of *Pé*.

8. DETAILS OF THE EXPERIMENTAL TECHNIQUE

The experimental procedure for measuring break-through curves is simple and will not be given here in much detail. Only the most important points will be mentioned in the following section.

The equilibrium experiments described were performed with the cation exchanger Dowex 50 × 8. The kinetic experiments were performed with the same resin and also with Amberlite IRC 50. In most cases the exchanger particles were sieved and a certain sieve-fraction was used. The particle diameter is not very important for the equilibrium experiments but it is important for the kinetic experiments. It is necessary to discuss the consequences of the swelling and shrinkage occurring in a bed of ion exchanger particles. These volume changes are much more pronounced in the case of Amberlite IRC 50 than for Dowex 50 × 8.

As a rule the exchange resin shows a shrinkage when there occurs an exchange, in which the displacing ions have a greater affinity to the resin than the displaced ions. Consequently a bed of ion exchange particles will normally shrink if $K_1 > 1$ (sharp front) and swell if $K_1 < 1$ (" equilibrium " break-through). This behaviour has some very important consequences for the measurement of break-through curves.

If in a percolation experiment $K_1 > 1$, a sharp break-through curve will result and shrinkage will occur. If the packing of the bed is not absolutely regular, the flow rate will be somewhat greater in the places with high porosity and smaller where the porosity is less. So, at the places with high porosity, the front will run ahead, causing more shrinkage.

In this way small and often inevitable differences in the bed porosity will grow more pronounced during the experiment, which means that a flow as described here is in principle unstable. Therefore experiments with sharp break-through curves should be mistrusted principally if no attention has been paid to this aspect.

If, on the other hand, $K_1 < 1$, the same reasoning leads to the conclusion that the results of a reverse or " equilibrium " break-through curve are much more to be trusted. Further the longitudinal mixing, resulting from an unequal flow rate, is much more serious in the case of the sharp break-through curve with great concentration gradients in the direction of flow than for the

equilibrium break-through where the concentration changes only slowly.

Therefore the experiments described in the first part of the article were mostly performed with normal glass columns, but the sharp break-through curves used in the second part, describing the kinetic results, were measured using an other type of column.

The wall A of this column (Fig. 17) is made of slightly extensible " plastic " material (e.g. silicone rubber). The lower part of this column is clamped (clamp D) on a short piece of glass tubing C, bearing a fritted glass disk B and a glass cock ending in a capillary. The construction is apparent from Fig. 17. The bed of exchanger particles in A can expand laterally producing a certain stress in the column wall. This stress will, on subsequent shrinkage, prevent any uneven packing in the bed practically completely. The break-through curves measured with this type of column were far better reproducible than those taken with glass columns. For a more complete description of these phenomena reference is made to [20].

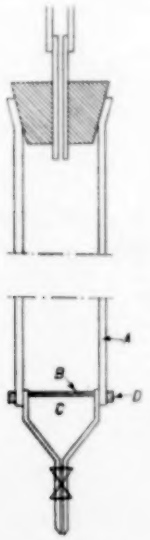

FIG. 17. " Plastic " column.

It is also possible to measure sharp break-through curves with a swelling bed, thus preventing the deleterious effects of shrinkage on a sharp break-through curve. For such a case it is necessary to make use of the weakly acidic character of the exchange groups of e.g. Amberlite IRC 50. These carboxylic groups are weakly dissociated if they are in the H^+ form. Therefore during the exchange of e.g. Na^+_L against H^+_R the following reaction occurs.

$$R\,COOH \rightleftharpoons R\,COO^- + H^+_R \qquad (34)$$

$$H^+_R + Na^+_L \rightleftharpoons Na^+_R + H^+_L \qquad (35)$$

The dissociation reaction (34) has such a small equilibrium constant K_1 that the H^+ ions are far more strongly bound to the resin than Na^+ ions. Therefore it is impossible to displace the H^+_R ions from the resin by a solution of NaCl or Na_2SO_4. It is possible, however, to draw reaction (35) to the right hand side by using an anion of a very weak acid. Then the following reaction will occur in the solution phase:

$$H^+_L + Z^- \rightleftharpoons HZ$$

If the dissociation constant K_d of (36) is much smaller than K_i of (34) the equilibrium of (35) will lie at the right hand side (or $K_i > 1$). This situation will occur if for Z^- the anion $H_2BO_3^-$ or OH^- is chosen.

But since the hydrogen in the resin phase occurs almost completely in the undissociated form, so without water of hydration the resin will swell considerably when the hydrogen is displaced by the hydrated Na^+ ions. So in this case a sharp break-through curve ($K_i > 1$) will be attended by a swelling bed.

Acknowledgements—The author is greatly indebted to H. KRAMERS for the scientific guidance he gave and for the very valuable help in preparing both this paper and the corresponding thesis.

T. HUIZENGA, P. G. SIBBALD and W. J. W. VERMIJS are thanked for the careful execution of some of the experimental work.

NOTATION

C = absolute concentration of one ion species in the fluid (kg eq./m³)
C_i = value of C at the interface between two phases (kg eq./m³)
C_0 = total concentration in the fluid (kg aq./m³)
C_1, C_2 = constants in (41)
C = constant
d = particle diameter (m)

$\mathfrak{D}_L$ = diffusion coefficient in the liquid phase (m^2/sec)

$\mathfrak{D}_R$ = diffusion coefficient in the resin phase (m^2/sec)

f = function of x in (5)

F = area of the cross-section of the column (m^2)

k = reaction rate constant in (37) (m^3/kg eq. sec)

k_L = partial mass transfer coefficient in the liquid phase (m/sec)

k_R = partial mass transfer coefficient in the resin phase (m/sec)

K_d = dissociation constant in (29) (kg mol/m^3)

K_i = dissociation constant of the active groups in the resin (kg mol/m^3)

K_L = total mass transfer coefficient for the liquid phase (m/sec)

K_R = total mass transfer coefficient for the resin phase (m/sec)

K_1 = equilibrium constant for uni-univalent exchange in (13)

K_2 = equilibrium constant for uni-divalent exchange in (33)

$l = \tau/s$ = dimensionless measure of the volume of fluid that has flowed through the column

l_m = special value of l, where $l = 1/[4x\,(1-x)]$

$m = y_i/x_i$ = slope of the line connecting the points (0, 0) and (x_i, y_i)

n = exponent of the Reynolds number

q = absolute concentration of one ion species in the resin (kg eq./m^3 bed volume)

q_i = value of q at the interface of two phases (kg eq./m^3 bed volume)

q_0 = total capacity of the exchanger (kg eq./m^3 bed volume)

R = volumetric flow rate of the fluid (m^3/sec)

R_L = partial resistance against mass transfer in the liquid phase (m^2sec/kg eq.)

R_R = partial resistance against mass transfer in the resin phase (m^2sec/kg eq)

$s = q_0 zF$ = total capacity of the bed (kg eq).

$S = 6\,(1-\epsilon)\,d$ = specific surface of the bed (m^2/m^3)

t = time (sec)

$v_0 = R/F$ = linear flow rate relative to the empty column (m/sec)

v_x = speed of displacement of the break-through curve through the bed (m/sec)

V_c = special value of ${}_cV_x$, where $l = 1$ (m^3)

V_{ex} = volume of fluid, that has flowed through the column, corrected for pore volume (m^3)

$x = C/C_0$ = relative concentration in the fluid.

x_b = value of x at the inflexion point of the break-through curve.

x_i = value of x at the interface between two phases

x^* = value of x in equilibrium with y according to (5)

$y = q/q_0$ = relative concentration in the resin

y_i = value of y at the interface between two phases

z = vertical co-ordinate (m)

γ = activity coefficient

δ = angle between the line, connecting the points $(x_i y_i)$ and (x, y_i) and the negative x-axis

ϵ = porosity

ν = kinematic viscosity (m^2/sec.)

$\tau = [t - (z/v_0)]\,C_0 R$ = total number of equivalents, that has flowed through cross-section z (kg eq.)

ϕ = function of x, $\sqrt{K_1}$ and l in (7)

Φ'' = mass flow per unit exchange-area (kg eq./m^2 sec)

$Sh = k_L/S\mathfrak{D}_L$ = Sherwood number

$Pé = v_0/S\,\mathfrak{D}_L$ = Péclet number

$Re = v_0/Sv$ = Reynolds number.

REFERENCES

[1] AMUNDSON N. R. *et al. J. Phys Chem.* 1952 **56** 683.

[2] BOYD G. E. and SOLDANO B. A. *J. Amer. Chem. Soc.* 1953 **75** 6091.

[3] CONWAY D. E. *et al. Trans. Faraday Soc.* 1954 **50** 512.

[4] DRANOFF J. and LAPIDUS L. *Industr. Engng. Chem.* 1957 **49** 1297.

[5] DUNCAN J. F. and LISTER B. A. J. *J. Chem. Soc.* 1949 3285.

[6] GILLILAND E. R. and BADDOUR R. F. *Industr. Engng. Chem.* 1953 **45** 330.

[7] GLUECKAUF E. *Trans. Faraday Soc.* 1955 **51** 1540.

[8] GLUECKAUF E. *J. Chem. Soc.* 1947 1302.

[9] HIESTER N. K. and VERMEULEN T. *Chem. Engng. Progr.* 1952 **48** 505.

[10] KLAMER K. Thesis, Delft 1957.

[11] KLAMER K. and VAN KREVELEN D. W. *Chem. Engng. Sci.* 1958 **7** 197.

[12] KLAMER K. *et al. Chem. Engng. Sci.* 1958 **7** 204.

[13] KRAMERS H. *Course on Packed and Fluidized beds*, Delft 1956.

[14] VAN KREVELEN D. W. and KREKELS J. T. C. *Rec. Trav. Chim. Pays-Bas.* 1948 **67** 512.

[15] LANDÖLT and BÖRNSTEIN *Zahlenwerte und Funktionen, aus Physik, Chemie, Astronomie, Geophysik und Technile* (6th edition) (edited by A. Euchen) Springer-Verlag, Berlin 1950.

[16] LEWIS G. N. and RANDALL M. *Thermodynamics*, McGraw-Hill, New York 1923.

[17] SILLÉN L. G. *Ark. Kemi* 1952 477 and 499.

[18] SUJATA A. D. *et al. Industr. Engng. Chem.* 1955 **47** 2193.

[19] THOENES D. Thesis, Delft 1957.

[20] WEVERS C. J. H. Thesis, Delft 1957.

The diffusivity of chlorine in water

(*Received* 17 *November* 1958)

We have recently determined the diffusion coefficient for chlorine in water by measuring the rate of absorption of pure chlorine gas into water in a wetted wall column. The measurements were performed at atmospheric pressure and at temperatures ranging from 10 to 35°C.

The experimental technique was exactly the same as employed by Nijsing *et al.* [1] and the hydrodynamic conditions of the laminar film were accurately known. As has been explained in [1] and in many other recent papers on the same subject, the rate of absorption can be calculated on the basis of the " penetration " theory. From this it follows that for physical absorption the absorption rate is proportional to $c^* \sqrt{D}$, the proportionality factor being fixed by the width and the height of the falling film and its surface velocity.

In this investigation the theory of physical absorption has been applied to the absorption of Cl_2 into water, although it is known that under equilibrium conditions the chlorine in water is partly hydrolysed. Thus we find from the data collected by Adams and Edmonds [2] that of the total amount of chlorine dissolved about 78 per cent is unhydrolysed at 10°C, 71 per cent at 20°C and 63 per cent at 30°C. However, from a paper by Shilov and Solodushenkov [3] it appears that at room temperature the hydrolysis reaction is completed well within 0·1 sec. Since the contact times in our film absorber were between 0·3 and 1 sec, we have assumed chemical reaction equilibrium throughout the liquid phase. In that case, the theory of physical absorption may be applied with c^* = the equilibrium solubility of chlorine in water (both hydrolysed and unhydrolysed) and D = the diffusivity of the equilibrium mixture of Cl_2, HOCl and HCl in water.

In Table 1 the values obtained for $c^* \sqrt{D}$ are given which have been corrected to a chlorine pressure of 760 mm Hg. Each value is the average of 3 – 5 experimental runs with different liquid velocities and in each run the film height was varied by a factor of 6. The maximum deviation of the individual $c^* \sqrt{D}$ values for one temperature from the average values indicated in Table 1 did not exceed ± 3 per cent. The mean deviation is about ± 1·5 per cent.

For calculating the values of D at the different temperatures, the solubility data of Adams and Edmonds [2] have been used. These are given in Table 1 together with the calculated values of D. If the solubilities between 10 and 25°C from the paper by Whitney and Vivian [4] are employed, the value of D becomes 5 per cent smaller at 10°C and 5 per cent larger at 25°C. It appears that the reliability of the diffusivities obtained in this investigation depends mainly on the solubility data adhered to.

Table 1. *Experimental values of* $c^* \sqrt{D}$ *and derived values of* D

Temp. (°C)	$c^* \sqrt{D}$ † (10^{-4} kg/m² sec²)	c^* [2] † (kg/m³)	D (10^{-9} m²/sec)
10·0	2·95	9·76	0·91
13·0	2·84	9·05	0·98
18·3	2·70	7·76	1·20
20·0	2·58	7·37	1·22
22·4	2·55	7·00	1·32
25	2·46	6·54	1·42
30	2·36	5·86	1·62
35	2·31	5·43	1·81

† At 760 mm Hg pressure.

The diffusivity values of Table 1 have been plotted against temperature in Fig. 1, together with the data obtained by Davidson and Cullen [5] from absorption experiments on wetted spheres. As to the dependence on temperature, their diffusivities for chlorine were rather discordant with those obtained for other sparingly soluble non-reacting gases with the same method. This is not the case with the chlorine diffusivities presented in this com-

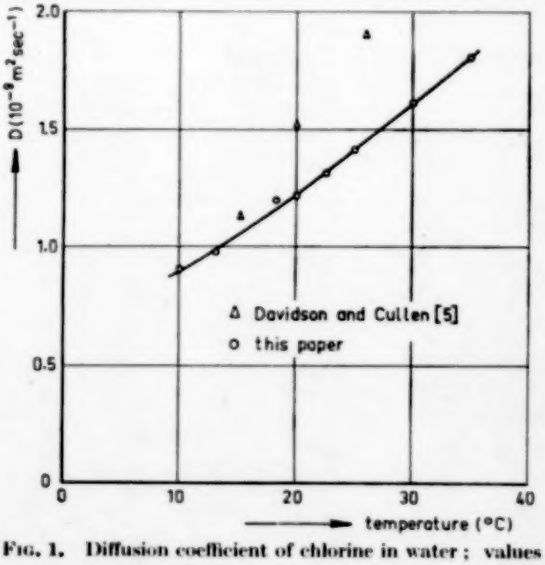

Fig. 1. Diffusion coefficient of chlorine in water; values from Table 1 vs. temperature.

munication. It appears that the Stokes – Einstein relationship holds well for these data ; the average value of $D\mu/T$ is $(4{\cdot}23 \pm 0{\cdot}07)\ 10^{-15}\ \mathrm{N\,^{\circ}K^{-1}}$.

Laboratorium voor Fysische Technologie H. Kramers
Technische Hogeschool R. A. Douglas
Delft, Netherlands R. M. Ulmann

References

[1] Nijsing R. A. T. O., Hendriksz R. H. and Kramers H., *Chem. Engng. Sci.* 1959 **10** 1/2.

[2] Adams F. W. and Edmonds R. G. *Industr. Engng. Chem.* 1937 **29** 447.

[3] Shilov E. A. and Solodushenkov S. N. *C. R. Acad. Sci. U.R.S.S.* 1936 **3** 17 ; Morris J. C. *J. Amer. Chem. Soc.* 1946 **68** 1692.

[4] Whitney R. P. and Vivian J. E. *Industr. Engng. Chem.* 1941 **33** 741.

[5] Davidson J. F. and Cullen E. J. *Trans. Inst. Chem. Engrs.* 1957 **35** 51.

Book Reviews

The Kinetics of Vinyl Polymerization by Radical Mechanism. C. H. Bamford, W. G. Barb, A. D. Jenkins and P. F. Cryan. Butterworths, London, 1958. 318 pp. 50s. $8.80.

Free radical polymerization has been the subject of extensive scientific research for a period of somewhat more than 20 years. During this time the nature of the phenomena involved has been established, together with a detailed mathematical treatment of the several processes which are believed to take place. Unlike the other processes for making high polymers the free radical process is now capable of quantitative description through the absolute velocity constants for the different steps involved.

The time is therefore ripe for the production of a single work on this subject, and it can only be a matter of satisfaction for all workers in the field to see that Dr. Bamford and some of his colleagues have found the time to write it. The work of the Maidenhead laboratory has made a number of important contributions to the understanding of free radical processes, especially in connection with the problems of trapped radicals and absolute velocity constants, and these are naturally well represented, (though not over represented) in the text.

The book covers all the important fields of radical polymerization. It begins with techniques of investigation and then deals with the measurement of absolute velocity constants for different monomers. Subsequent chapters show how these quantities work out in terms of homogeneous and heterogeneous polymerizations. Evidence is presented showing how the reactions are affected by the isolation of free radicals in emulsion particles or by their fixation in gels or precipitated polymer particles. Other chapters deal with copolymerization, of which a useful condensed presentation is given, and the kinetics of inhibition and gelation.

A book with this title naturally contains a good deal of mathematics, but it may also be read with advantage by those who do not wish to go through all the mathematical arguments in detail. The inclusion of an author index would have been an advantage, as the book should become an important reference source for future workers in the field.

R. N. Haward

Kurzes Handbuch der Brennstoff- und Feuerungstechnik. W. Gumz: Springer Verlag, Berlin–Göttingen–Heidelberg, 1953. (2. Aufl.) 583 S. DM 45.

Das 1942 in erster Auflage erschienene und seit 1952 in 2. Auflage vorliegende Buch gibt auf knappen Raum (575 S.) in 4 Hauptabschnitten — Physikalische Grundgesetze, die Brennstoffe, Verbrennung, Vergasung, Verbrennungs- und Vergasungsvorgänge — eine umfassende Einführung in alle Fragen und Probleme, die bei der praktischen Verbrennung der herkömmlichen gasförmigen, flüssigen und festen Brennstoffe auftreten. Die moderne Feuerungstechnik wird von dem Verfasser als angewandte Physikalische Chemie aufgefasst, die neben der Thermodynamik in immer steigendem Masse genaue Kenntnis der Strömungslehre verlangt.

In diesem Sinne widmet der Autor etwa ein Fünftel seines Buches den diesbezüglichen physikalischen und physikalisch-chemischen Grunderscheinungen. In einer konzentrierten Aufzählung aller wichtigen Gesetzmässigkeiten wird dem Feuerungstechniker gezeigt, was es evtl. alles zu berücksichtigen gilt. In einem Kapitel über die Brennstoffe findet sich eine Beschreibung der physikalischen und chemischen Stoffeigenschaften sowie der Bewertungsmöglichkeit durch Verbrennungswärme, Reaktionsfähigkeit und Zündeigenschaften. Auf 60 Seiten sind ausserdem im einzelnen die Aufarbeitungs (und Veredelungs) methoden dargestellt. Im Mittelpunkt des Buches steht als besonders wertvoller Beitrag eine eingehende und kritische Einführung in die verschiedenen Berechnungsmöglichkeiten des Verbrennungsvorganges unter besonderer Berücksichtigung des I–t — Diagramms, zu dessen Entwicklung der Verfasser selbst entscheidend beigetragen hat.

Bemerkenswert ist die Fülle der zusammengetragenen Zitate, die besonders vollzählig sein dürften, da der Verfasser durch seinen langjährigen Aufenthalt in den USA guten Einblick in die dortige auch weniger leicht zugängliche Literatur hatte Etwa 200 treffend ausgewählte Abbildungen und rund 100 Zahlentafeln unterstützen die konzentrierte Darstellung.

Man darf den Versuch als gelungen betrachten, durch den hier dem Praktiker ein Buch an die Hand gegeben wird, das bis zu den Grundlagen führt und nicht in einer äusseren Beschreibung steckenbleibt. Die vertiefte Darstellung bietet sicherlich auch dem Forscher manche Anregung.

Es wäre zu wünschen dass es dem Verfasser in Fortführung seiner verdienstvollen Arbeit gelingen möge, das Buch ständig auf neuzeitlichem Stand zu halten. Bei einer Neuauflage wäre dann evtl. die chemische Kinetik mehr als bisher zu berücksichtigen. Das immer stärker werdende Eindringen kinetischer Betrachtungen in die praktischen Anwendungen lässt dieses Gebiet zu einer eigenständigen Disziplin neben Thermodynamik, Strömungslehre etc. werden. Weiterhin könnte vielleicht überlegt werden, ob ein Abschnitt über die wichtigsten Grundergebnissne der Flammenforschung mit in das Kapitel über die Grundgesetze aufzunehmen wäre.

F. Fetting.

VOL. 10 1959

BOOKS RECEIVED

S. S. Penner: Chemistry Problems in Jet Propulsion. International Series of Monographs on Aeronautical Sciences and Controlled Flight. Pergamon Press 1957.

R. L. Butzka: Plastic Sheet Forming. Reinhold and Chapman and Hall 1958.

N. F. L. Megson: Phenolic Resin Chemistry. Butterworths 1958.

R. G. Fowler and D. I. Mayer: Physics for Engineers and Scientists. Allyn and Bacon 1958

A. M. Lovelace, W. Postelnek and D. A. Rausch: Aliphatic Fluorine Compounds. ALS Monograph No. 138. Reinhold 1958.

G. W. Gray (editor): Steric Effects in Conjugate Systems. Academic Press and Butterworths 1959.

A. G. Jones: Analytical Chemistry: Some New Techniques. Academic Press and Butterworths 1958.

D. H. Desty (editor): Gas Chromatography. Academic Press and Butterworths 1958.

B. Lenhert (editor): Electromagnetic Phenomena in Cosmical Physics. Cambridge University Press 1958.

I.U.P.A.C.: Nomenclature of Organic Chemistry. Butterworths 1958.

I.U.P.A.C.: Nomenclature of Inorganic Chemistry 1957. Butterworths 1959.

K. Diels and R. Jaeckel: Leybold Vakuum-Taschenbuch für Laboratorium und Betrieb Springer-Verlag 1958.

F. Trotman-Dickenson: Free Radicals: An Introduction. Methuen 1959.

SELECTION OF CURRENT PAPERS FROM NON-CHEMICAL ENGINEERING JOURNALS OF INTEREST TO CHEMICAL ENGINEERS

E. McLAUGHLIN: Viscosity and self-diffusion in liquids. *Trans. Faraday Soc.* 1959 **55** 29-38.

R. V. JONES: The detection of thermal radiation using linear expansion. *Proc. Roy. Soc.* 1959 A **249** 100-113.

V. C. LIU: On the separation of gas mixtures by suction of the thermal boundary layer. *Quart. J. Mech. Appl. Math.* 1959 **12** 1-13.

D. R. DAVIES: Heat transfer by laminar flow from a rotating disk at large Prandtl numbers. *Quart. J. Mech. Appl. Math.* 1959 **12** 14-21.

Y. P. VARSHNI and S. N. SRIVASTAVA: Viscosity of normal paraffins. *Proc. Phys. Soc.* 1959 **73** 153-159.

W. C. WINNING. Some observations concerning the viscosity–temperature behaviour of hydrocarbons. *J. Inst. Petrol.* 1959 **45** 9-15.

P. GROOTENHUIS: The mechanism and application of effusion cooling. *J. Roy. Aero. Soc.* 1959 **63** 73-89.

J. W. MARTIN: An experimental method for diffusion and extraction studies across the liquid–liquid interface. *Nature (Lond).* Jan. 31st 1959 **183** 312-313.

F. FRANKS and D. J. G. IVES: Effect of low concentrations of alcohols on the interfacial tension between water and hydrocarbons. *Nature (London).* Jan. 31st 1959 **183** 316-317.

P. H. PRICE: Alternative method of correlating forced convection heat transfer data. *Brit. J. Appl. Phys.* 1959 **10** 135-138.

D. J. RYLEY: Experimental determination of the atomizing efficiency of a high-speed spinning disk atomizer. *Brit. J. Appl. Phys.* 1959 **10** 43-47.

R. E. GIBSON: A heat conduction problem involving a specified moving boundary. *Quart. Appl. Math.* 1959 **16** 426-430.

H. BURROW: The eddy diffusivity in annular flow. *J. Roy. Aero. Soc.* 1959 **63** 180-181.

H. W. DOUGLAS and J. BURDEN: The surface charge and sedimentation of Thoria suspensions. Part 2. The sedimentation of dilute and concentrated suspensions in relation to particle size and the Verweg–Overbeek theory of sol stability. *Trans. Faraday Soc.* 1959 **55** 356-362.

C. HARRIS: Correlation of sedimentation rates by dimensionless groups. *Nature (Lond.)* Feb. 21st 1959 **183** 530-531.

SELECTION OF CURRENT SOVIET PAPERS OF INTEREST TO CHEMICAL ENGINEERS*

M. M. KOTON: New polymers, their properties and practical application. *Zh. prikl. Khim.* 1959 **32** 6-21.

Z. Z. VYSOTSKI and V. V. SHALYA: Properties of silica gels obtained by drying silicic acid gel under vacuum. *Zh. prikl. Khim.* **32** 35-39.

M. F. LANTRATOV and A. F. ALABISHEV: Equilibrium diagram of the system NaOH–Na_2CO_3–NaCl. *Zh. prikl. Khim.* 1959 **32** 65-70.

G. N. GASYUK, A. G. BOLSHAKOV, A. V. KORTNEV and P. YA. KRAYNY: Coefficients of mass transfer in gaseous phase. *Zh. prikl. Khim.* 1959 **32** 95-99. A general correlation is established for the gas phase mass transfer coefficient in terms of dimensionless groups.

V. I. ATROSHCHENKO and N. A. GABRYA: On the rate of dissolution of methane and hydrogen–nitrogen mixture in condensing ammonia. *Zh. prikl. Khim.* 1959 **32** 99-104.

V. G. GLEIM, I. K. SHELOMOV and B. R. SHIDLOVSKI: On processes leading to formation of drops as the result of bursting of bubbles at gas–liquid interfaces. *Zh. prikl. Khim.* 1959 **32** 218-222.

D. I. OROCHKO, T. Kh. MELIK-AKHNAZAROV and T. P. ZINOVEVA: Reactor arrangement for chemical processes employing fluidized beds. *Khim. Nauka i Prom.* 1958 **3** 694-703.

P. I. LUKYANOV: Reactor arrangement for pyrolysis of crude oil to ethylene. *Khim. Nauka i Prom.* 1958 **3** 703-715.

V. M. RAMM and A. YU. ZAKGEIM: Theory and technology of absorption. *Khim. Nauka i Prom.* 1958 **3** 715-724. Literature survey covering the period 1955–58. 100 references.

N. I. GELPERIN and A. G. LYAKUMOVICH: Extraction from solution. *Khim. Nauka i Prom.* 1958 **3** 725-735. Literature review of recent work on liquid–liquid extraction. 68 references.

M. E. AEROV and V. A. MALYUSOV: New developments in rectification. *Khim. Nauka i Prom.* 1958 **3** 736-745. Literature survey. 140 references.

L. A. AKOPYAN, A. N. PLANOVSKI and A. G. KASATKIN: On calculation of packed columns operating under optimum conditions. *Khim. Nauka i Prom.* 1958 **3** 745-748. Correlation in terms of dimensionless groups.

M. YU. LURYE: Contemporary problems in the technology of drying. *Khim. Nauka i Prom.* 1958 **3** 748-752.

A. B. BASSEL and N. I. GELPERIN: Heat transfer equipment of high intensity. *Khim. Nauka i Prom.* 1958 **3** 753-767. Review of heat transfer equipment for increased heat recovery. 50 references.

V. I. SOKOLOV: Technology of centrifuging. *Khim. Nauka i Prom.* 1958 **3** 768-776. Literature survey of recent advances in centrifuging. 21 references.

N. V. SHPANOV: Industrial filtration. *Khim. Nauka i Prom.* 1958 **3** 777-782. Literature review. 25 references.

V. V. IVANOV: Advances in construction of chemical pumps. *Khim. Nauka i Prom.* 1958 **3** 782-789. Literature review. 10 references.

V. I. TETERYUKOV: Rotary vacuum pumps with liquid piston. *Khim. Nauka i Prom.* 1958 **3** 790-797.

A. A. GRYAZNOV: High-vacuum diffusion pumps. *Khim. Nauka i Prom.* 1958 **3** 798-802.

I. I. KORNILOV: Corrosion resistant titanium and its alloys. *Khim. Nauka i Prom.* 1958 **3** 803-807.

G. V. SAMSONOV: Prospects for application of refractory compounds in the chemical industry. *Khim. Nauka i Prom.* 1958 **3** 807-811.

S. V. DOBROVOLSKI, K. K. GOFMEISTER and P. N. LAMEKHOV: Manufacture of phthalic nitrile from phthalic anhydride and ammonia. *Khim. Prom.* 1958 458-463.

V. M. VLASENKO, G. K. BORESKOV and G. E. BRAUDE: Catalytic removal of carbon dioxide from hydrogen–nitrogen mixtures. *Khim. Prom.* 1958 473-475.

B. A. CHERTKOV: Coefficients of heat transfer in cooling of flue gases in packed scrubbers. *Khim. Prom.* 1958 487-491.

---

*To assist readers, translations of any article appearing in the above list can be obtained at a reasonable charge. All orders should be addressed to the Administrative Secretary of the Pergamon Institute at either 4 Fitzroy Square, London W.1, or 122 East 55th Street, New York 22, whichever is more convenient.

M. M. Egorov, V. F. Kiselev, K. G. Krasilnikov and V. V. Murina: Effect of the nature of silica gel and quartz surface on their adsorption properties. III. Heats of wetting of silica by various liquids. *Zh. fiz. Khim.* 1959 **33** 65-73.

A. K. Skryabin: The process of extraction. *Zh. fiz. Khim.* 1959 **33** 74-77. Curves of change of concentration with distance in a spray column have been obtained by solution of differential equations for extraction regarded as a statistical process obeying the Einstein–Smoluchowski equation.

V. V. Karasev and B. V. Deryagin: Determination of surface viscosity from the kinetics of thinning of wetting liquid films in the blowing-off process. *Zh. fiz. Khim.* 1959 **33** 100-106.

G. G. Devyatikh, N. Kh. Aglinlov and I. A. Frolov: Effect of rate of distillate removal on separating efficiency of a rectification column. *Zh. fiz. Khim.* 1959 **33** 161-164.

A. Yu. Koshevnik, M. M. Kusakov and N. M. Lubman: Effect of surface acting agents on the motion of gas bubbles in hydrocarbon liquids. *Zh. fiz. Khim.* 1959 **33** 197-203.

D. P. Dobychin and T. F. Tellinskaya: Rapid method of determination of surface area of sorbents by adsorption. *Zh. fiz. Khim.* 1959 **33** 204-207.

L. F. Vereshchagin, A. A. Semerchan and S. S. Sekoyan: On disintegration of a rapid water stream. *Zh. tekh. Fiz.* 1959 **29** 45-50.

L. E. Ber: Method of solution of problems of non-isothermal turbulent convection between two parallel plates. *Zh. tekh. Fiz.* 1959 **29** 61-69.

O. B. Ptitsin: Hydrodynamics of polymer solutions. I. Diffusion and sedimentation of branched macromolecules. *Zh. tekh. Fiz.* 1959 **29** 75-93.

L. D. Berman: Some regularities of simultaneous mass and heat transfer processes in heterogeneous systems. *Zh. tekh. Fiz.* 1959 **29** 94-106.

I. I. Vorovich and V. I. Yudovich: Steady flow of a viscous fluid. *Dokl. Akad. Nauk SSSR* 1959 **124** 542-545.

ERRATUM

Aris R. Diffusion and reaction in flow systems of Turner's structures. *Chem. Engng. Sci.* 1959 **10** 80.

In Fig. 1 on p. 82 $x = 0$ should read $v = 0$